THE ADSORPTION AND DISSOCIATION OF AsH_3 and B_2H_6 MOLECULES ON STEPPED Ge(100) SURFACE

A THESIS SUBMITTED TO
THE GRADUATE SCHOOL OF NATURAL AND APPLIED SCIENCES
OF
MIDDLE EAST TECHNICAL UNIVERSITY

BY

MUSTAFA TÜRKMENOĞLU

IN PARTIAL FULFILLMENT OF THE REQUIREMENTS
FOR
THE DEGREE OF MASTER OF SCIENCE
IN
PHYSICS

JULY 2011

Approval of the thesis:

THE ADSORPTION AND DISSOCIATION OF AsH_3 and B_2H_6 MOLECULES ON STEPPED Ge(100) SURFACE

submitted by MUSTAFA TÜRKMENOĞLU in partial fulfillment of the requirements for the degree of **Master of Science in Physics Department, Middle East Technical University** by,

Prof. Dr. Canan Özgen
Dean, Graduate School of **Natural and Applied Sciences** _____

Prof. Dr. Sinan Bilikmen
Head of Department, **Physics** _____

Prof. Dr. Şenay Katırcıoğlu
Supervisor, **Physics Dept., METU** _____

Examining Committee Members:

Prof. Dr. Nizami Hasanli
Physics Dept., METU _____

Prof. Dr. Şenay Katırcıoğlu
Physics Dept., METU _____

Prof. Dr. Hamit Yurtseven
Physics Dept., METU _____

Assoc. Prof. Akif Esendemir
Physics Dept., METU _____

Assoc. Prof. Barış Akaoğlu
Physics Engineering Dept., Ankara University _____

Date: 22/07/2011

I hereby declare that all information in this document has been obtained and presented in accordance with academic rules and ethical conduct. I also declare that, as required by these rules and conduct, I have fully cited and referenced all material and results that are not original to this work.

Name, Last name: MUSTAFA TÜRKMENOĞLU

Signature :

ABSTRACT

THE ADSORPTION AND DISSOCIATION OF AsH_3 AND B_2H_6 MOLECULES ON STEPPED Ge(100) SURFACE

Türkmenoğlu, Mustafa
M.Sc., Department of Physics
Supervisor: Prof. Dr. Şenay Katırcıoğlu
July 2011, 96 pages

In this work, the doping processes of the S_A type stepped Ge (100) surface by arsine (AsH_3) and diborane (B_2H_6) gas flow have been simulated seperately by the possible adsorption and dissociation models. The most stable adsorption and dissociation models of AsH_3 and B_2H_6 on stepped Ge(100) surface have been determined by the local minimum total energy and/or binding energy calculations based on Hartree-Fock Theory. The present calculations have shown that, the step region (both up and down terraces) of the stepped Ge (100) surface has the most attractive sites for the initial adsorption stages of the gas molecules. It has been found that the thermodynamically preferred structures in the dissociation paths of arsine and diborane are the same; AsH_3 , BH_3 (fragment of diborane), AsH_2 and BH_2 products prefer to be bounded to a single surface Ge atom, but AsH and BH prefer to be bridged between two adjacent surface Ge atoms. It has been also found that, at the first step of the adsorptions, AsH_3 can only dissociate to AsH_2, but BH_3 can dissociate to both BH_2 and BH. This remarkable result has showed that dissociation of BH_3 on Ge(100) surface can be easier than AsH_3's. According to the optimization calculations, the dissociation path has started with the adsorption of AsH_3 (or BH_3) on the electron deficient side (buckled down) of the Ge dimer bond and ended with the occupation of the empty Ge sites in the surface layers by As (or B) atom substitutionally. In the present work, the beginning of the n – (or p-) type doping of the stepped Ge(100) surface has been illustrated by the As (or B) electronic states obtained in the optical energy gap of Ge very close to HOMO (or LUMO) energy edge.

Keywords: Arsine (AsH_3), Diborane (B_2H_6), Stepped Ge(100), Adsorption, Dissociation, Hartree-Fock (HF).

ÖZ

AsH_3 VE B_2H_6 MOLEKÜLLERİNİN BASAMAKLI Ge(100) YÜZEYİNE YAPIŞMASI VE AYRIŞMASI

Türkmenoğlu, Mustafa
Yüksek Lisans, Fizik Bölümü
Tez Yöneticisi: Prof. Dr. Şenay Katırcıoğlu
Temmuz 2011, 96 sayfa

Bu çalışmada, S_A tipi basamaklı Ge(100) yüzeyinin Arsine (AsH_3) ve Diborane (B_2H_6) gaz akışıyla ayrı ayrı katkılanması, olası yapışma ve çözünme modelleriyle simule edilmiştir. AsH_3 ve B_2H_6'nın basamaklı Ge(100) yüzeyi üzerinde en kararlı yapışma ve çözünme modelleri Hartree-Fock kuramına dayalı lokal en düşük toplam enerji ve/veya bağlanma enerjisi hesaplamalarıyla belirlenmiştir. Yapılan hesaplamalar basamaklı Ge(100) yüzeyinin basamak bölgesinin (üst ve alt teraslar) gaz moleküllerinin başlangıç yapışma aşaması için en çekici bölge olduğunu göstermiştir. Arsine ve diborane'nin çözünme yolları üzerinde termodinamik olarak tercih ettikleri yapıların benzer olduğu bulunmuştur; AsH_3, BH_3 (Diborane parçası), AsH_2 ve BH_2 çözünme ürünleri sadece bir Ge yüzey atomuna bağlanmayı tercih ederlerken, AsH ve BH komşu iki Ge yüzey atomu arasında köprü olmayı tercih etmişlerdir. Bu çalışmada ayrıca, yapışma aşamasının ilk adımında AsH_3'ün sadece AsH_2'ye fakat BH_3'nün hem BH_2 hem de BH'a ayrıştığı bulunmuştur. Bu kayda değer sonuç BH_3'ün Ge(100) yüzeyinde AsH_3'den daha kolay çözünebileceğini göstermiştir. Optimizasyon hesaplamalarına göre, çözünme yolu AsH_3'ün (veya BH_3) Ge dimer bağının elektron eksik tarafına (aşağıya bükülmüş) yapışmasıyla başlamış ve yüzey tabakaları içinde Ge atomu tarafından terkedilmiş yerlerin As (veya B) atomları tarafından doldurulmasıyla sonlanmıştır. Sunulan çalışmada, basamaklı Ge(100) yüzeyinin n- (veya p-) tipi katkılanmasının başlaması Ge'un optik enerji boşluğunda HOMO (veya LUMO) enerji ucuna yakın As (veya B) elektronik durumlarının elde edilmesiyle açıklanmıştır.

Anahtar Kelimeler: Arsine (AsH_3), Diborane (B_2H_6), Basamaklı Ge(100), Yapışma, Çözünme (Ayrışma), Hartree-Fock (HF).

to my father…

ACKNOWLEDGEMENTS

First and foremost, I would like to express my deepest gratitude to my thesis supervisor, Prof. Dr. Şenay Katırcıoğlu for her indispensable support, invaluable advice and guidance throughout the whole study.

I would like to thank TUBITAK ULAKBIM. The reported numerical calculations in this thesis are performed using TUBITAK ULAKBIM High Performance and Grid Computing Center (TR-Grid e-Infrastructure).

I would like to express my deepest gratitude to my family for their love, support, encouragement and patience throughout my carrier.

TABLE OF CONTENTS

LIST OF TABLES

TABLES

LIST OF FIGURES

FIGURES

CHAPTER 1

INTRODUCTION

Nowadays, Germanium (Ge) material is coming into prominence again in device technology. The recent works [1-3] have showed that its high low-field hole mobility is interesting for high-mobility nano-devices applications, while its band gap (suitable for light absorption at communication wavelengths) is attractive in modern optoelectronics for fabrication of high-quality photo-detectors [4-6]. The use of the Germanium materials (n- and p- type Ge) for the electronic devices manufacturing was started at the beginning of the electronic age. In the 1950 and 1960s, a huge amount of data on the preparation of Ge with certain carrier type and concentration during the crystal growth and device manufacturing were reported by various research groups [7-10]. In these works, the superior low-field carrier mobility and small band gap energy were reported to be main features for Ge. Although the Ge material with high hole and electron mobility has considered to be important in device applications, the building electronic devices on germanium was left years ago because of its unstable oxides (germanium oxides), poor dielectric properties and temperature dependent electrical properties due to low energy band gap. Therefore, in the last three decades, instead of Ge, Silicon (Si) gained recognition as a dominant substrate for electronic devices especially, with its good quality oxide layer. Consequently, Si completely dominated the microelectronic industry although the first transistor was fabricated on Ge. But, according to a recent work [11], the continuous scaling into nanometer region of the Complementary Metal Oxide Semiconductor (CMOS) technology (for n- and p- type MOS transistors) brings silicon to its limits. Hence, in the next few years, it will no longer be possible to follow Moore's law (describes a long-term trend in the history of computing hardware, in which the number of transistors per square inch on an integrated circuit

has doubled approximately every two years) with silicon devices. For this reason, the investigations on new materials and innovative device design have been restarted. Along these lines there is a renewed interest in Ge as a possible candidate to replace silicon in a future integrated devices technology because its appealing properties like higher carrier mobility [12]. The Ge electronic devices could be faster than Si ones. On the other hand, the heterostructures consisting of alternate Ge and Si layers grown on Si were recognized to be a new class of materials in the last decade for modulated band gap engineering [13-14]. For exploring Ge's renewed application in semiconductor devices, the previously reported fundamentals of Ge such as the preparation conditions with a certain carrier type and concentration, the carrier mobility and its dependence on the carrier concentration, knowledge on the sticking and segregation coefficients of various dopants, have all been tried to be reevaluated in the recent works [15-20] from a current point of view.

Arsenic (As) and Boron (B) are usually used n- and p- type dopants for Ge, respectively. In the doping process, B atoms have been provided with diborane (B_2H_6) gas flow during or after the growth of Ge materials by gas- phase molecular beam epitaxy (GP-MBE) [21-22], solid-phase molecular beam epitaxy (SP-MBE) [23] or chemical vapor deposition (CVD) techniques [2, 6, 20, 24-25]. The thermally or photochemically activated B_2H_6 gas molecules or their fragments first adsorb on Ge surface, then decompose to further corresponding precursors and finally reduce to B atoms by desorption of H atoms from the surface [2, 6, 20-21, 23-25]. In recent works [2, 6, 20, 25] the application of heat treatment in low pressure CVD technique has intended the doping reaction and migration of B atoms in Ge sample. In Ref. [24], plasma-enhanced CVD with the surface irradiated by a 193 nm, 50 Hz pulsating laser was performed to synthesize boron films from B_2H_6 + He gas flow at a pressure of 200Pa. In this process, plasma was employed to generate precursor radicals (BH_3, BH_2, BH) for the growth while the irradiation was intended for photochemical enhancement of the surface processes such as again migration and growth reactions. In another work [21], the p-type doping was provided with Boron concentration of $8x10^{21}/cm^3$ by B_2H_6 gas molecules in the temperature range of 325-600^oC during the epitaxial growth of Ge(100) layers from Ge_2H_6 gas flow. In the same work [21], the

exhibited temperature programmed desorption (TPD) spectra associated with dideuteride, monodeuteride and deuterium desorption from Ge surface indicated the decomposion of B_2H_6 on Ge(100) surface. The growth of p-type Ge(100) surface was also reported in Ref. [22] by GP-MBE technique with B concentration of $4x10^{19}/cm^3$ in the temperature range of 300-400°C. Therefore p-type (by B atoms) doping of Ge materials have been initiated by the adsorption of BH_3 precursors on the surface and ended by the deposition of B atoms depending on the rate of desorption of H atoms from the surface. In the literature, Tertiarybutylarsine (TBAs) and Arsine (AsH_3) gas were frequently used n-type dopant source for Ge [26-28] and SiGe materials [29] in metal-organic vapor phase epitaxy (MOVPE) and CVD techniques. However, the Ge materials have been generally doped by As atoms in ion implantation method at room temperature [19] or under the heat treatment [17, 30]. In Ref. [26], the concentration of As atoms in Ge sample was limited to approximately $1x10^{19}/cm^3$ in the temperature range of 500-700°C. According to the structural works on As doped Ge surfaces [27-28], TBAs or AsH_3 gas flow forms facets on Ge surfaces having different miscut directions by etching. Particularly, the faceting on Ge (955) and Ge(11 3 3) surfaces were identified by scanning tunneling microscopy (STM) images when the samples were annealed under AsH_3 partial pressure of 1.2 torr at 560°C for 20 min exposure time [27]. The etching and faceting were determined to be removed on Ge surfaces by reducing the temperature, TBAs (or AsH_3) partial pressure and total TBAs (or AsH3) exposure time [27]. The different faceting structures due to different annealing temperatures were also identified on As-terminated vicinal Ge(100) surface by STM, X-ray photoemission spectroscopy (XPS) and low energy electron diffraction (LEED) measurements [28].

In the literature, the morphology of Ge surfaces has been also investigated to determine the different surface structures effective on the adsorption of dopant precursors. Especially, equilibrium surfaces of vicinal Ge (100) have been studied in detailed experimentally [31-38]. In the literature, the structure of Ge(100) surface is reported to be very similar to Si(100). The surface atoms on both Si(100) and Ge(100) dimerize resulting in (2x1) reconstruction [31-46]. The dimerization of the surface atoms first proposed by Schlier et al [47] for Si(100) and Ge(100) surfaces

was first imaged on Si(100) surface in real space by STM [39-40]. The dimerization of the surface atoms is derived by the reduction of surface energy due to the reduction in the number of dangling bonds from two to one for each surface atom. In STM images of Si(100) [39-40] both buckled (asymmetric) and non-buckled (symmetric) dimers were determined. While the symmetric dimer bonds are in the plane of the surface, asymmetric dimmer bonds make an angle with the surface. In time averaged STM images of Ge(100) and Si(100) [33-34, 43-44] all the dimer bonds were determined to be buckled (asymmetric) with a length of ~2.45A^{o} [36]. According to analysis given in these works [33-34, 43-44] the buckled dimers had flip flop motion and the symmetric appearing dimers are imaged as a result of a time average of the two configurations (up and down) of buckled dimers. The tilt angle of the parallel dimer bonds on Ge(100) surface are associated with the displacement of electron density from buckled down to buckled up Ge atom. The tilt angle of the asymmetric dimers out of the surface plane is ~14° [36]. The surface dimers of Si(100) and Ge(100) were also proposed to be buckled by Chadi [48]. In this work [48], the total energy calculations of the dimerized surface without imposing any symmetry constraints have indicated that the surface dimers spontaneously buckle, and the symmetric dimers are unstable.

The analysis of STM images have also illustrated that there are surface defects on Ge (100) and Si(100) as well as the asymmetric dimers, such as steps, missing dimer defects, or kink atoms [31-38, 43-44, 49-50]. In Ref. [36], Zandvliet has shown that STM images of vicinal Ge(100) can provide quantitative estimates for energetic parameters, such as the step free energy, the kink creation energy, the step–step interaction energies, and the energy of the facet. Because of the high coordination around the step edge the sites of the atomic steps are dominant to initiate the adsorption, chemical reaction, and catalysis. In light of the high resolution scanning tunneling microscopy (STM) [31-32, 36, 49-50], LEED [35-38], ultraviolet photoemission spectroscopy (UPS) [35, 37], and XPS [35-37] measurements, the main structure of vicinal Ge(100) surfaces are terraces (step up and down) formed by asymmetrically dimerized Ge surface atoms either in (1x2) or (2x1) domains. Two types of stepped structures, S_A and S_B, have been observed on vicinal Ge(100) surfaces for the small miscut angles towards the [110] direction [31-32, 35-36, 37-

38]. However, for the large miscut angles, the stepped structure was determined to be D_B (or D_A) type [35-38] with a double atomic height at the step edge. These most probable types of steps were first modeled and labeled by Chadi [51] for vicinal Si(100) surfaces. According to the definition of D_B (or D_A) type steps [51] dimer bonds on both upper and lower terraces are parallel (or perpendicular) to the step edge. In the case of the S_A (or S_B) type step edges, the dimer rows of the upper and lower terraces are parallel (or perpendicular) and perpendicular (or parallel) respectively, to step edge direction. Since the kink formation energy was reported to be significantly lower in S_B steps than in S_A, S_B steps contain many more thermally excited kinks than in S_A [52]. In Ref. [31], the STM images of vicinal Ge(100) surface were explained by both rebonded and nonbonded S_B step edges. But the STM images of the same system were explained by only bonded S_B step edges in Ref. [32]. The D_B (or D_A) type steps were first observed on STM images of vicinal Ge(100) and Si(100) surfaces by Wierenga et al [49]. The coexistence of S_B (or S_A) and D_B (or D_A) type steps on Ge(100) and Si(100) surfaces were reported in Ref. [50] for a range of miscut angle. The formation of steps has been reinvestigated by spot profile analysis of LEED (SPA-LEED), UPS, and XPS measurements in Ref. [35] for vicinal Ge(100) samples having miscut angles of 2.7 ^{o} and 5.4^o. Tegenkamp et al [35] have reported that the vicinal Ge(100) surface with miscut angle of 2.7^o have mainly terraces which are separated by steps of single atomic height (S_A or S_B). The average upper and lower terrace sizes and the monatomic step height of the sample were determined to be 29.9, 14.9 and 1.40 A^o, respectively, by diffraction analysis [35, 38]. According to the qualitative results of SPA-LEED, the terraces which are separated by double atomic height (D_A or D_B) were determined to be also present on the same sample with a small fraction (~1%). The fraction of double steps were found to be increased (~50%) when the miscut angle of vicinal Ge(100) was taken to be 5.4^o [35]. A recent work [37] has indicated that the double steps can be induced on vicinal Ge(100) surfaces by Si adsorption under an appropriate kinetic growth conditions. All these works [31-36, 38, 43-44] have indicated that the critical value of the miscut angle is ~6° to have D_A or D_B types steps on Ge(100) surface. The corresponding critical value of the miscut angle is 4° for Si(100) surface.

Although a considerable experimental and a few theoretical efforts have been devoted to understand the kinematics of stepped Ge(100) surfaces, there isn't any experimental or theoretical work investigating the decomposition stages of AsH_3 and B_2H_6 in the n- and p- type doping processes of stepped Ge(100). This work aims to compensate the lack of the literature by presenting a systematic theoretical study about the possible adsorption and dissociation models of AsH_3 and B_2H_6 on stepped Ge(100) surfaces. In the present work, the most probable dissociation paths for AsH_3, and B_2H_6 on stepped Ge(100) surfaces have been determined by the local minimal energy calculations based on Hartree-Fock theory. The binding energy of the fragments (AsH_3, AsH_2, AsH, As, and BH_3, BH_2, BH, B) has been also calculated in the adsorption and decomposition models of arsine and diborane gas molecules by

$$E_{binding} = E_{model} - E_{surface} - E_{fragment} \tag{1.1}$$

Here, E_{model}, $E_{surface}$, and $E_{fragment}$ are the total energies of the adsorption (or dissociation) models, stepped Ge(100) surface with necessary dangling bonds, and the fragment molecules (or atoms), respectively. In the present work, the kink free vicinal Ge(100) surface with a small miscut angle has been simulated by a cluster having (2x1) and (1x2) dimerized domains separated by kink free S_A type step.

This thesis is organized as follows: In chapter II, the calculation method used in this work is explained and formulated, in chapter III, the stepped Ge(100) surface is modeled by a cluster, in Chapters IV and V the dissociation paths of AsH_3 and B_2H_6 on stepped Ge(100) surfaces are examined, and finally conclusion of the whole present works is outlined in chapter VI.

CHAPTER 2

HARTREE-FOCK THEORY

2.1 Introduction

In the present work, the total energy of the cluster models involving the decomposition steps of AsH_3 and BH_3 molecules on stepped Ge(100) surface has been calculated by Hartree-Fock theory. Since the present cluster models consist of many interacting atoms (Ge, H, As (or B)) with many interacting electrons the present calculations deal with the solution of many body problem defined in Quantum mechanics.

The many-body problem is a general name for a vast category of physical problems pertaining to the properties of microscopic systems made of a large number of interacting particles. Microscopic here implies that quantum mechanics has to be used to provide an accurate description of the system. In such a quantum system, the repeated interactions between particles create quantum correlations, or entanglement. As a consequence, the wave function of the system is a complicated object holding a large amount of information, which usually makes exact and/or analytical calculations impractical. Thus, many-body theoretical physics most often relies on a set of approximations specific to the problem at hand, and ranks among the most computationally intensive fields of science. Since the present cluster models have limited the number of atoms, the present many body problem has been defined for a molecular system.

2.2 The Schrödinger Equation

In quantum mechanics, the Schrödinger equation describes the wavefunction of a particle:

$$\{-\frac{h^2}{8\pi^2 m}\nabla^2 + V\}\Psi(\vec{r},t) = \frac{ih}{2\pi}\frac{\partial\Psi(\vec{r},t)}{\partial t} \tag{2.1}$$

In this equation, $\Psi(r,t)$ is the wave function, m is the mass of the particle, h is Planck's constant, and V is the potential field in which the particle is moving. The energy of the particle can be obtained by solving the Eq. 2.1 for Ψ, subject to the appropriate boundary conditions. If V is not a function of time, the Schrödinger equation can be simplified by separation of variables mathematical technique. In this technique the wave function is written as the product of a spatial function and a time function:

$$\Psi(\vec{r},t) = \psi(\vec{r})\tau(t) \tag{2.2}$$

The substitution of these new functions into Eq. 2.1 gives two equations, one of which depends only the position of the particle and the other of which is a function of time only. Since the potential field, $V(\vec{r})$, is considered to be time independent, the problem is entirely the solution of the time independent Schrödinger equation:

$$H\psi(\vec{r}) = E\psi(\vec{r}) \tag{2.3}$$

Where E is the energy of the particle, and H is the Hamiltonian operator, equal to:

$$H = \frac{-h^2}{8\pi^2 m}\nabla^2 + V(\vec{r}) \tag{2.4}$$

Eq. (2.3) is an eigen value equation, eigen values are the energies corresponding to the different stationary states of the particle.

2.3 The molecular Hamiltonian

The Schrödinger equation for a collection of particles like a molecule is very similar with the Schrödinger equation written for a particle (Eq. (2.1)):

$$H_{mol}\Psi(\vec{r},t) = E\Psi(\vec{r},t) \tag{2.5}$$

In this case, $\Psi(\vec{r},t)$ would be a function of the coordinates of all the particles in the system as well as time. Therefore the spatial function, in time independent Schrödinger equation (Eq. 2.3), is a function of the positions of the electrons, $\vec{r}$, and the nuclei, $\vec{R}$, within the molecule. The position of a particular electron or nucleus is described below by $\vec{r}_i$ or $\vec{R}_A$, respectively. The molecular Hamiltonian, H_{mol}, is made up of kinetic and potential energy:

$$H_{mol} = T + V \tag{2.6}$$

The kinetic energy operator (T) is a summation of ∇^2 over all the particles in the molecule:

$$T = -\frac{h^2}{8\pi^2}\sum_k \frac{1}{m_k}\left(\frac{\partial^2}{\partial x_k{}^2} + \frac{\partial^2}{\partial y_k{}^2} + \frac{\partial^2}{\partial z_k{}^2}\right) \tag{2.7}$$

or

$$T = -\frac{h^2}{8\pi^2}\sum_k \frac{1}{m_k}\nabla_k{}^2(x,y,z) \tag{2.8}$$

The potential energy component is the Coulomb repulsion between each pair of charged entities:

$$V = \frac{1}{4\pi\pi_o}\sum_j \sum_{k<j} \frac{e_j e_k}{\Delta\vec{r}_{jk}} \tag{2.9}$$

where $\Delta\vec{r}_{jk}$ is the distance between the two particles, and e_j and e_k are the charges on particles j and k, respectively. For an electron, the charge is –e, for a nucleus the charge is Ze, where Z is the atomic number for that atom. Thus for a molecule with

N electrons and M nuclei, the H_{mol} is written explicitly in atomic unit of length ($a_o = \frac{h^2}{4\pi^2 m_e e^2}$):

$$H_{mol} = -\frac{1}{2}\sum_{i=1}^{N}\nabla_i^2 - \sum_{A=1}^{M}\frac{1}{2M_A}\nabla_A^2 - \sum_{i=1}^{N}\sum_{A=1}^{M}\frac{Z_A}{\Delta\vec{r}_{iA}} + \sum_{i=1}^{N}\sum_{j>i}^{N}\frac{1}{\Delta\vec{r}_{ij}} + \sum_{A=1}^{M}\sum_{B>A}^{M}\frac{Z_A Z_B}{\Delta\vec{R}_{AB}} \qquad (2.10)$$

Here, M_A is the ratio of the mass of the nucleus A to the mass of an electron and Z_A is the atomic number of nucleus A. The Laplacian operators, ∇_i^2 and ∇_A^2 involve the differentiation with respect to the coordinates of the ith electrons and A^{th} nucleus. The first and second terms in Eq. (2.10) are the total kinetic energies of the electrons and nuclei. The fourth and fifth terms of Eq. (2.10) define the total electron-electron and nuclei-nuclei repulsion interactions. The third term in the same equation defines the Coulomb attraction between the electrons and nuclei. The above Hamiltonian (Eq. (2.10) gives the energies in Hartrees and the lengths in Bohrs.

An exact solution to the Schrödinger equation (Eq. (2.5)) is not possible for any molecular systems. However, a number of simplifying assumptions and procedures make an approximate solution possible for a large of molecules like in the present work. Since there are no known solutions for many-electron systems, the problem is solved numerically. One of the numerical solution methods to Schrödinger equation is provided by Hartree-Fock theory. The Hartree-fock theory is formulated below using the Refs. [53-56].

2.4. The Hartree-Fock Theory

The Hartree–Fock method is typically used to solve the time-independent Schrödinger equation for a multi-electron atom or molecule. In Hartree–Fock approximation, the equations are solved using a nonlinear method such as iteration, which gives rise to the name “self-consistent field method”. The Hartree–Fock method makes five major simplifications in order to deal with the solution of the Schrödinger equation (Eq. (2.5)):

- The Born-Oppenheimer approximation is inherently assumed. The full molecular wave function is actually a function of the coordinates of each of the nuclei, in addition to those of the electrons.
- The relativistic effects are completely neglected.
- Each energy eigen function is assumed to be describable by a single Slater determinant, an antisymmetrized product of one-electron wave functions (i.e., orbitals).
- The variational solution is assumed to be a linear combination of a finite number of basis functions which are chosen to be orthogonal.
- The mean field approximation is implied. Effects arising from deviations from this assumption, known as electron correlation, are completely neglected for the electrons of opposite spin, but are taken into account for electrons of parallel spin.

2.4.1 Born-Oppenheimer Approximation

Born-Oppenheimer (BO) Approximation is the first of several approximations used to simplify the solution of the Schrödinger equation. It is based on the observation, that the electrons are much lighter particles than the nuclei. The electron-nucleus mass ration M/m_e amounts to 1836 for a proton and to order of 10^4 for typical elements such as carbon or silicon. Due to their smaller mass electrons bound in the potential of the nuclei move more rapidly than the heavy nuclei themselves and on the average follow their motion. Therefore the electron distribution within a molecular system depends on only the positions of the nuclei and not on their velocities. In BO approximation the molecular wave function, $\psi \equiv \psi(r, R)$, is written as a product of a nuclear and electronic wave function:

$$\psi(\vec{r}, \vec{R}) = \Phi_{elec}(\vec{r}, \vec{R})\Phi_{nuc}(\vec{R}) \tag{2.11}$$

The molecular wave function for a particular electron position r_i and nuclear position R_A is

$$\psi(\vec{r}_i, \vec{R}_A) = \Phi_{elec}(\vec{r}_i, \vec{R}_A)\Phi_{nuc}(\vec{R}_A) \tag{2.12}$$

The above definition of the molecular wave function in BO approximation separates the nuclear and electronic motions, and consequently allows the two parts of the problem to be solved independently. In the first part of the BO approximation the electronic Schrödinger equation is solved, yielding the wave function, $\Phi_{elec}(\vec{r},\vec{R})$, depending on electrons only. During this solution the nuclei are fixed in a certain configuration, very often the equilibrium configuration. Since nuclei are much heavier and move more slowly than electrons, in the electronic Hamiltonian the kinetic energies of the nuclei are neglected and repulsion between the nuclei is considered to be constant:

$$H_{elec} = -\frac{1}{2}\sum_{i=1}^{N}\nabla_i^2 - \sum_{i=1}^{N}\sum_{A=1}^{M}\frac{Z_A}{\Delta\vec{r}_{iA}} + \sum_{i=1}^{N}\sum_{j>i}^{N}\frac{1}{\Delta\vec{r}_{ij}} + \sum_{A=1}^{M}\sum_{B>A}^{M}\frac{Z_A Z_B}{\Delta\vec{R}_{AB}} \tag{2.13}$$

This Hamiltonian is then used in the Schrödinger equation describing the motion of the electrons in the field of fixed nuclei:

$$H_{elec}\Phi_{elec}(\vec{r},\vec{R}) = E_{elec}(\vec{R})\Phi_{elec}(\vec{r},\vec{R}) \tag{2.14}$$

The solution function, $\Phi_{elec}(\vec{r},\vec{R})$, in Eq. (2.14) is antisymmetric and required to be normalized. The E_{elec} resulted from Eq. (2.14) is nuclear coordinate functional and describes the potential energy surface for the molecular system.

Accordingly, in the second part of the BO approximation, E_{elec} is also used as the effective potential for the nuclear Hamiltonian:

$$H_{nuc} = T_{nuc}(\vec{R}) + E_{elec}(\vec{R}) \tag{2.15}$$

or

$$H_{nuc} = -\sum_{A=1}^{M}\frac{1}{2M_A}\nabla_A^2 + E_{elec}(\vec{R}) \tag{2.16}$$

This Hamiltonian is used in the Schrodinger equation for nuclear motion:

$$H_{nuc}\Phi_{nuc}(\vec{R}) = E\Phi_{nuc}(\vec{R}) \tag{2.17}$$

describing the vibrational, rotational, and translational states of the nuclei.

In the present work, the total energy values of the considered cluster models are resulted from the eq. (2.14) for fixed optimized coordinates of Ge, H, and the corresponding dopant atoms.

2.4.2 Molecular Orbitals

According to the third assumption considered in Hartree-Fock theory the electronic wave function $\Phi_{elec}(\vec{r})$ in Eq. (2.14), (for fixed nuclei configuration), is Hartree product of molecular orbitals:

$$\Phi_{elec}(\vec{r}_1, \vec{r}_2, ..., \vec{r}_N) = \varphi_1(\vec{r}_1)\varphi_2(\vec{r}_2).....\varphi_N(\vec{r}_N) \tag{2.18}$$

However, such a function is not satisfactory for fermions, such as electrons, because the wave function is not antisymmetric. For the two- particle case, an antisymmetric wave function can be mathematically described as follows:

$$\Phi_{elec}(\vec{r}_1, \vec{r}_2) = -\varphi_2(\vec{r}_2)\varphi_1(\vec{r}_1) \quad \text{for} \quad \Phi_{elec}(\vec{r}_1, \vec{r}_2) = \varphi_1(\vec{r}_1)\varphi_2(\vec{r}_2) \tag{2.19}$$

Since the interchanging two of the $\vec{r}_i$'s does not change the sign of the Eq. (2.18), the wave function is not antisymmetric. Therefore the Hartree product does not satisfy the Pauli principle. This problem can be overcome by taking a linear combination of all Hartree products.

The antisymmetric wave function for the two-particle case can be written as the linear combination of both Hartree producs:

$$\Phi_{elec}(\vec{r}_1, \vec{r}_2) = \frac{1}{\sqrt{2}}\{\varphi_1(\vec{r}_1)\varphi_2(\vec{r}_2) - \varphi_1(\vec{r}_2)\varphi_2(\vec{r}_1)\} \tag{2.20}$$

or in the Slater determinant expression

$$\Phi_{elec}(\vec{r}_1, \vec{r}_2) = \frac{1}{\sqrt{2}}\begin{vmatrix} \varphi_1(\vec{r}_1) & \varphi_2(\vec{r}_1) \\ \varphi_1(\vec{r}_2) & \varphi_1(\vec{r}_2) \end{vmatrix} \tag{2.21}$$

where the coefficient, $\frac{1}{\sqrt{2}}$, is the normalization factor. This wave function is antisymmetric and no longer distinguishes between fermions. Moreover, it also goes to zero if any two wave functions or two fermions are the same. This is equivalent to satisfying the Pauli Exclusion Principle.

The Slater determinant for the two-particle case is:

$$\Phi_{elec}(\vec{r}_1, \vec{r}_2) = \frac{1}{\sqrt{2}} \begin{vmatrix} \varphi_1(\vec{r}_1)\alpha(1)\varphi_1(\vec{r}_1)\beta(1) & \varphi_2(\vec{r}_1)\alpha(1)\varphi_2(\vec{r}_1)\beta(1) \\ \varphi_1(\vec{r}_2)\alpha(2)\varphi_1(\vec{r}_2)\beta(2) & \varphi_2(\vec{r}_2)\alpha(2)\varphi_2(\vec{r}_2)\beta(2) \end{vmatrix} \tag{2.22}$$

when the electron spin is taken into account. Here, two spin functions are defined as follows:

$$\alpha(\uparrow) = 1 \quad \text{spin up}, \quad \alpha(\downarrow) = 0 \quad \text{spin down}$$

$$\beta(\uparrow) = 0 \quad \text{spin down}, \quad \beta(\downarrow) = 1 \quad \text{spin up} \tag{2.23}$$

Therefore $\alpha(1)$ is the value of α for electron 1. The product of the molecular orbital, $\varphi(\vec{r}_i)$ and a spin function α (or β) is defined as a spin orbital, a function of both the electron's location and its spin.

2.4.3 Slater determinant for a molecular system

The expression of the antisymmetric wave function (Eq. 2.21) can be generalized to n number of electrons by writing it as a Slater determinant. For an n-electron system, a closed shell wave function can be built particularly by defining n/2 molecular orbitals:

$$\Phi_{elec}=\frac{1}{\sqrt{N!}}\begin{vmatrix} \varphi_1(\vec{r}_1)\alpha(1) & \varphi_1(\vec{r}_1)\beta(1) & \varphi_2(\vec{r}_1)\alpha(1) & \varphi_2(\vec{r}_1)\beta(1)\ldots. & \varphi_{\frac{n}{2}}(\vec{r}_1)\alpha(1) & \varphi_{\frac{n}{2}}(\vec{r}_1)\beta(1) \\ \varphi_1(\vec{r}_2)\alpha(2) & \varphi_1(\vec{r}_2)\beta(2) & \varphi_2(\vec{r}_2)\alpha(2) & \varphi_2(\vec{r}_2)\beta(2)\ldots. & \varphi_{\frac{n}{2}}(\vec{r}_2)\alpha(2) & \varphi_{\frac{n}{2}}(\vec{r}_2)\beta(2) \\ \vdots & \vdots & \vdots & \vdots & \vdots & \vdots \\ \varphi_1(\vec{r}_i)\alpha(i) & \varphi_1(\vec{r}_i)\beta(i) & \varphi_2(\vec{r}_i)\alpha(i) & \varphi_2(\vec{r}_i)\beta(i)\ldots. & \varphi_{\frac{n}{2}}(\vec{r}_i)\alpha(i) & \varphi_{\frac{n}{2}}(r_i)\beta(i) \\ \varphi_1(\vec{r}_j)\alpha(j) & \varphi_1(\vec{r}_j)\beta(j) & \varphi_2(\vec{r}_j)\alpha(j) & \varphi_2(\vec{r}_j)\beta(j)\ldots. & \varphi_{\frac{n}{2}}(\vec{r}_j)\alpha(j) & \varphi_{\frac{n}{2}}(\vec{r}_j)\beta(j) \\ \vdots & \vdots & \vdots & \vdots & \vdots & \vdots \\ \varphi_1(\vec{r}_n)\alpha(n) & \varphi_1(\vec{r}_n)\beta(n) & \varphi_2(\vec{r}_n)\alpha(n) & \varphi_2(\vec{r}_n)\beta(n) & \varphi_{\frac{n}{2}}(\vec{r}_n)\alpha(n) & \varphi_{\frac{n}{2}}(\vec{r}_n)\beta(n) \end{vmatrix} \tag{2.24}$$

Here, the electrons are assigned to these orbitals in pairs of opposite spin.

2.4.4 Basis sets

The fourth assumption given for Hartree-fock theory involves expressing the molecular orbitals as linear combinations of a pre-defined set of one electron functions known as basis functions. Here any set of appropriately defined functions may be used. An individual molecular orbital is defined as:

$$\varphi_i = \sum_{\mu=1}^{N} C_{\mu i}\chi_\mu \tag{2.25}$$

where the coefficients $C_{\mu i}$ are known as the molecular orbital expansion coefficients. The normalized $\chi_1\chi_2.....\chi_N$ are the basis functions. Larger number of well chosen wave functions yields more accurate approximations to the molecular orbitals. In the present work Gaussian –type atomic functions ($e^{-\alpha r^2}$) provided by Gauss03 package [57] are used as basis functions.

2.4.5 The variational principle

The problem has now become how to solve Eq. 2.14 for the set of molecular orbital expansion coefficients, $C_{\mu i}$. Hartree-Fock theory takes advantage of the variational

principle, which says that "the expectation value of the known Hamiltonian for any normalized wave function must be greater than the actual ground state energy corresponds to the exact wave function of the system". In the present molecular hamiltonian (Eq. (2.14)), the energy $E_{elec}(\vec{R})$ corresponds to the exact wave function, $\Phi_{elec}(\vec{r},\vec{R})$. According to the variational principle since the ground state antisymmetric normalized wave function of the electronic coordinates are defined to be the linear combinations of any set of appropriate basis functions (Eq. (2.25)), the solution of the Eq. 2.14, which we will denote it $\Xi_{elec}(r,R)$, gives the expectation value of the energy greater than the energy for the exact wave function, Φ_{elec} :

$$E_{var} = \frac{<\Xi(\vec{r},\vec{R})|H_{mol}|\Xi(\vec{r},\vec{R})>}{<\Xi(\vec{r},\vec{R}|\Xi(\vec{r},\vec{R})>} \tag{2.26}$$

and

$$E_{var}\Xi_{elec}(\vec{r},\vec{R}) > E_{elec}\Phi_{elec}(\vec{r},\vec{R}) \tag{2.27}$$

Thus the problem solving the Eq. 2.14 becomes one of finding the set of coefficients, $C_{\mu i}$, that minimize the energy of the resultant wave function $\Xi_{elec}(r,R)$:

$$\frac{\partial E_{var}}{\partial \Xi_i(\vec{r}_i,\vec{R})} = 0 \qquad \text{or} \qquad \frac{\partial E_{var}}{\partial \varphi_i(\vec{r}_i,\vec{R})} = 0 \tag{2.28}$$

with the fourth assumption of the Hartree –Fock theory ($\int\int \varphi_i^* \varphi_j d\vec{r}_i d\vec{r}_j = \delta_{ij}$).

2.4.6 The Roothaan-Hall Equations

The equations (2.26) and (2.28) yield the Fock equation:

$$\hat{F}\varphi_i = \varepsilon_i \varphi_i \tag{2.29}$$

in which the Fock operator, $\hat{F}$, is an effective one electron Hamiltonian for an orbital φ. Therefore Fock operator involves one electron integrals of kinetic and nuclear-electron attraction operators:

$$-\frac{1}{2}\nabla_i^2(\vec{r}_i) - \sum_{A=1}^{M}\frac{Z_A}{\Delta\vec{r}_{iA}} \tag{2.30}$$

and two electron integrals of $\frac{1}{\vec{r}_{ij}}$: $\hat{J} - \hat{K}$, for which

$$\hat{J}\varphi_i = \left\{\sum_{j=1}^{N}\int\varphi_j(\vec{r}_j)\frac{1}{\vec{r}_{ij}}\varphi_j(\vec{r}_j)d\vec{r}_j\right\}\varphi_i(\vec{r}_i) \tag{2.31}$$

and

$$\hat{K}\varphi_i = \left\{\sum_{j=1}^{N}\int\int\varphi_j(r_j)\frac{1}{\vec{r}_{ij}}\varphi_i(\vec{r}_i)d\vec{r}_i d\vec{r}_j\right\}\varphi_j(\vec{r}_j) \tag{2.32}$$

In Eq. (2.29) ε_i is the orbital energy. Therefore, finding a many electron wave function is reduced to finding a series of one electron orbitals in Eq. (2.29).

The basis set expansion of the wave function used in Eq. (2.29) leads to the following equations describing the molecular expansion coefficients, $C_{\nu i}$ derived by Roothaan and by Hall [58-59]:

$$\sum_{\nu=1}^{N}(F_{\mu\nu} - \varepsilon_i S_{\mu\nu})C_{\nu i} = \vec{0} \qquad \mu = 1,2,.....,N \tag{2.33}$$

Or

$$FC_i = \varepsilon_i SC_i \tag{2.34}$$

Here, each element in Eq. (2.34) is a matrix. ε is a diagonal matrix of orbital energies. Each term of ε_i is the one-electron orbital energy of molecular orbital χ_i.

The matrix C in Eq. (2.34) shows a column vector of molecular orbital coefficients. The matrix S indicates the overlap between the orbitals:

$$S_{\mu\nu} = \int\chi_\mu^*(\vec{r}_i)\chi_\nu(\vec{r}_i)d\vec{r}_i \tag{2.35}$$

In Eq. (2.34) F is called the Fock matrix, and it represents the average effects of the field of all the electrons on each orbital:

$$F_{\mu\nu} = \int\chi_\mu^*(\vec{r}_i)\hat{F}\chi_\nu(\vec{r}_i)d\vec{r}_i \tag{2.36}$$

or

$$F_{\mu\nu} = \int \chi_\mu^*(\vec{r}_i)(-\frac{1}{2}\nabla_i^2(\vec{r}_i) - \sum_{A=1}^{M} \frac{Z_A}{\Delta\vec{r}_{iA}})\chi_\nu(\vec{r}_i)d\vec{r}_i + \sum_{j=1}^{N}\int\int \chi_\mu^*(\vec{r}_i)\chi_\mu(\vec{r}_i)(\frac{1}{\vec{r}_{ij}})\chi_\nu^*(\vec{r}_j)\chi_\nu(\vec{r}_j)d\vec{r}_i d\vec{r}_j$$

$$-\sum_{j=1}^{N}\int\int \chi_\mu^*(\vec{r}_i)\chi_\nu(\vec{r}_j)(\frac{1}{\vec{r}_{ij}})\chi_\nu^*(\vec{r}_i)\chi_\mu(\vec{r}_j)d\vec{r}_i d\vec{r}_j \qquad (2.37)$$

In the above equation, the first term (H_{ii}) involves one electron integrals of kinetic and nuclear-electron attraction operators, the second and third terms (J_{ij} and K_{ij}) define the Coulomb and exchange integrals, respectively. The diagonalization of the Fock matrix gives the energies correspond to the molecular orbitals. The energy of the of the ith electron can be written as:

$$\varepsilon_i = H_{ii} + \sum_{j=1}^{N}(J_{ij} - K_{ij}) \qquad (2.38)$$

2.4.7 Solving the Roothaan-Hall Equations

Since the the Roothaan-Hall Equations ((Eq. (2.33 or 2.34)) are not linear they must be solved iteratively. The procedure is called the Self-Consistent Field (SCF) method. At convergence, the energy is at a minimum, and the orbitals generate a field which produces the same orbitals. The solution produces a set of orbitals (φ_i), both occupied and unoccupied. The total number of orbitals is equal to the number of basis functions used. Under Hartree-Fock treatment, each electron sees all of the other electrons as an average distributions, there is no instantaneous electron-electron interaction included. The solution steps of the Roothaan-Hall Equations are outlined below:

1. choose a basis set (χ_μ)
2. calculate all the one ($H_{\mu\nu}$) and two electron integrals ($J_{\mu\nu}$ and $K_{\mu\nu}$)
3. obtain an initial guess for all the molecular orbital coefficients C_i
4. use the current C_i construct a new Fock matrix (F)
5. solve $FC_i = \varepsilon_i SC_i$ for a new set of C_i

6. if the new C_i are different from the old C_i, go back to step 4.

2.4.8 Hartree–Fock algorithm

In the self consistent field calculations of Hartree–Fock theory, the solution steps (1-6) are fallowed in iteration method. Iteration in computing is the repetition of a process within a computer program. The algorithmic flowchart illustrating the SCF iteration of Hartree –Fock method within Gauss03 [57] program is simply given in Fig 2.1.

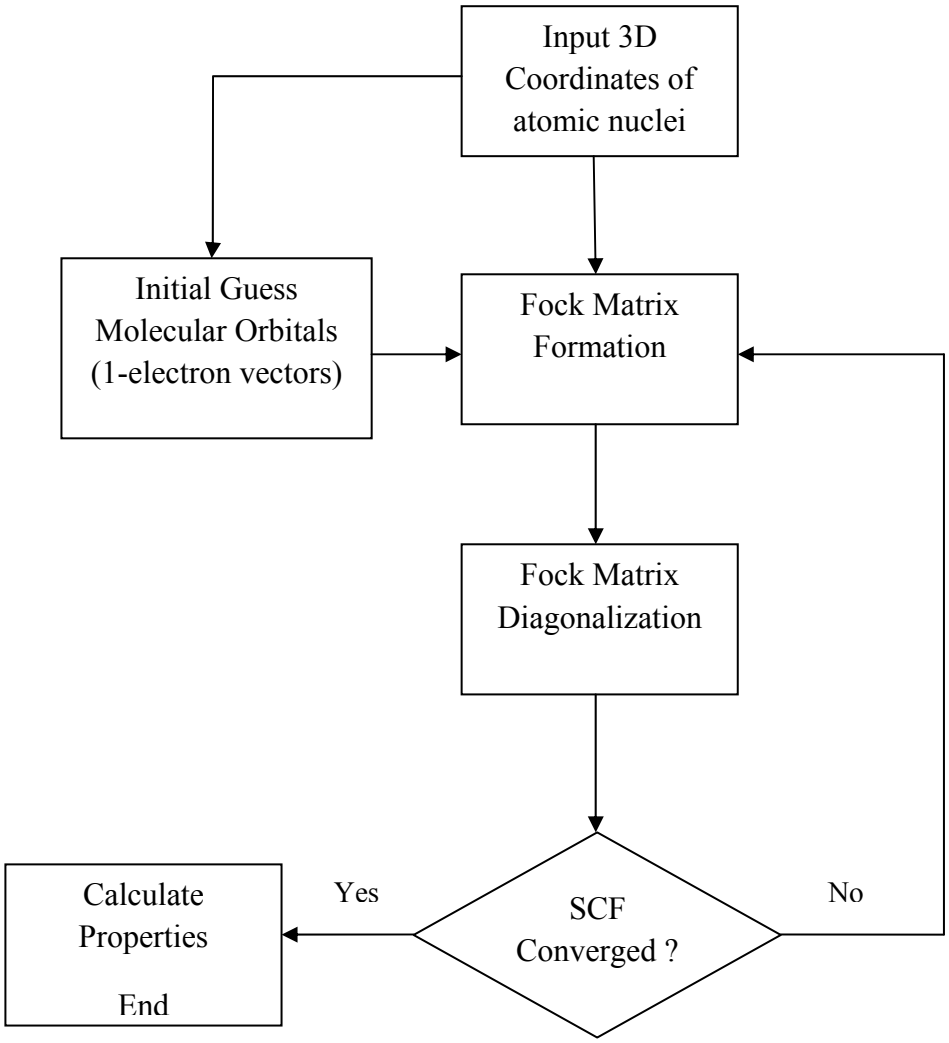

FIG. 2.1. The algorithmic flowchart illustration of the SCF iteration of Hartree – Fock method within Gauss03 program.

At the last step of the algorithm, the ground state molecular orbital energies are obtained for the occupied and unoccupied molecular states. The energy of the highest occupied molecular orbital (HOMO) and the energy of the least unoccupied molecular orbital (LUMO) are important reference energy levels to find out the energy of the impurity states defined for a doped host molecule. Furthermore the calculated molecular orbital energies obtained at the last step of the Hartree-Fock algorithm can be used to calculate the total energy of the molecular structure:

$$E_{tot} = \sum_{i=1}^{N} \varepsilon_i + \sum_{A=1}^{M} \sum_{B>A}^{M} \frac{Z_A Z_B}{R_{AB}} \tag{2.39}$$

The repetition of the above self consistent iteration cycle for different positions of the atoms provides the lowest energy corresponding to the optimized geometry of the system. All the calculations outlined in this chapter are provided by Gauss03 package [57].

CHAPTER 3

STEPPED Ge(100) SURFACE

3.1 Introduction

The bulk Ge crystallizes in diamond structure. The diamond structure consists of two interpenetrated fcc structures. The second fcc is displaced with respect to the first one along the main diagonal of the cubic structure by a distance of $\frac{a\sqrt{3}}{4}$. Here, a is the lattice constant with the value of 5.658 A^0 [60] for Ge. The conventional unit cell of the Ge bulk structure is pictured in Fig. 3.1. There are two Ge atoms in the unit cell located at (0,0,0) and (a/4, a/4, a/4). The electron configuration of Ge is $1s^2 2s^2 2p^6 3s^2 3p^6 3d^{10} 4s^2 4p^2$. The four valence electrons on 4s and 4p orbitals are responsible to form four covalent bonds around each Ge atom. Therefore, each Ge atom is surrounded by four nearest neighbor atoms in $\frac{a\sqrt{3}}{4}$ distance. The Ge bulk structure sliced along $\langle 100 \rangle$ directions gives Ge(100) surfaces. The unreconstructed Ge(100) surface consists of unit cells with an area of $\frac{a\sqrt{2}}{2} \times \frac{a\sqrt{2}}{2}$ in (1x1) dimension. There is one Ge atom in each unit cell with two uncompensated (dangling) bonds. While the two dangling bonds are extending outside of the surface, the other two bonds bond the surface Ge atoms to the next layer of the Ge(100) (1x1) surface. The top view of the Ge(100) (1x1) surface is pictured in Fig. 3.2(a) for two sublayers. In Fig. 3.2(a), the open and closed circles define the position of the first and second sublayer Ge atoms, respectively.

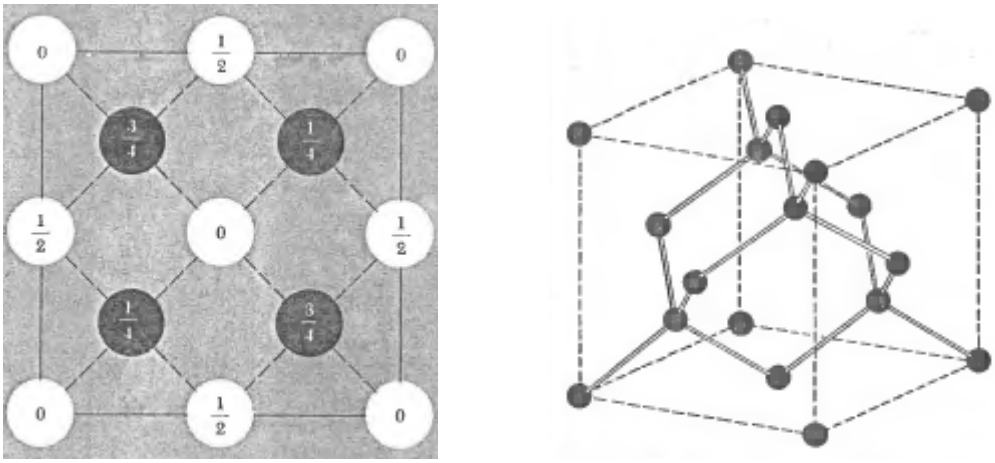

(a) **(b)**

FIG. 3.1. The top (a) and side (b) view of the conventional unit cell of the Ge bulk structure [60].

The studies in the past have clearly showed that Ge(100) surface has both strong short range and energetically weaker moderate-range reconstructions as well as Si(100). At room temperature, the short range interaction forces the nearest neighbor atoms on Ge(100) (1x1) surface to form rows of dimers in a new Ge(100) (2x1) structure. As it is mentioned in the first chapter, the reconstruction reduces the surface energy by eliminating half of Ge's dangling bonds. The necessary energy in reconstruction was reported to be quite strong (≥ 1 eV) [41]. The rows of dimers with (2x1) periodicity were observed clearly on Ge(100) surface by LEED [35, 37-38, 41] and STM [33-34, 39-40, 43-44] images. According to the results of these works [33-35, 37-41], one Ge atom is pushed up and the other is pushed down on the same dimer bond, so that the dimer is buckled or asymmetric. Therefore the dimers are tilted along $\langle 110 \rangle$ direction and form dimer row structure on Ge(100) surface. The line up of dimer bonds is associated with the displacement of electron density from buckled down to buckled up atom. The structure of dimer rows on Ge(100) (2x1) surface were also proposed theoretically [48] and the asymmetric dimers being more stable than the symmetric ones was found by total energy calculations. In another theoretical work [61], the energetic stability of asymmetric dimers has been examined by Ising model. Because of the electron displacement from buckled down

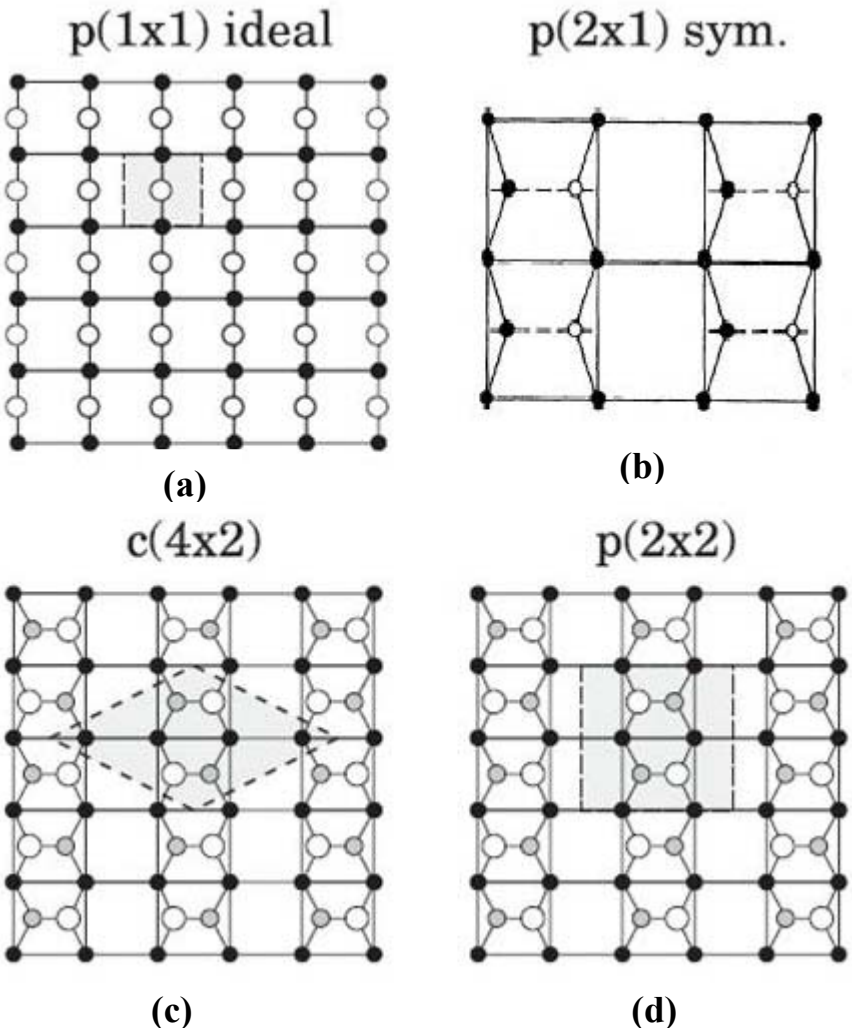

FIG. 3.2. Ge (100) surface with (a) unreconstructed (1x1) unit cell, b) p(2x1) dimer reconstruction, (c) c(4x2) dimer reconstruction, (d) p(2x2) dimer reconstruction.

to buckled up, the asymmetric dimers are treated as interacting spins in this model. Therefore all the spins defined for the structure of asymmetric dimers on Ge(100) (2x1) are totally aligned like in ferromagnetic case. The top view of the Ge(100) (2x1) surface is pictured in Fig. 3.2(b) with two sublayers. In Fig. 3.2(b), the open and closed circles define the position of the first and second sublayer Ge atoms, respectively. The asymmetric dimer bonds on Ge(100) surface make it possible to form other larger surface reconstructions such as p(2x2), c(4x2), p(4x1) [48]. They are energetically weaker moderate-range reconstructions. Among these reconstructions, c(4x2) and p(2x2) were found to be the lowest energy reconstructions with their nearly degenerate energies by ab-initio calculations [61, 62]. According to LEED [41, 63] and STM [34, 64, 65] images, (2x1) structure of

Ge(100) surface changes to c(4x2) and p(2x2) periodicities at temperatures lower than 250 K. In c(4x2) reconstruction, the bonds along the same and different rows are arranged in the order of "zig-zag". Therefore the dimers on the same and different rows are either buckled up or down at every two dimers. In p(2x2) reconstructions, while the asymmetric dimers are in zig-zag type order from one row to other, they are all either in buckled up or down order along the same row. The stability of the asymmetric dimers for c(4x2) and p(2x2) reconstructions was studied within Ising model [36, 61] by treating the dimers as spins like in antiferromagnetic case. The top view of the c(4x2) and p(2x2) reconstructions on Ge(100) surface are pictured in Fig. 3.2(c) and (d). In these figures, the open and shaded circles show the positions of the buckled up and buckled down first layer Ge atoms on the same dimer bonds, respectively. The closed circles in the same figures define the positions of the second layer Ge atoms.

3.2 Stepped Ge(100) surface

As it is introduced in chapter I, atomic steps, kinks or missing dimer type defects can be formed on the crystal surfaces during the growth process. Since the step edges are more attractive to initiate the adsorption, chemical reactions and catalysis, the investigations in the literature have been usually focused on defected crystal surfaces having single or double atomic steps. According to the outline introduced in chapter I, vicinal Ge(100) surface can have single (S_A or S_B) or double (D_A or D_B) atomic steps when the miscut angle is less or greater than ~6°, respectively [31-36, 38, 43-44]. For both types of step structures, the step edge is the boundary between the upper and lower terraces. Since the rows of dimers on the upper and lower terraces are parallel and perpendicular to the step edge, the upper and lower terraces in S_A type vicinal surface are defined by (2x1) and (1x2) reconstructions. The reconstruction is in (1x2) and (2x1) periods on the upper and lower terraces, respectively, for S_B type steps. However, the reconstruction is same for both terraces, i.e. (2x1) for D_A and (1x2) for D_B type steps. The top view of the steps structures, S_A, S_B, D_A, and D_B are given in Fig. 3.3. In Fig. 3.3, the open big and small circles define the positions of the first layer dimerized Ge atoms on the upper and lower terraces of

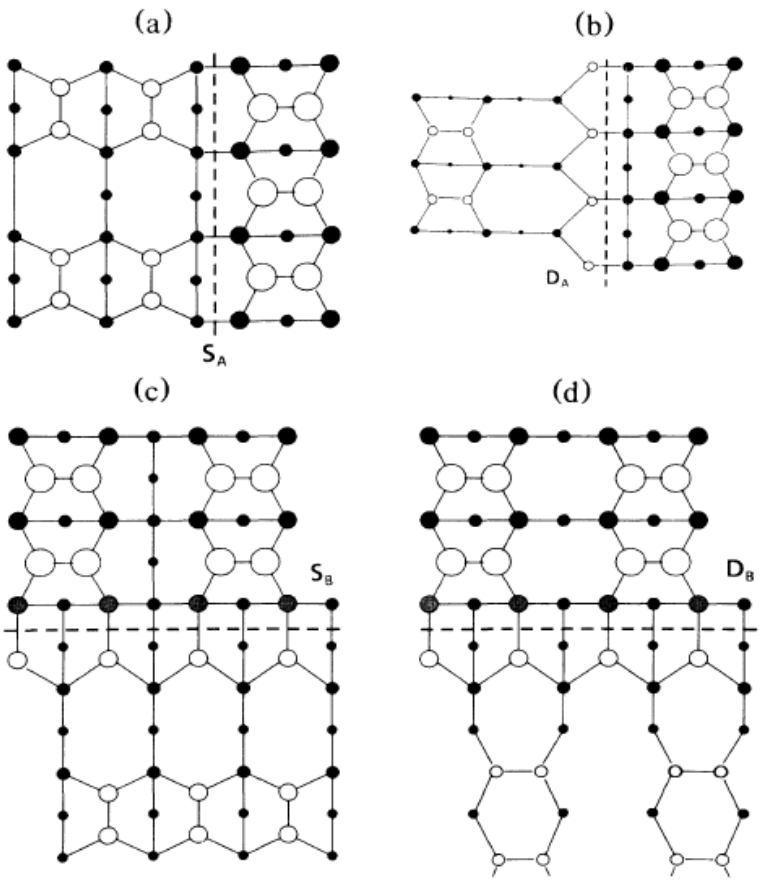

FIG. 3.3. Top views of (a) S_A, (b) D_A, (c) S_B, and (d) D_B steps.

the step models, respectively. In the same figure, the positions of the second and third layer Ge atoms on the upper and lower terraces of the step models are shown by the closed circles having different sizes. Since the aim of this project is to find out only the effect of step on the reaction mechanisms, the vicinal Ge(100) surface is considered to be kinks free. Therefore the present kinks free Ge(100) surface could have either S_A or S_B type steps. In the present work, the vicinal Ge(100) surface is determined to be S_A type instead of S_B. Because S_A type steps have relatively less attractive kinks than S_B [52]. The prototype of the kinks free vicinal Ge(100) surface with S_A type step is modeled by a cluster consists of nine and eight sublayers on the upper and lower terraces, respectively. The (2x1) and (1x2) periods on the upper and lower terraces are formed by three and two dimer rows, respectively in the cluster model. All the dimer bonds in the stepped Ge(100) cluster are asymmetric with a length of 2.54A^o and a tilt angle of ~14°. Because of the compensation of the

dangling bonds at the step edge, the dimer bonds are elongated with respect to the ones on the flat Ge(100)(2x1) surface. Since the present calculations are based on optimized structures, the initial length and tilt angle of the asymmetric dimer bonds on Ge(100) cluster do not need to be determined precisely. The length and tilt angle of the asymmetric dimer bonds on optimized stepped Ge(100) cluster are determined to be 2.50A^{o} and ~4°, respectively. The S_A type stepped Ge(100) cluster with hydrogenated dangling bonds is pictured in Fig. 3.4.

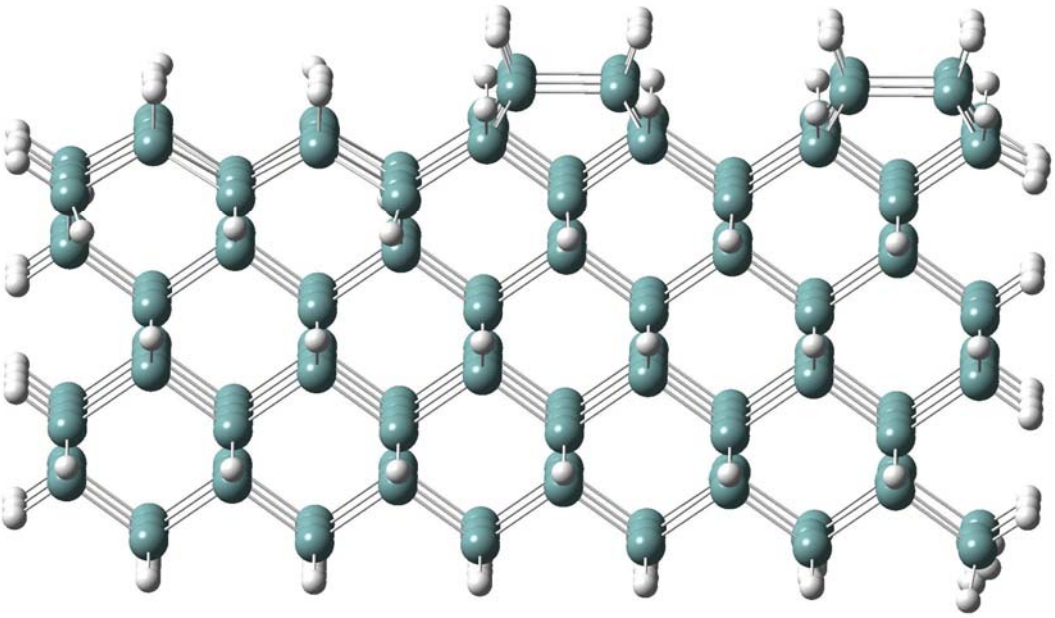

(a)

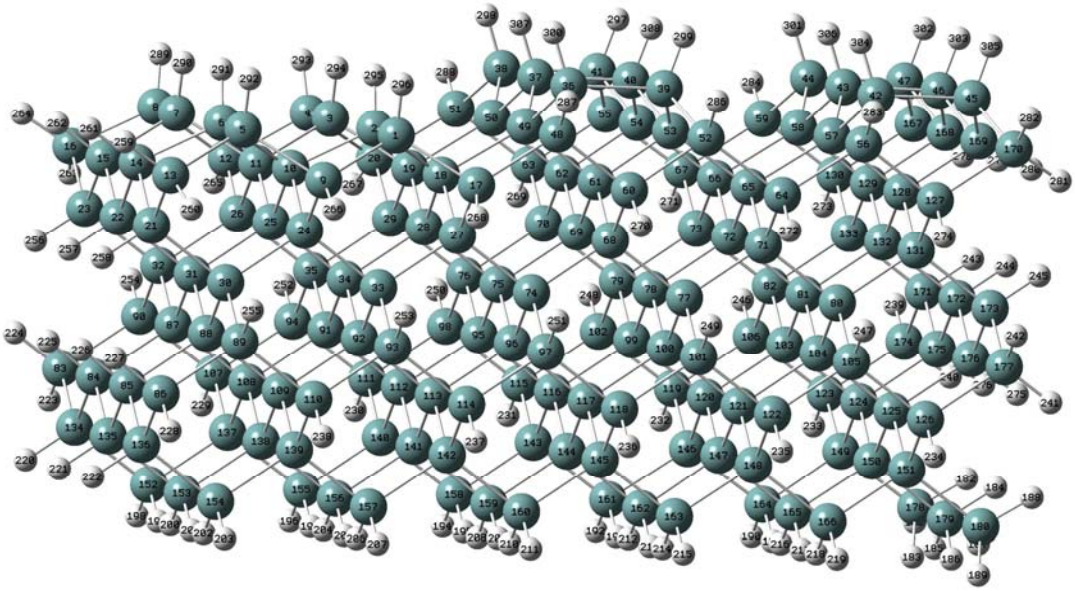

(b)

FIG. 3.4. The side view (a) and the perspective (b) of the S_A type stepped Ge(100) cluster with hydrogenated dangling bonds.

CHAPTER 4

RESULTS:1
STEPPED Ge(100) SURFACE EXPOSED TO ARSİNE GAS

4.1. Introduction

In the present work, the n-type doping process of the Ge sample exposed to arsine gas has been simulated by the possible adsorption and dissociation models of AsH_3 on stepped Ge(100) surface. The total energy and the binding energy have been calculated for the models and AsH_3, AsH_2 , AsH, As, respectively, to find out the initial stages of the doping process of Ge(100) surface by Arsenic atoms.

4.2 Adsorption of AsH_3 on Stepped Ge(100) surface

In the present work, the adsorption of AsH_3 molecule on S_A type stepped Ge(100) surface has been investigated by considering single and double open surface bonds on step-down and step-up terraces. In the first group adsorption models ($MAsH_3$mod1-$MAsH_3$mod8), AsH_3 molecule is adsorbed to the step-down ($MAsH_3$mod1-$MAsH_3$mod4) and step-up ($MAsH_3$mod5-$MAsH_3$mod8) terraces via an open Ge bond taken at the step and close to the step regions. Since the stepped Ge(100) surface has asymmetric dimer bonds, the adsorption of AsH_3 is considered for both buckled-up and buckled-down Ge atoms, separately. The other open bonds of the stepped Ge surface are saturated by H atoms. The adsorption input models of AsH_3 on S_A type stepped Ge surface having single open bond are pictured in Fig. 4.1,

Model	Initial Structure	Optimized Structure
$MAsH_3$mod1	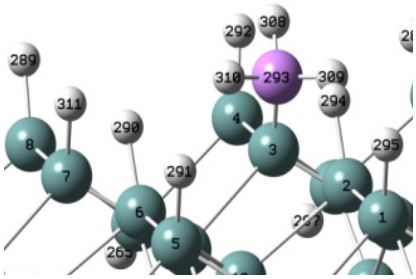	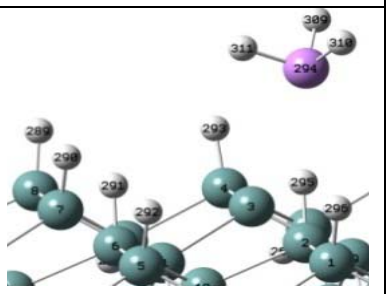
$MAsH_3$mod2	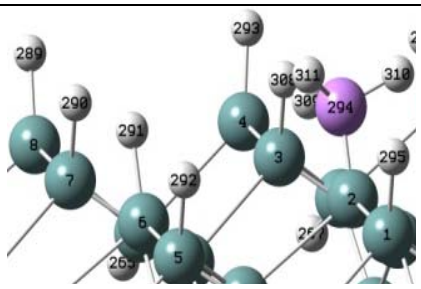	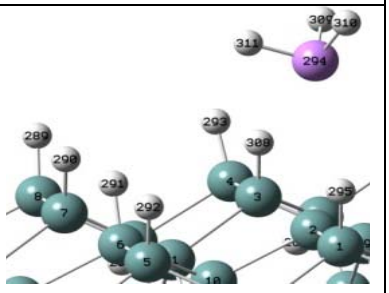
$MAsH_3$mod3	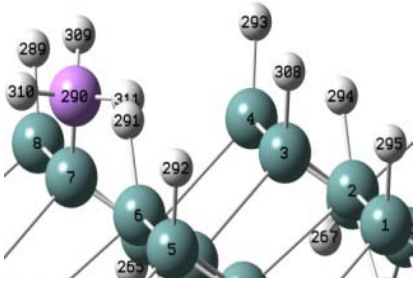	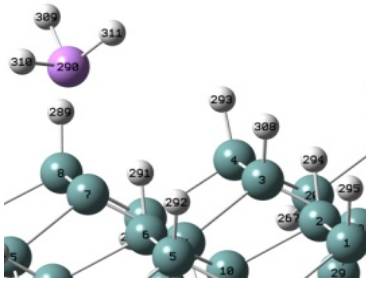
$MAsH_3$mod4	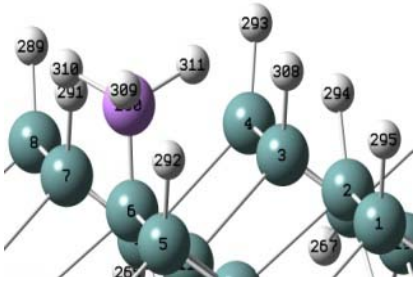	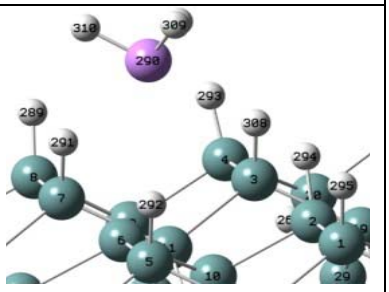
$MAsH_3$mod5	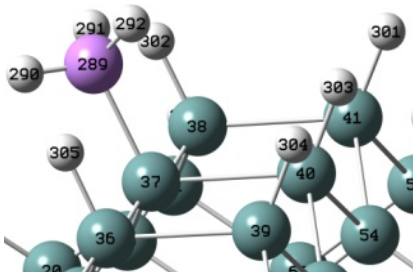	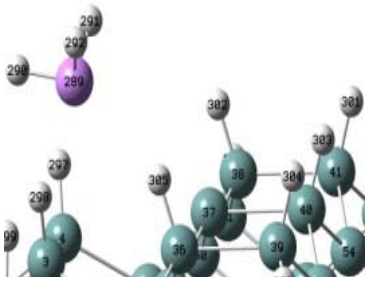

FIG. 4.1. The initial and optimized adsorption models of AsH_3 on stepped Ge(100) surface having single open bond.

Model	Initial Structure	Optimized Structure
$MAsH_3$mod6	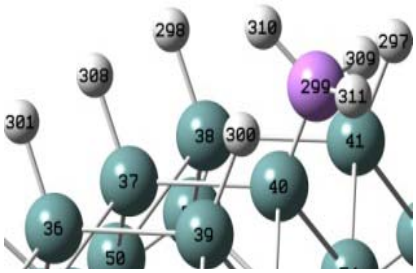	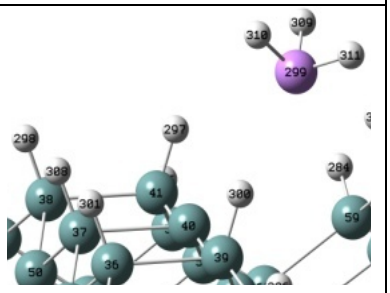
$MAsH_3$mod7	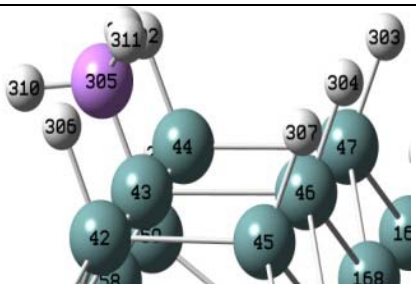	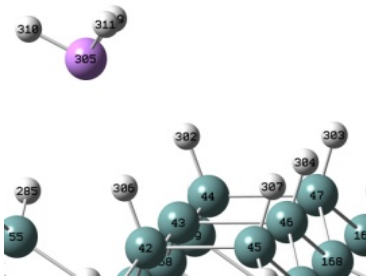
$MAsH_3$mod8	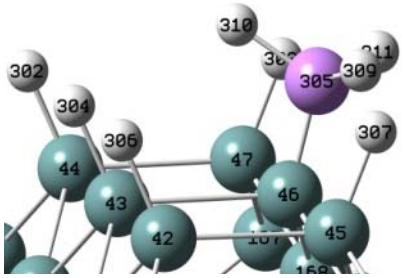	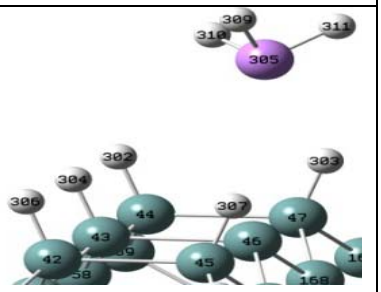

FIG. 4.1. (Cont.)

by the labels of the surface Ge atoms given in Fig. 3.4. As an example, in $MAsH_3$mod1 structure, AsH_3 molecule is adsorbed to buckled-down side of the dimer bond via third Ge atom when the other surface atoms are totally compensated by H atoms. In the present work, the input geometries of the adsorption models are optimized by minimizing their total energies. The optimized structures of $MAsH_3$mod1 - $MAsH_3$mod8 models are pictured in Fig. 4.1. The total energy of each optimized model is given in Table 4.1. The binding energy of AsH_3 in each optimized adsorption model has been also calculated by Eq. (1.1) and tabulated in Table 4.1. The total energy calculations have shown that, the most probable adsorption model is $MAsH_3$mod2 in which AsH_3 is initially adsorbed to the buckled

TABLE 4.1. The structural parameters, the total energy, and the binding energy of AsH_3, for the optimized adsorption models of AsH_3 on stepped Ge(100) surface having single open bond.

Model	Bond Length(A^o)			Tilt angle (degree)	Total Energy (a.u.)	Binding Energy (eV)
	Ge-As	As-H	Dimer Ge-Ge			
$MAsH_3$mod1	4.21	1.45	2.45	3.5	-371613.8565	-5.113
$MAsH_3$mod2	4.20	1.45	2.50	0.5	-371613.8571	-5.129
$MAsH_3$mod3	4.26	1.45	2.45	5.8	-371613.8556	-5.102
$MAsH_3$mod4	4.29	1.45	2.49	0.5	-371613.8563	-5.112
$MAsH_3$mod5	4.20	1.45	2.47	1	-371613.8563	-5.105
$MAsH_3$mod6	4.28	1.45	2.47	1	-371613.8562	-5.102
$MAsH_3$mod7	4.36	1.45	2.48	0.9	-371613.8560	-5.099
$MAsH_3$mod8	4.33	1.45	2.48	0.2	-371613.8558	-5.104

up Ge atom at the step region of the step-down terrace. Since the total energies of the stepped Ge(100) surfaces (having single open bond at different sites) have found to be approximately the same (-369402.7350 - (-369402.7355) a.u), the most probable adsorption model ($MAsH_3$mod2) has been also confirmed by the binding energy of AsH_3. The minimum binding energy of AsH_3 is calculated to be -5.129eV for $MAsH_3$mod2 structure. Although the total energies of the models (Table 4.1) are very close to each other, there is a small energy difference of 0.038eV between the step down models ($MAsH_3$mod1-$MAsH_3$mod4) in which AsH_3 is initially adsorbed to the step and closed to the step regions. The energy difference is calculated to be 0.014eV for corresponding models ($MAsH_3$mod5-$MAsH_3$mod8) of the step-up terrace. On the other hand, the total energy of the most probable adsorption model ($MAsH_3$mod2) is found to be ~0.022eV lower than the total energies of the step-up

models. In all adsorption models ($MAsH_3$mod1-$MAsH_3$mod8), AsH_3 molecule has been suspended on the open Ge bond after optimization. In most probable adsorption model ($MAsH_3$mod2), AsH_3 molecule has suspended on the open bond of the second Ge atom with a Ge-As distance of 4.20 A^o. The asymmetric dimer bond structure of the surface is found to be not changed by optimization.

The adsorption of AsH_3 on stepped Ge(100) surface with two open bonds has been defined by unbridged $MAsH_3$mod9-$MAsH_3$mod14 and bridged $BAsH_3$mod1-$BAsH_3$mod5 models. Since the total energies of the adsorption models at the step region are found to be lower than those of the others in the group of $MAsH_3$mod1-$MAsH_3$mod8 models, the two open bonds are considered at the step region for both terraces. The two open surface bonds are either on the same or adjacent dimer bonds. In $MAsH_3$mod9-$MAsH_3$mod14 models, AsH_3 molecule is initially adsorbed to one of the open bond when the other bond is open. The two open bonds considered on the step-down and step-up terraces have also allowed forming bridge adsorption models ($BAsH_3$mod1-$BAsH_3$mod5). In Fig. 4.2, the initial and optimized models correspond to two dangling bonds of the surface are pictured by the labels of Ge atoms given in Fig. 3.4. The total energies of the optimized bridged and optimized unbridged adsorption models have been listed in Table 4.2. The optimized unbridged adsorption models ($MAsH_3$mod9-$MAsH_3$mod14) have expressed two kinds of structures; when the model has two open bonds on the same dimer bond, AsH_3 remains on the initial adsorption bond leaving the other bond as open ($MAsH_3$mod9, $MAsH_3$mod10, $MAsH_3$mod13), but when the two open bonds are on the adjacent dimers, AsH_3 dissociates into AsH_2 and H fragments ($MAsH_3$mod11, $MAsH_3$mod12, $MAsH_3$mod14). Similarly, when the bridged adsorption models are considered on the same dimer bond ($BAsH_3$mod1, $BAsH_3$mod4), AsH_3 breaks the bridge and adsorbs to one of the open bond after optimization. But in the other bridged adsorption models ($BAsH_3$mod2, $BAsH_3$mod3, $BAsH_3$mod5), initially AsH_3 makes a bridge between the adjacent dimers and decomposes to AsH_2 and H fragments spontaneously after optimization. Therefore when the stepped Ge terraces with more

Model	Initial Structure	Optimized Structure
$MAsH_3$mod9	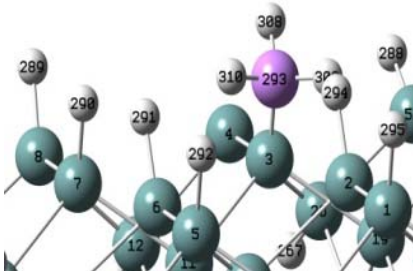	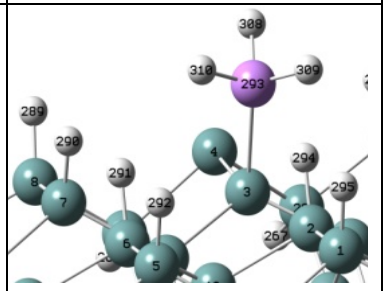
$MAsH_3$mod10	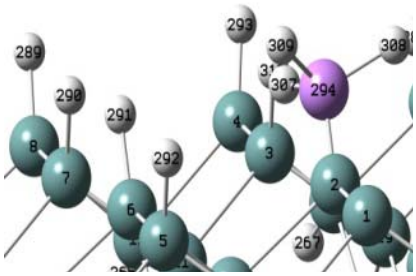	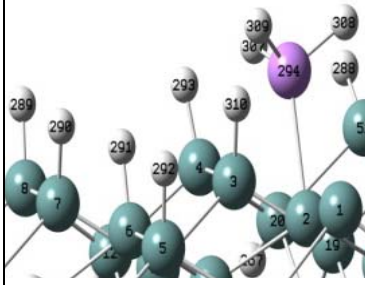
$MAsH_3$mod11	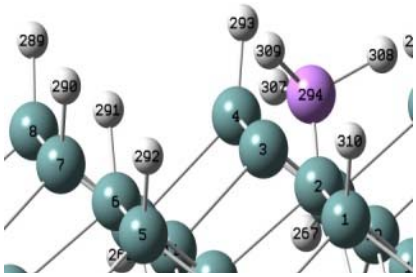	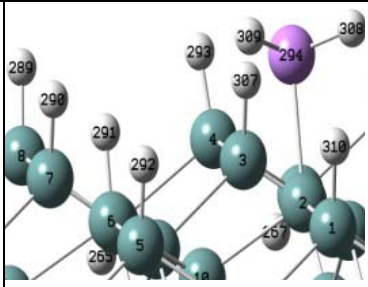
$MAsH_3$mod12	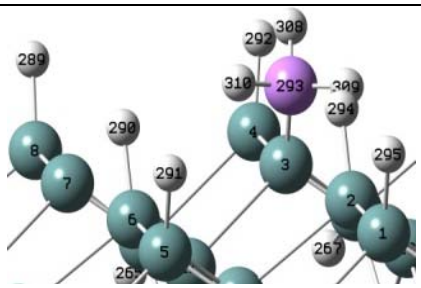	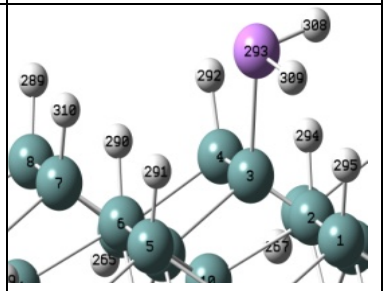
$MAsH_3$mod13	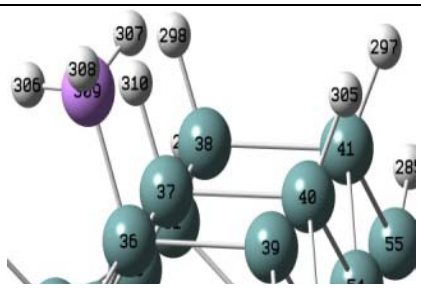	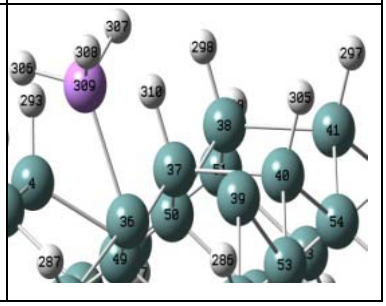

FIG. 4.2. The initial and optimized adsorption models of AsH_3 on stepped Ge(100) correspond to two dangling bonds of the surface.

Model	Initial Structure	Optimized Structure
$MAsH_3$mod14	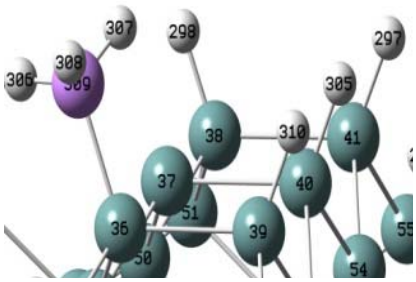	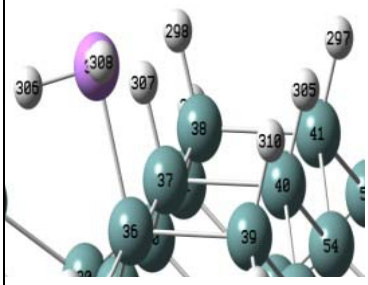
$BAsH_3$mod1	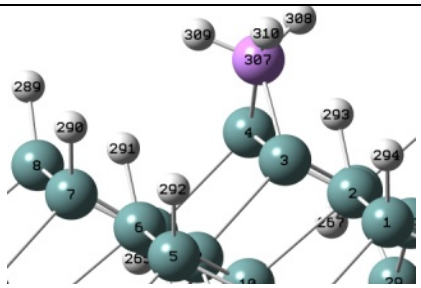	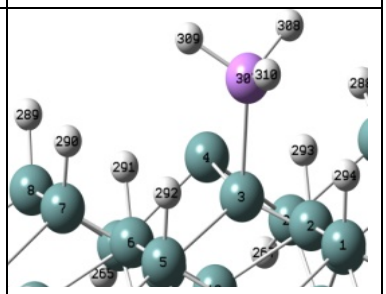
$BAsH_3$mod2	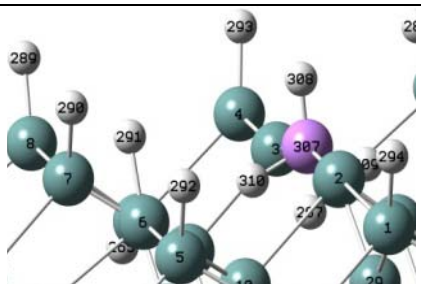	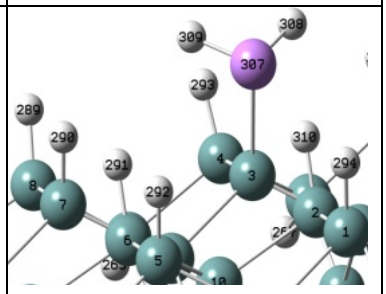
$BAsH_3$mod3	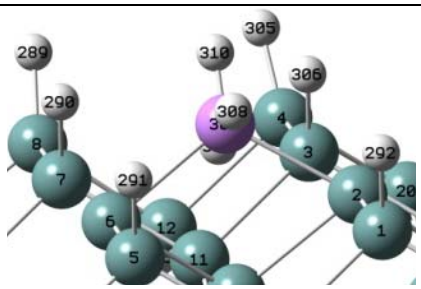	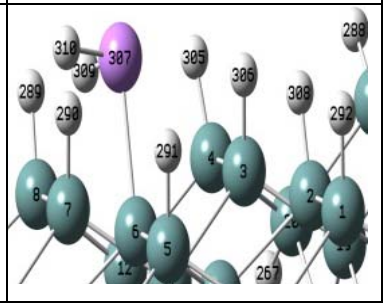

FIG. 4.2. (Cont.)

than one dangling bonds on the same or different dimers adjacent to each other have been exposed to arsine gas, AsH_3 molecules will be adsorbed to the surface either directly or dissociatively. The most probable direct adsorption models of AsH_3 are obtained by optimization of $BAsH_3$mod1 and $BAsH_3$mod4 models on the step-down and step-up terraces respectively. The binding energy of AsH_3 are calculated (Eq. 1.1) to be -6.544 and -6.789eV in $BAsH_3$mod1 and $BAsH_3$mod4, respectively. Since

Model	Initial Structure	Optimized Structure
BAsH3mod4	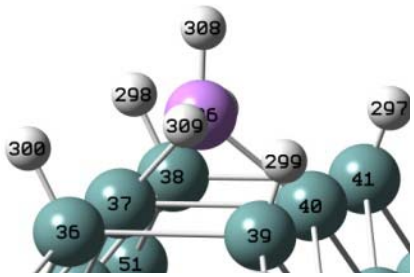	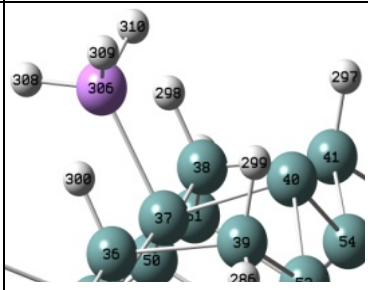
BAsH3mod5	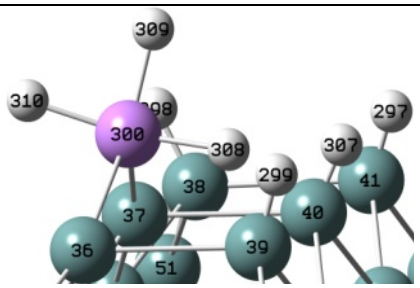	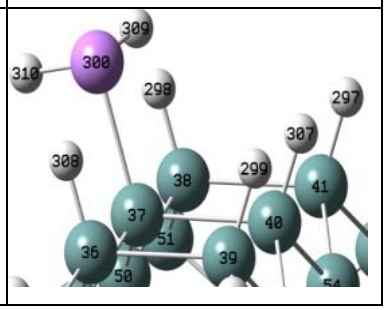

FIG. 4.2. (Cont.)

the adsorption of AsH_3 to the surface is not provided actually in the most probable structure of $MAsH_3$mod2 (Fig.4.1 and Table 4.1), the binding energy of AsH_3 in this model is higher than those in optimized $BAsH_3$mod1 and $BAsH_3$mod4 structures (Fig. 4.2 and Table 4.2). In optimized $BAsH_3$mod1 and $BAsH_3$mod4 models, AsH_3 has adsorbed to the buckled down bond of the dimer with a bond length of ~2.51A^o and increased the buckled angle (tilt angle) of the dimer after optimization. In these most probable models, the dimer bond is found to be elongated (2.50-2.56 A^o) by the adsorption of AsH_3 molecule. According to the total energies given in Table 4.2, the most probable dissociation models of AsH_3 in (AsH_2, H) form are obtained when AsH_3 molecule makes a bridge between the rows of the dimers on both step-down ($BAsH_3$mod3) and step-up ($BAsH_3$mod5) terraces. Although the AsH_3 molecule is also dissociated into AsH_2 and H fragments in the optimized $MAsH_3$mod11, $MAsH_3$mod12, $MAsH_3$mod14, and $BAsH_3$mod2 models, the total energies correspond to their local minima are all higher than the total energy of $BAsH_3$mod3 model. The binding energies of AsH_2 calculated by Eq. (1.1) are -6.073 and -5.967eV (Table 4.2) for the most probable structures of $BAsH_3$mod3 and $BAsH_3$mod5, respectively. Therefore the adsorption of AsH_2 on step-down terrace is

TABLE 4.2. The structural parameters, the total energy, and the binding energy of AsH_3 (or AsH_2), for the optimized adsorption models of AsH_3 on stepped Ge(100) correspond to two dangling bonds of the surface.

Model	Bond length(A^o)			Tilt angle (degree)	Total Energy (a.u.)	Binding Energy (eV)
	Ge-As	As-H	Dimer Ge-Ge			
$MAsH_3$mod9	2.52	1.45	2.53	16.2	-371613.2050	-6.391
$MAsH_3$mod10	2.52	1.45	2.59	20.0	-371613.2048	-6.386
$MAsH_3$mod11	2.38	1.45	2.51	0.2	-371613.3677	-5.970 for AsH_2
$MAsH_3$mod12	2.38	1.45	2.47	4.4	-371613.3669	-5.948 for AsH_2
$MAsH_3$mod13	2.50	1.45	2.58	19.7	-371613.2106	-6.666
$MAsH_3$mod14	2.38	1.45	2.50	0.6	-371613.3674	-5.984 for AsH_2
$BAsH_3$mod1	2.51	1.45	2.50	15.8	-371613.2106	-6.544
$BAsH_3$mod2	2.38	1.45	2.47	4.4	-371613.3681	-5.980 for AsH_2
$BAsH_3$mod3	2.38	1.45	2.42	9.8	-371613.3712	-6.073 for AsH_2
$BAsH_3$mod4	2.51	1.45	2.56	19.7	-371613.2151	-6.789
$BAsH_3$mod5	2.38	1.45	2.48	0	-371613.3677	-5.967 for AsH_2

stronger than the adsorption on step-up terrace. The bond length between AsH_2 and the surface Ge atom is found to be 2.38A^o in both most probable structures, $BAsH_3$mod3 and $BAsH_3$mod5. The optimized geometries of $BAsH_3$mod3 and $BAsH_3$mod5 have illustrated that, H atoms appeared by the dissociation of AsH_3 will be adsorbed to one of the open surface bonds. Hence at this initial stage of the doping process, AsH_3, AsH_2, and H will be appeared totally on the stepped Ge(100) surface depending on the positions of the open bonds in front of AsH_3 molecules.

4.3 Adsorption of AsH_2 on Stepped Ge(100) surface

At this stage of the work, molecular adsorption of AsH_2 on stepped Ge surface has been confirmed by the optimization of unbridged and bridged adsorption models pictured in Fig. 4.3. The structural parameters and the total energies of the considered models are tabulated in Table 4.3. It is found that, AsH_2 prefers molecular adsorption actually in all considered adsorption models. In all optimized unbridged and bridged models AsH_2 is found to be bounded to one of the open surface bond with a bond length of 2.38 A^o while the other bond is open. This outcome has excluded the spontaneous dissociative adsorption of AsH_2 on stepped Ge surface. Since the adsorption of AsH_2 is studied directly, the binding energy of AsH_2 (Table 4.3) in $MAsH_2$mod1-$MAsH_2$mod5 and $BAsH_2$mod1-$BAsH_2$mod5 is lower by ~2 eV than those (Table 4.2) in the dissociative adsorption models of AsH_3. But, the most probable adsorption model of AsH_2 among the models in Table 4.3 (dissociative adsorption models of AsH_3) and table 4.2 is found to be the same in which AsH_2 is bounded to the buckled down of the dimer.

4.4 Adsorption of AsH on Stepped Ge(100) surface

The adsorption of AsH_2 molecule on the surface has been expected to be followed by the adsorption of AsH molecule when one of the H atoms of AsH_2 has formed H_2 molecule with an adjacent H atom and desorbed from the surface. At his stage, the surface H atoms remained by the dissociation of AsH_3 (as AsH_2 and H) make the built up of H_2 molecules possible.

In the present work, the adsorption of AsH on stepped Ge(100) surface has been modeled again by unbridged (MAsHmod1-MAsHmod5) and bridged (BAsHmod1-BAsHmod5) models on the step-down and step-up terraces. The initial and optimized adsorption models of AsH are totally pictured in Fig. 4.4 by the labels of surface Ge atoms given in Fig. 3.4. In unbridged models, two open bonds are considered either on the same or adjacent dimer bonds. Therefore AsH molecule is adsorbed to one of the open bonds, when the other bond is open. In bridged models, AsH makes a

Model	Initial Structure	Optimized Structure
$MAsH_2$mod1	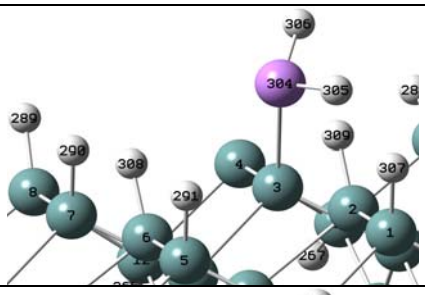	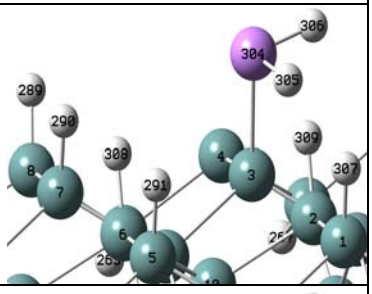
$MAsH_2$mod2	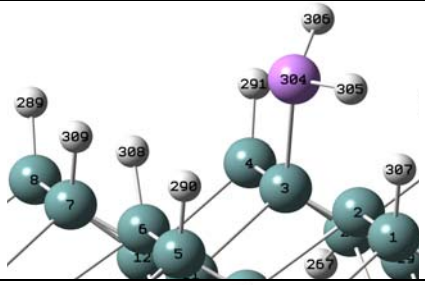	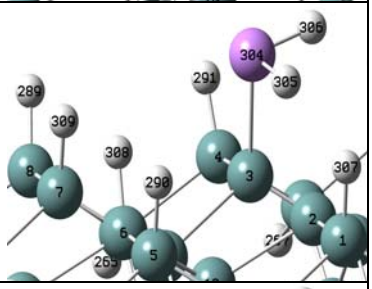
$MAsH_2$mod3	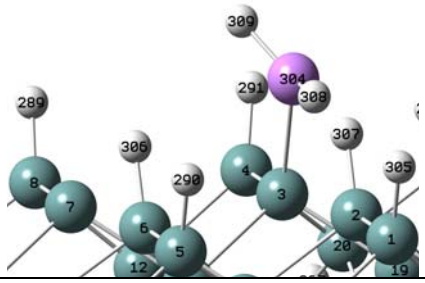	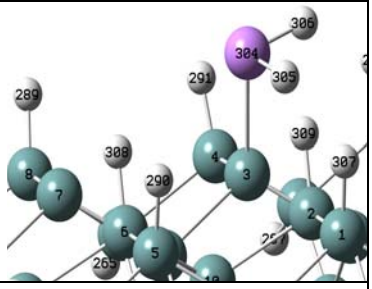
$MAsH_2$mod4	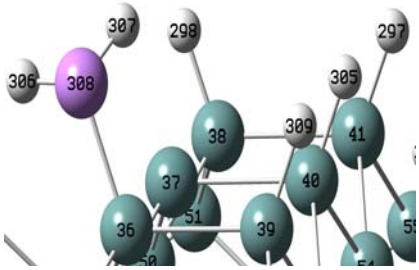	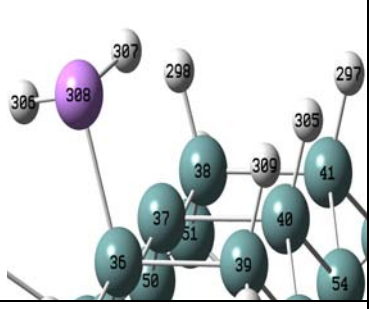
$MAsH_2$mod5	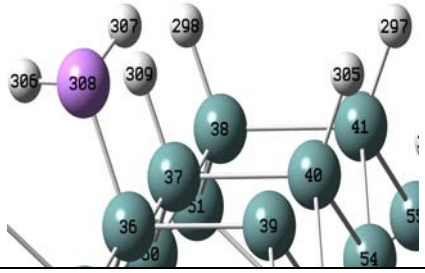	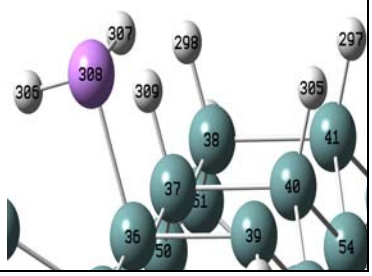

FIG. 4.3. The initial and optimized adsorption models of AsH_2 on stepped Ge(100) surface.

Model	Initial Structure	Optimized Structure
$BAsH_2$mod1	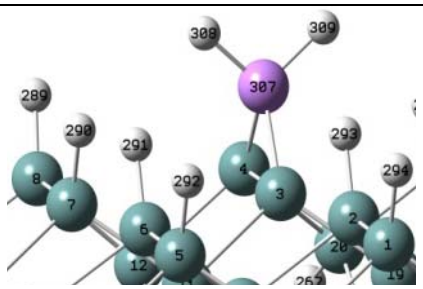	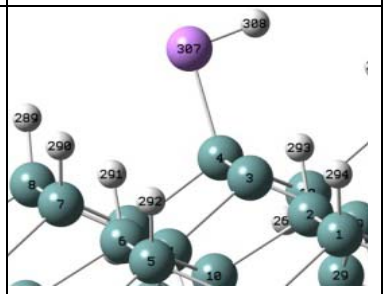
$BAsH_2$mod2	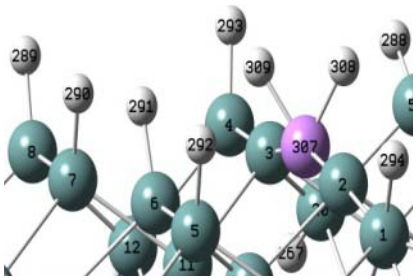	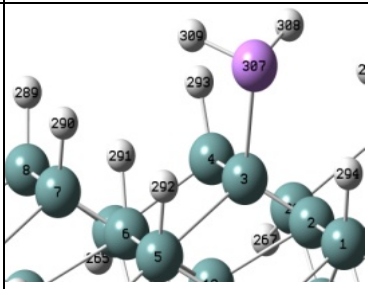
$BAsH_2$mod3	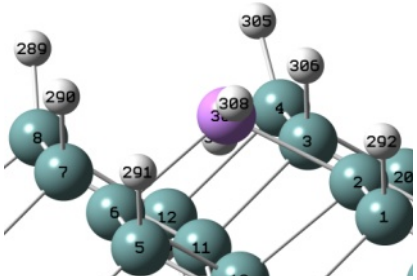	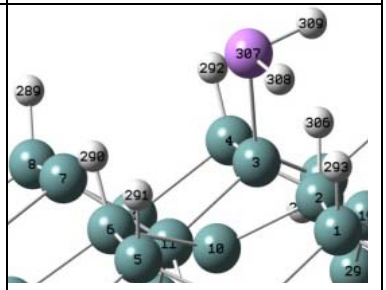
$BAsH_2$mod4	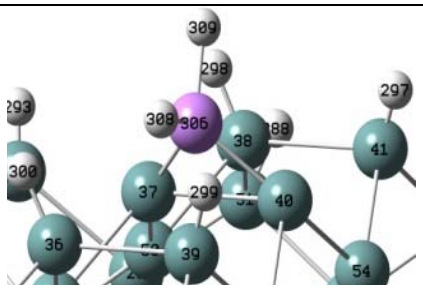	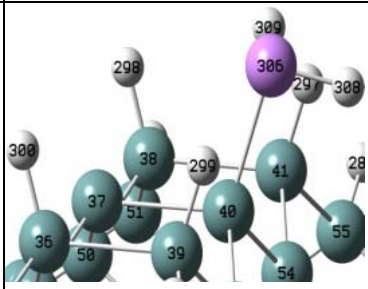
$BAsH_2$mod5	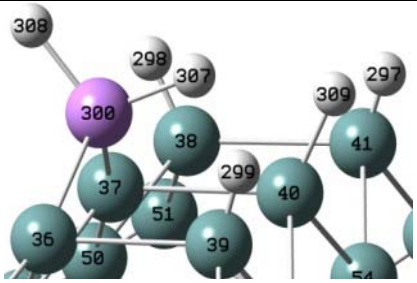	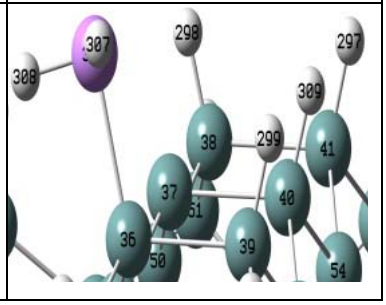

FIG. 4.3. (Cont.)

TABLE 4.3. The structural parameters, the total energy, and the binding energy of AsH_2, for the optimized adsorption models of AsH_2 on stepped Ge(100) surface.

Model	Bond length(A^o)			Tilt angle (degree)	Total Energy (a.u.)	Binding Energy (eV)
	Ge-As	As-H	Dimer Ge-Ge			
$MAsH_2$mod1	2.38	1.45	2.46	3.7	-371612.7402	-7.902
$MAsH_2$mod2	2.38	1.45	2.47	4.4	-371612.7413	-8.661
$MAsH_2$mod3	2.38	1.45	2.47	4.4	-371612.7403	-8.628
$MAsH_2$mod4	2.38	1.45	2.50	0.5	-371612.7408	-7.956
$MAsH_2$mod5	2.38	1.45	2.49	0.2	-371612.7405	-8.032
$BAsH_2$mod1	2.38	1.45	2.46	3.4	-371612.7453	-8.040
$BAsH_2$mod2	2.38	1.45	2.47	4.4	-371612.7427	-8.653
$BAsH_2$mod3	2.38	1.45	2.46	4	-371612.5798	-8.628
$BAsH_2$mod4	2.38	1.45	2.48	1.5	-371612.7410	-8.046
$BAsH_2$mod5	2.38	1.45	2.50	0.6	-371612.7417	-7.981

bridge between the open bonds either on the same as adjacent dimer bonds. The total energies of the models given in Table 4.4 have indicated that, AsH has preferred to make a bridge between the open bonds after optimization. The tendency of AsH to the bridged models has been also found in some optimized unbridged adsorption models (MAsHmod2, MAsHmod4, MAsHmod5). The most probable adsorption model of AsH corresponds to the minimum of the total energy is obtained when AsH makes a bridge between the open bonds on the same dimer bond of the step-down (BAsHmod1) and step-up (MAsHmod5) terraces. In optimized structures of these models, AsH is bonded to two surface Ge atoms with a bond length of 2.36A^o and binding energy of ~ -10.7eV (Table 4.4). The optimized bridged models

Model	Initial Structure	Optimized Structure
MAsHmod1	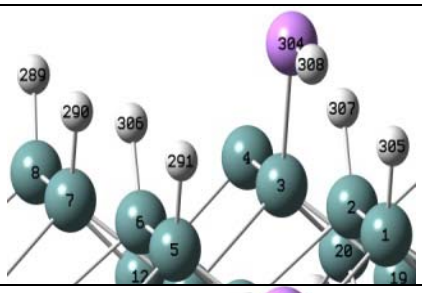	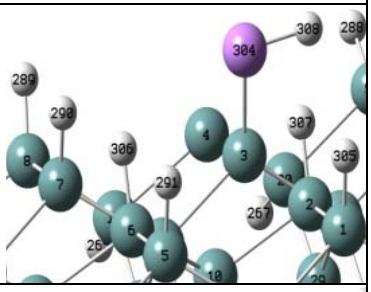
MAsHmod2	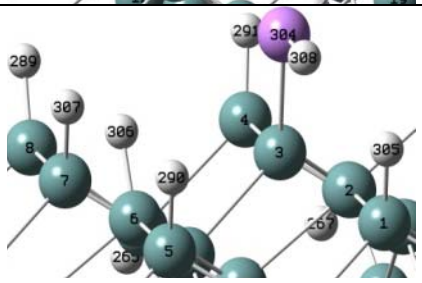	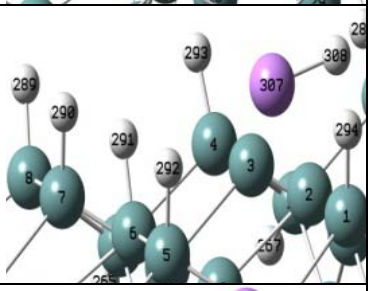
MAsHmod3	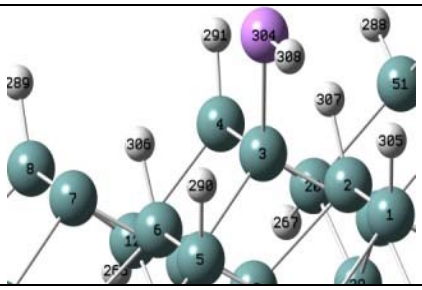	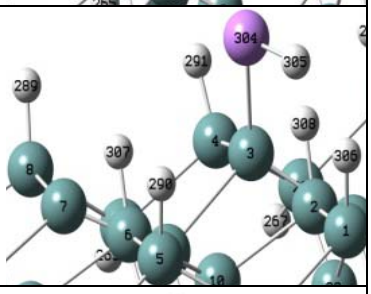
MAsHmod4	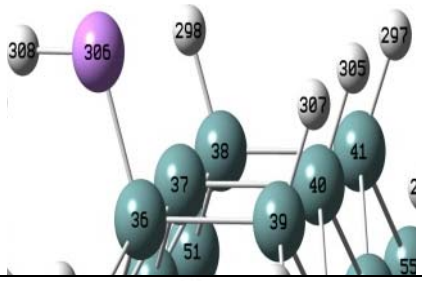	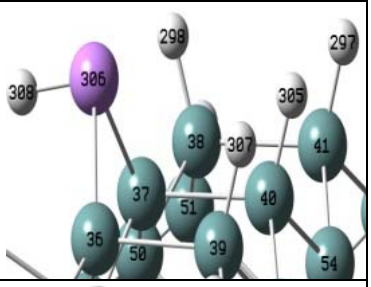
MAsHmod5	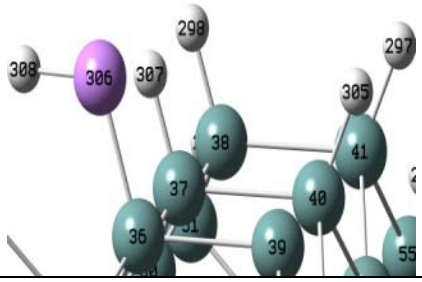	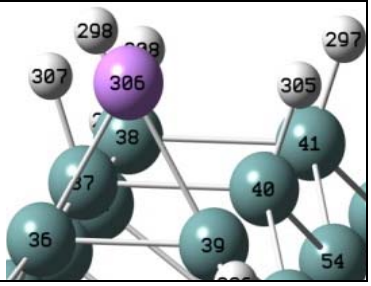

FIG. 4.4. The initial and optimized adsorption models of AsH on stepped Ge(100) surface.

Model	Initial Structure	Optimized Structure
BAsHmod1	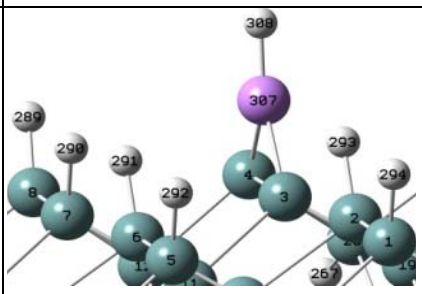	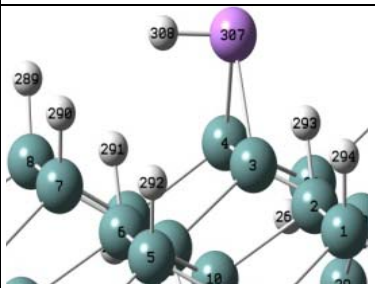
BAsHmod2	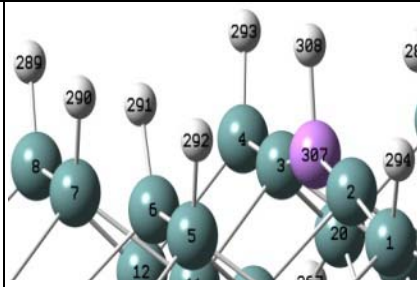	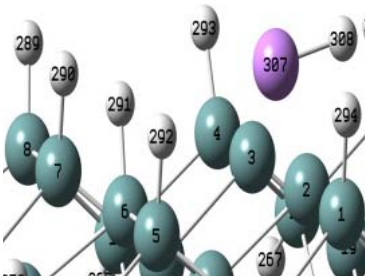
BAsHmod3	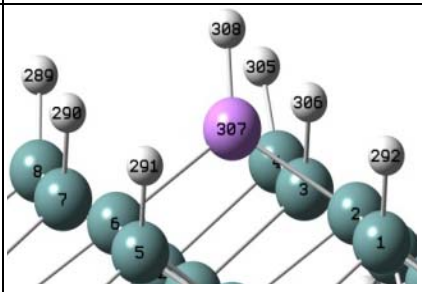	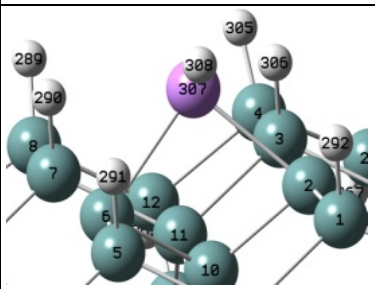
BAsHmod4	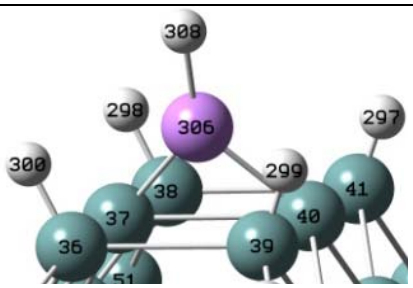	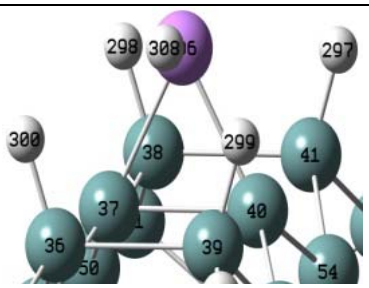
BAsHmod5	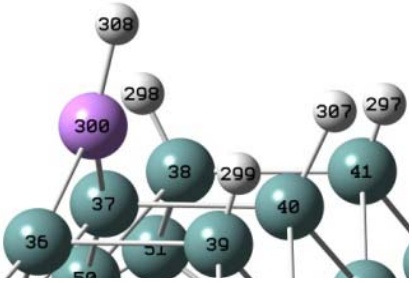	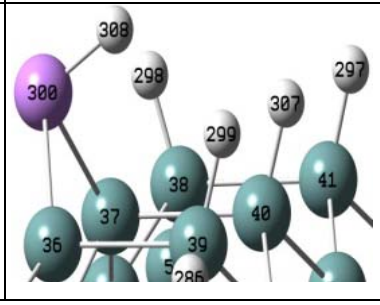

FIG. 4.4. (Cont.)

TABLE 4.4. The structural parameters, the total energy, and the binding energy of AsH for the optimized adsorption models of AsH on stepped Ge(100) surface.

Model	Bond length(A^o)			Tilt angle (degree)	Total Energy (a.u.)	Binding Energy (eV)
	Ge-As	As-H	Dimer Ge-Ge			
MAsHmod1	2.16	1.45	2.87	19	-371612.0410	-7.105
MAsHmod2	2.65	1.45	2.71	18	-371612.0792	-8.874
MAsHmod3	2.25	1.45	2.47	4.5	-371612.0164	-7.160
MAsHmod4	2.53	1.45	2.50	9.1	-371612.1264	-9.467
MAsHmod5	2.36	1.45	2.36	0.9	-371612.1682	-10.688
BAsHmod1	2.36	1.45	2.34	4.8	-371612.1716	-10.658
BAsHmod2	2.66	1.45	2.76	16.4	-371612.0814	-8.933
BAsHmod3	2.55	1.45	2.51	5.6	-371612.1150	-9.842
BAsHmod4	2.36	1.45	2.35	0.6	-371612.1680	-10.683
BAsHmod5	2.51	1.45	2.49	8	-371612.1292	-9.543

(BAsHmod2- BAsHmod4) have also indicated that AsH can make bridge between the adjacent dimers when one of the open bond on the same dimer is compensated by another fragment, H.

4.5 Adsorption of As atom on Stepped Ge(100) surface

In this stage of the doping process of Ge sample, AsH_3 molecule of the arsine gas is expected to be reduced to As atom by

$$AsH+H \longrightarrow As+H_2$$

reaction. Here, H_2 molecule, built up by H atom of AsH fragment and one of the adjacent surface H atom, has desorbed from the surface. The atomic adsorption of As has been examined by again unbridged (MAsmod1-MAsmod5) and bridged (BAsmod1-BAsmod5) models. It is examined whether the bridge model of AsH (Fig. 4.4) is broken or not during desorption of H_2 from the surface. The initial and optimized adsorption structures of As on stepped Ge(100) surface are pictured in Fig. 4.5. The total energies of the models and the binding energy of As in these models are tabulated in Table 4.5. It is found that the adsorption of As on step-down and step-up terraces depend on the position of the open surface bonds. As atom has preferred to make the bridge structure between two Ge surface atoms when the open bonds are on the same dimer bond. Therefore the bridge structure of AsH on the same dimer (Fig. 4.4) has been saved on both step-down and step-up terraces by the adsorption of As. However, the bridge structures of AsH between the adjacent dimers (Fig. 4.4) have been found to be broken during the reduction of AsH to As. The bridge structure of As on the same dimer bond of the step-down terrace is characterized with the binding energy of -10.634eV and Ge-As bond length of 2.36A^o in the optimized structure of BAsmod1. Similarly the bridge model of As atom (BAsmod4) on the same dimer bond of the step-up terrace becomes prominent by the binding energy of -10.661eV. On the other hand, the As atom has preferred the buckled down Ge atoms on both step-down and step-up terraces when the bridge structure of AsH between the adjacent dimers is broken during the desorption of H_2 from the surface. In these most probable structures, MAsmod2 (or BAsmod2) and MAsmod5, the binding energy of As is calculated to be -10.936 and -10.237eV, respectively. The Ge-As bond length is found to be 2.37A^o in the direct adsorption models.

Model	Initial Strucure	Optimized Structure
MAsmod1	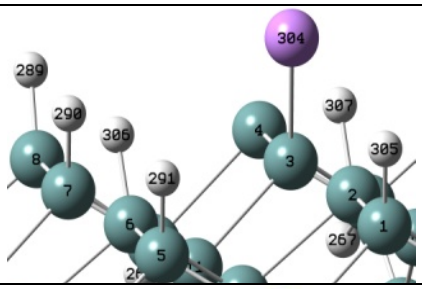	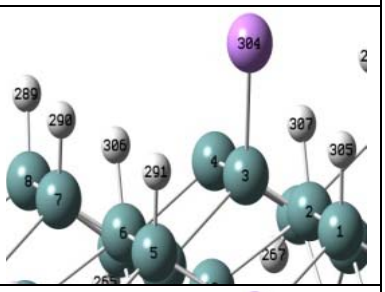
MAsmod2	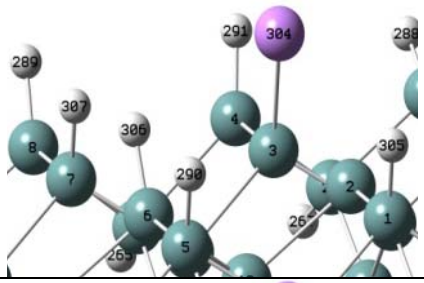	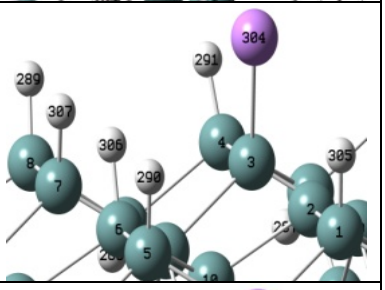
MAsmod3	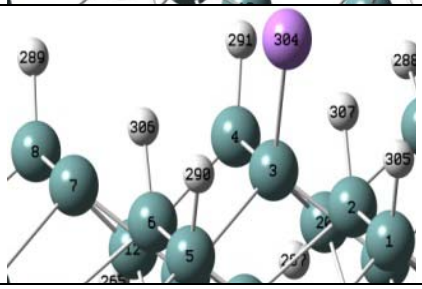	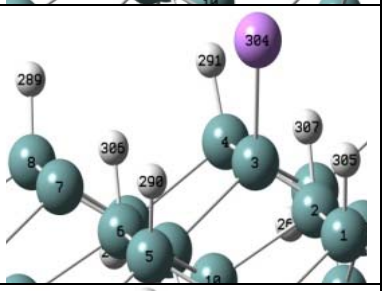
MAsmod4	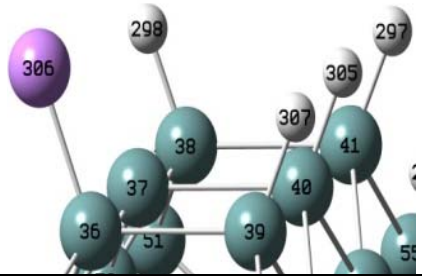	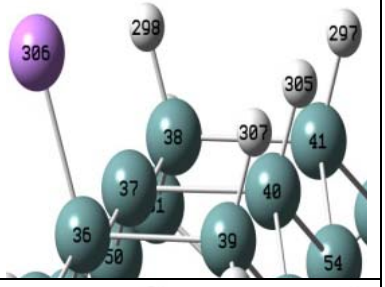
MAsmod5	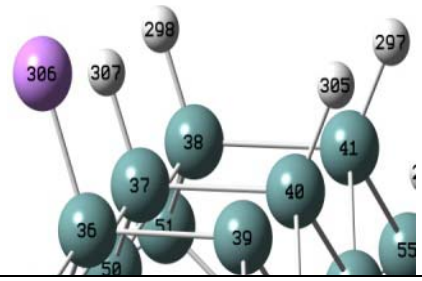	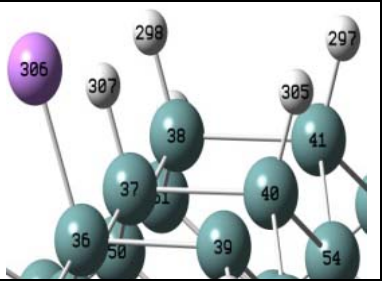

FIG. 4.5. The initial and optimized adsorption models of As atom on stepped Ge(100) surface.

Model	Initial Strucure	Optimized Structure
BAsmod1	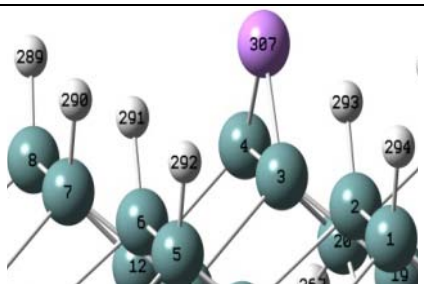	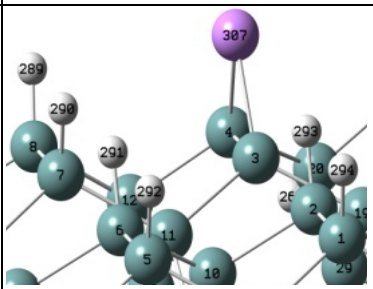
BAsmod2	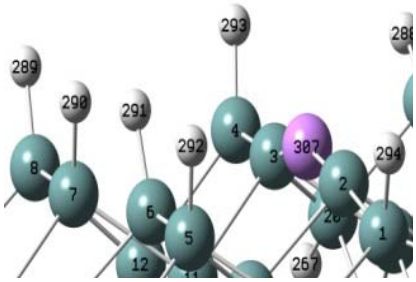	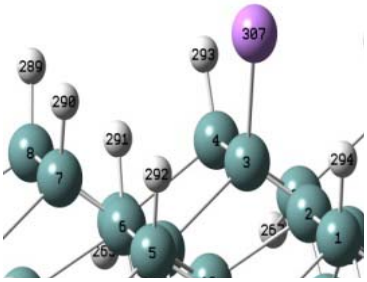
BAsmod3	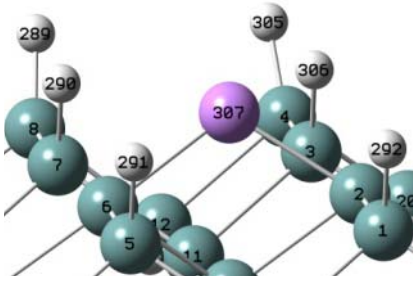	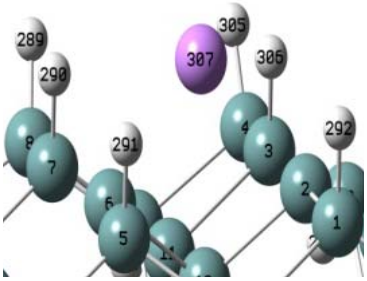
BAsmod4	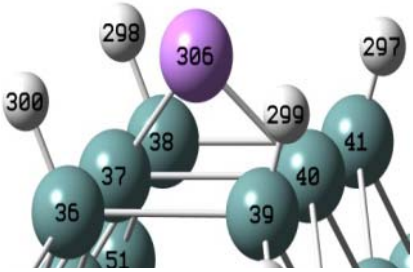	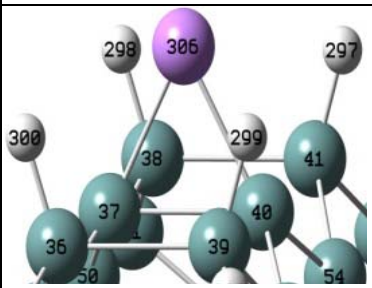
BAsmod5	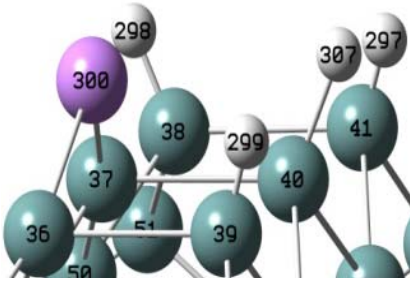	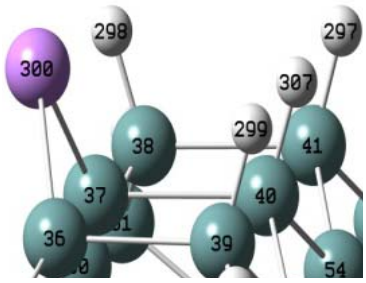

FIG. 4.5. (Cont.)

TABLE 4.5. The structural parameters, the total energy, and the binding energy of As, for the optimized adsorption models of As on stepped Ge(100) surface.

Model	Bondlength (A^o)		Tilt angle (degree)	Total Energy (a.u.)	Binding Energy (eV)
	Ge-As	Dimer Ge-Ge			
MAsmod1	2.37	2.46	5.6	-371611.5614	-10.163
MAsmod2	2.36	2.47	5.5	-371611.5630	-10.936
MAsmod3	2.36	2.47	5	-371611.5619	-10.9
MAsmod4	2.36	2.50	0	-371611.5627	-10.294
MAsmod5	2.37	2.50	0.4	-371611.5617	-10.237
BAsmod1	2.36	2.34	4.7	-371611.5787	-10.634
BAsmod2	2.37	2.47	5.3	-371611.5634	-10.947
BAsmod3	2.59	2.51	4.8	-371611.5217	-9.807
BAsmod4	2.36	2.35	0.5	-371611.5752	-10.661
BAsmod5	2.53	2.50	4.3	-371611.5343	-9.464

4.6 Diffusion of As atom through the layers of Stepped Ge(100) surface

In the last stage, the doping of stepped Ge(100) is simulated by the diffusion of the As atom towards the layers of the surface. During the diffusion, As atoms can have a sit between the surface Ge atoms breaking the Ge-Ge bonds or occupy substitutional

or interstitial places of the surface. The setting of As atoms between the surface Ge atoms on the step-down and step-up terraces is defined by BBAsmod1 and BBAsmod2 structures, respectively. The initial and optimized geometries, and the total energies of these models are given in Fig. 4.6 and Table 4.6, respectively. It is found that As atoms of these models push the adjacent Ge atoms out site the surface and occupy the empty places of Ge atoms after optimization. The binding energy of As in BBAsmod1 and BBAsmod2 structures is calculated (Eq. 1.1) to be -7.312 and -4.087eV, respectively. The other models SAsmod1-SAsmod3 and IAsmod1-IAsmod3 pictured in Fig. 4.6 have defined the substitutional and interstitial occupation sites of As atom on the stepped Ge(100) surface, respectively. In SAsmod1-SAsmod3 models, one site of Ge atom in the layers of the stepped Ge(100) surface is initially occupied by As atom. The main structures of these models are not changed after optimization (Fig. 4.6). The binding energy of As is calculated to be -3.843, -6.902, and -14.509eV for optimized SAsmod1, SAsmod2 and SAsmod3 structures, respectively. It is found that the initial structures of IAsmod1-IAsmod3 models are changed mainly after optimization (Fig. 4.6). The IAsmod1 model in which As atom is interstitial in the valley between the step-down and step-up terraces is converted to a bridge model between the layers of the terraces by optimization. Similarly the IAsmod2 model in which As atom interstitially between the 1st and 2nd layers of the step-down terrace is changed to a bridge model between the adjacent Ge atoms on the 1st and 2nd layers of the step-down terrace. It is also found that, the interstitial site of As in IAsmod3 has not been saved after optimization. In optimized IAsmod3 structure, As atom has left its interstitial site and got out from the layers of the surface to make a bridge between the Ge atoms on the same dimer. The breakdown of the interstitial models (IAsmod1-IAsmod3) have indicated that As atoms do not prefer the interstitial sites during the doping process of the stepped Ge(100) surface. The binding energy of As is calculated to be -5.238, -9.080 and -8.022eV in optimized IAsmod1, IAsmod2 and IAsmod3 structures, respectively. The binding energy of As in all BBAsmod1-BBAsmod2, SAsmod1-SAsmodmod2 and IAsmod1- IAsmod3 structures are found to be higher than that in the most probable adsorption models in which As atom is adsorbed to the step-down and step-up terraces with bridge (BAsmod1, BAsmod4) and unbridged (MAsmod2, MAsmod5) models. This outcome illustrates that, the substitutional

Model	Initial Structure	Optimized Structure
BBAsmod1	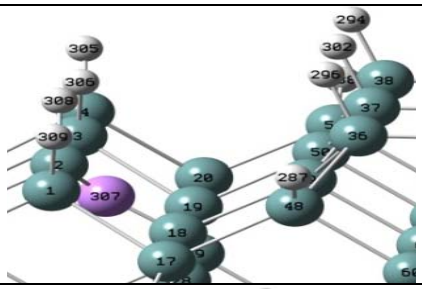	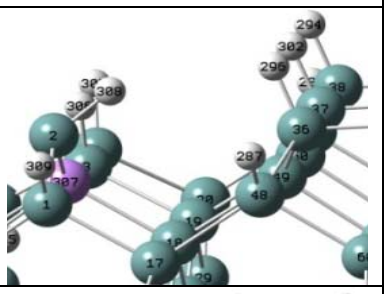
BBAsmod2	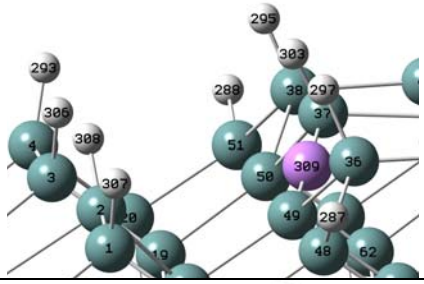	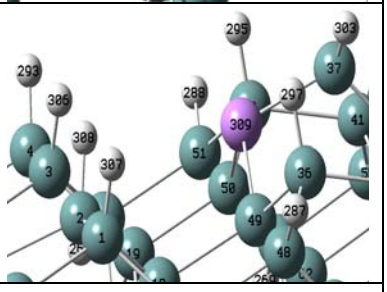
SAsmod1	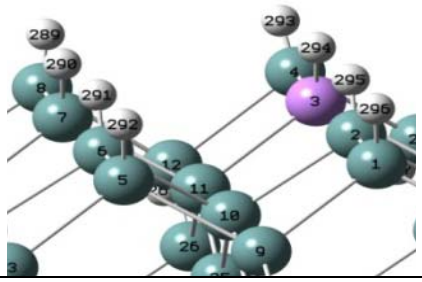	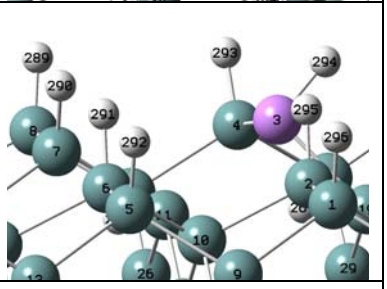
SAsmod2	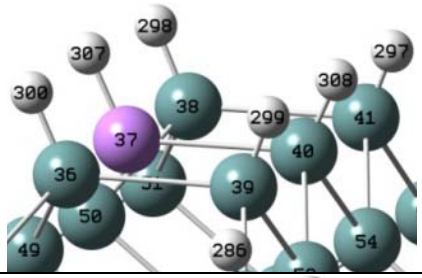	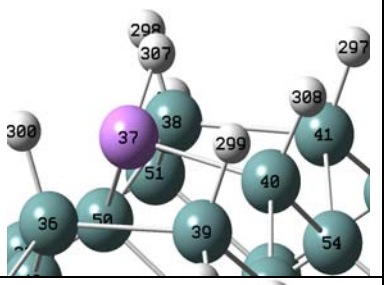
SAsmod3	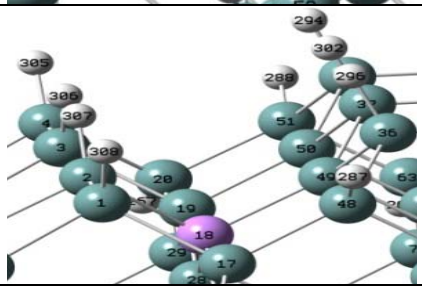	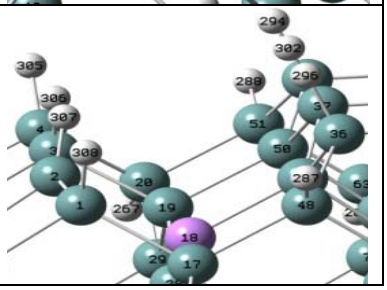

FIG. 4.6. The initial and optimized diffusion models of As atom on stepped Ge(100) surface.

Model	Initial Structure	Optimized Structure
IAsmod1	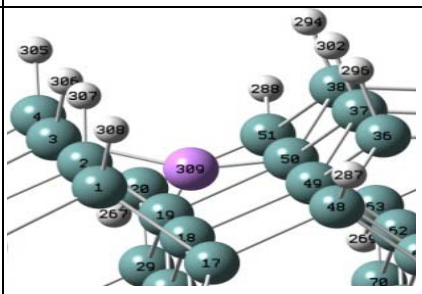	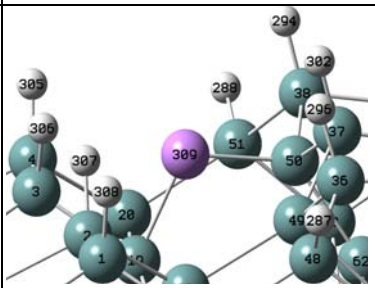
IAsmod2	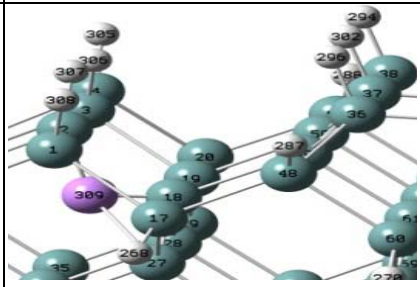	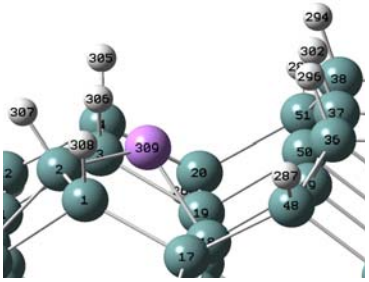
IAsmod3	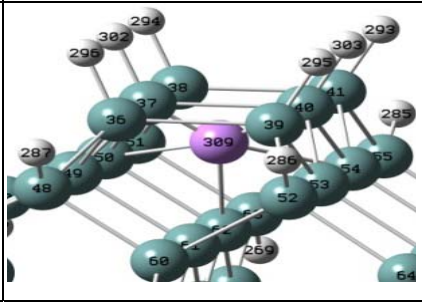	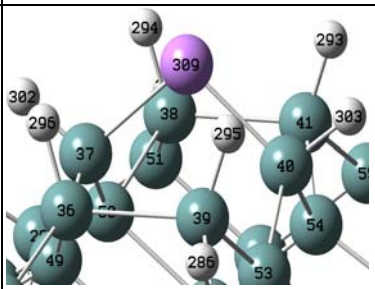

FIG. 4.6. (Cont.)

(SAsmod1-SAsmod2) and bridged models obtained by optimization of BBAsmod1-BBAsmod2 and IAsmod1-IAsmod3 structures can be obtained on the stepped Ge(100) surface by adjusting the laboratory conditions. On the other hand the binding energy of As in SAsmod3 is found to be highly lower than that of the most probable adsorption models on the step-down and step-up terraces. Therefore As atoms can diffuse through the layers in the laboratory conditions and occupy the empty sites of the stepped Ge(100) surface.

TABLE 4.6. The structural parameters, the total energy, and the binding energy of As, for the optimized diffusion models of As atom on stepped Ge(100) surface.

Model	Bond length (A^o)		Tilt angle (degree)	Total Energy (a.u.)	Binding Energy (eV)
	As-Ge	Dimer Ge-Ge			
BBAsmod1	2.34(up) 2.43(back)	---	---	-371612.8873	-7.311
BBAsmod2	2.34(up) 2.43(back)	---	---	-371612.7689	-4.087
SAsmod1	2.45 (dimer) 2.45 (back)	---	0.9	-369560.8856	-3.843
SAsmod2	2.46(dimer) 2.45(back)	---	2	-369560.8951	-6.902
SAsmod3	2.48	---	---	-369560.6993	-14.509
IAsmod1	2.28	2.43	7.5	-371612.8111	-5.238
IAsmod2	2.33	2.39	14	-371612.9523	-9.080
IAsmod3	2.38	---	---	-371612.9135	-8.022

In the present work, the density of states (DOS) of optimized SAsmod3 is plotted in Fig. 4.7 for the states around the highest occupied molecular orbitals (HOMO) and the lowest unoccupied molecular orbitals (LUMO) of the stepped Ge(100) surface. The DOS of stepped Ge(100) surface based on single point total energy calculations is also included to Fig. 4.7 for comparison. Both profiles seeing in Fig. 4.7 are generated by Gaussian broadening technique with broadening of 0.2eV. This broadening level is found to be sufficient to observe the features around the HOMO and LUMO clearly. Since all the dangling bonds of the stepped Ge(100) surfaces with and without As atom are passivated by H atoms the energy separation between the LUMO and HOMO can be seen obviously. The energy separation between LUMO and HUMO corresponds to the optical gap between the conduction and valance band of bulk Ge. Since the stepped Ge(100) surfaces with and without As

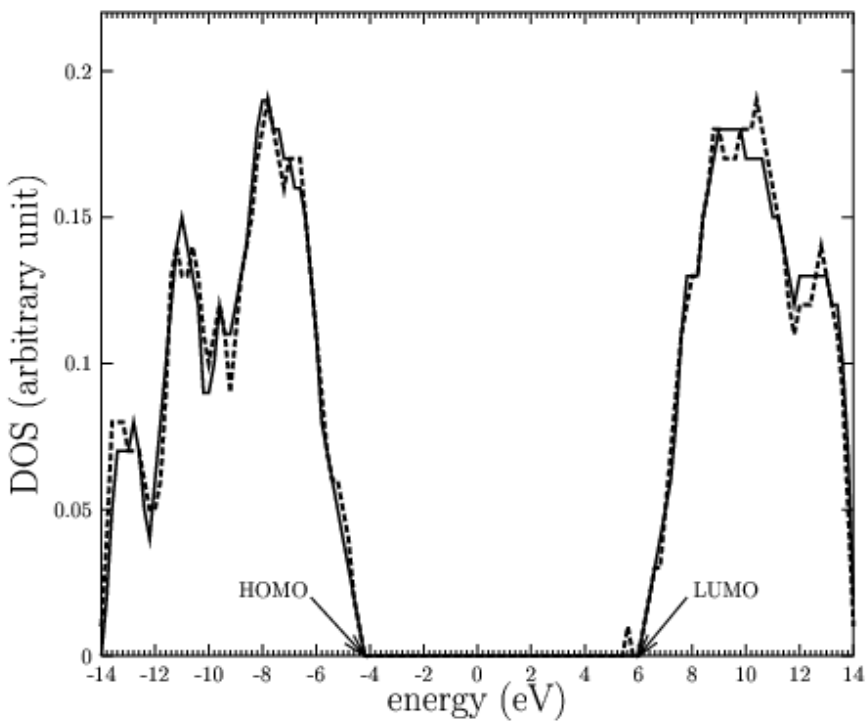

FIG. 4.7. DOS of optimized stepped Ge(100) surface models with (dotted line) and without (solid line) As atom.

atom are modeled as clusters (not periodic structure) the energy difference between LUMO and HUMO (~10eV) is much greater than the actual energy gap of bulk Ge (0.67eV) structure. As it is well known in the literature, the energy gap between LUMO and HOMO increases when the size of the cluster is decreased [66, 67]. Fig 4.7 illustrates the effect of As atom on DOS of stepped Ge(100) surface obviously. The DOS calculations of stepped Ge(100) surface have given an empty energy range between the HOMO and LUMO edges, but the same calculations on the stepped Ge(100) surface with a substitutional As atom (SAsmod3 model) have presented a feature at about 5.5eV. Therefore the substitutional As atom initiates the doping process of stepped Ge(100) surface by giving a feature very close to the LUMO edge. The feature of As states in Fig. 4.7 defines the donor energy level of n- type stepped Ge(100) surface. Since the ratio between the number of As atom and Ge atoms in the SAsmod3 model is just 1/180, the height of the As states is much lower than that of Ge states. The As donor energy level is presently calculated to be 0.5eV (referenced to LUMO edge) with respect to the reported value of 12.7meV

(referenced to the conduction band edge of bulk Ge) [60]. Since the present calculations have been done with a cluster model instead of a bulk Ge, it is considered to be weak for the determination of the exact value of the donor energy level. But it is found to be able to present the existence of the donor energy level very close to the edge of the LUMO.

4.7 Conclusion

In the present work, the decomposition steps of arsine molecule on stepped Ge(100) surface have been investigated to determine the reaction paths in the doping process. It is shown that the dissociation of AsH_3 is provided by coming away of H atoms step by step; first AsH_3 molecule adsorbs to a dangling bond of the buckled down Ge atom close to the step edge, then the dissociation steps start and finally AsH_3 reduces to As atom on the stepped Ge(100) surface. It is also presently showed that AsH_3 dissociates into AsH_2+H directly for certain adsorption models ($MAsH_3$mod11, 12, 14 and $BasH_3$mod2,3,5) just after the adsorption. Since the direct dissociation of AsH_3 was not identified on the flat Ge(100) surface [68], it is considered to be originated from much coordination of the stepped Ge(100) surface.

In the literature, the arsine-Ge surface systems were considered be important because of the faceting due to etching [26-28]. The steps like facets were determined to be controlled by the laboratory conditions; reducing the temperature, partial pressure and exposure time of AsH_3 the facets can be removed. This experimental outcome shows that faceting is directly related to the decomposition rate of AsH_3 and the desorption rate of Ge atoms from the surface. In Ref. [28] the etching of the Ge(100) surface by As atoms were controlled with 2 torr of Tertiarybutylarsine gas flow, 510°C of annealing temperature and 20min of exposure time to have arsenic terminated S_A type stepped Ge(100) surface like the As adsorbed stepped Ge(100) surface of the present work. Therefore As doped S_A type Ge(100) surface can be obtained in the laboratory with the step by step dissociation of AsH_3 as it is identified in our work. On the other hand, the substitional occupation of the stepped Ge(100)

surface by As atom identified in this work for the last step of the dissociation is confirmed by the As concentration of $1x10^{19}/cm^3$ measured in As doped Ge(100) surface [26] at 500-700°C. Because this concentration is consistent to the vacancies (irregular vacancies or empty Ge sites) generated in the Ge surface for the temperature range of 500-700°C with the vacancy formation energy of 0.59eV [69]. The occupation of the empty Ge sites by As atoms obtained by the present total energy calculations is also confirmed by the Ge-As dimers observed on the STM images of the As activated S_A type stepped Ge(100) surface [28]. Therefore As atoms prefer to occupy empty Ge sites instead of interstitial sites of the surface.

CHAPTER 5

RESULTS: 2
STEPPED Ge(100) SURFACE EXPOSED TO DIBORANE GAS

5.1 Introduction

The diborane gas molecule consists of two BH_3 molecules. In p-type doping process of stepped Ge(100) surface by diborane gas flow, B_2H_6 gas molecules can dissociate into BH_3, BH_2, BH, and finally B fragments. In this part of the present work, first the most stable geometry and the decomposition stages of diborane molecule have been examined and then the adsorption of the fragments of B_2H_6 on stepped Ge(100) surface have been studied by total energy calculations.

5.2 B_2H_6 molecular models

The two BH_3 molecules in B_2H_6 can bond to each other through either Boron or Hydrogen atoms. In the present work, three B_2H_6 molecular models are considered. In one of the bonding model, two planar BH_3 molecules with D_{3h} trigonal symmetry can bond to each other through the B-B bond. The two BH_3 molecules of this model are coincided when B_2H_6 is observed along B-B bond. In another bonding model, the BH_3 molecules in C_{3v} symmetry are also connected to each other through the B-B bond. The dihedral angle ($HB\hat{}BH$) between the B-H bonds of BH_3 molecules is 180°. Therefore, the two BH_3 molecules are not coincided along the B-B bond. In other possible bonding model, the first BH_3 molecule is attached to the second one through one of the H atom of the second BH_3 molecule. The planes of the BH_3

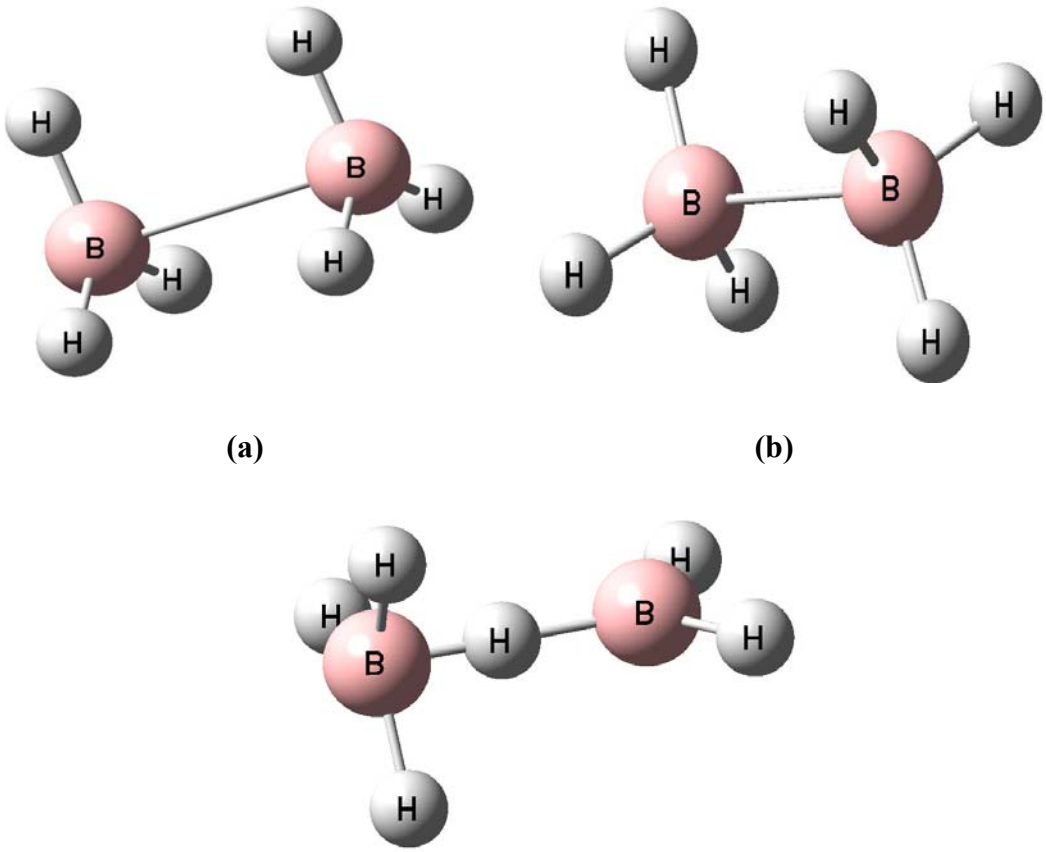

FIG. 5.1. The possible bonding models of BH_3 in B_2H_6 structure.

molecules both in D_{3h} symmetry are perpendicular to each other. The possible bonding models of BH_3 in B_2H_6 structure are pictured in Fig. 5.1. The length of B-B and B-H bonds in B_2H_6 models are taken to be ~ 1 and ~ 0.6 A^o, respectively. The present three models are defined with the acronyms of $M1B_2H_6$, $M2B_2H_6$, and $M3B_2H_6$.

5.2.1 Dissociation of B_2H_6

In the present work, the initial geometries of $M1B_2H_6$, $M2B_2H_6$, and $M3B_2H_6$ are optimized by total energy calculations. Since the doping of any substrate by B atoms is initiated with the dissociation of diborane gas molecules, the optimization is

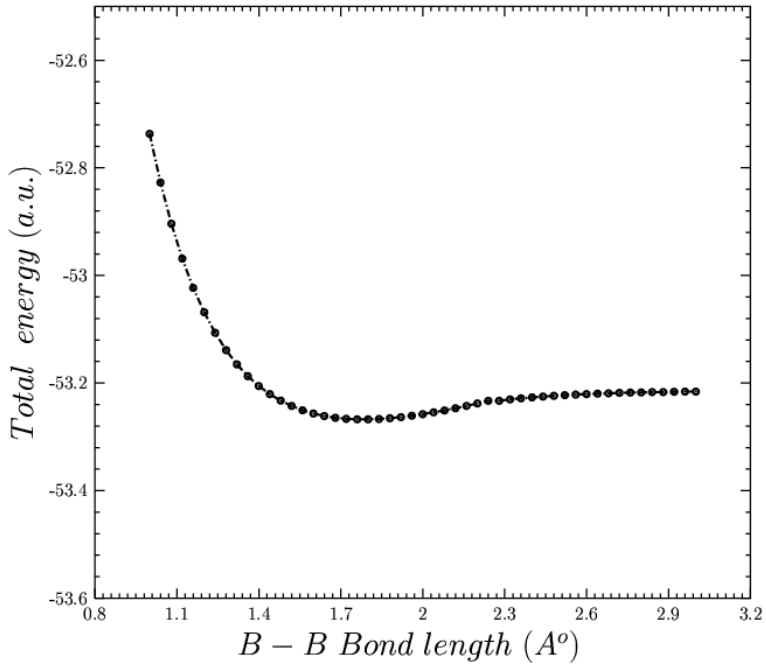

FIG. 5.2. The total energy versus B-B bond length for $M1B_2H_6$ model.

performed by increasing the length of B-B and B-H bonds in $M1B_2H_6$, $M2B_2H_6$, and $M3B_2H_6$ models, respectively. The total energy values are plotted as a function of

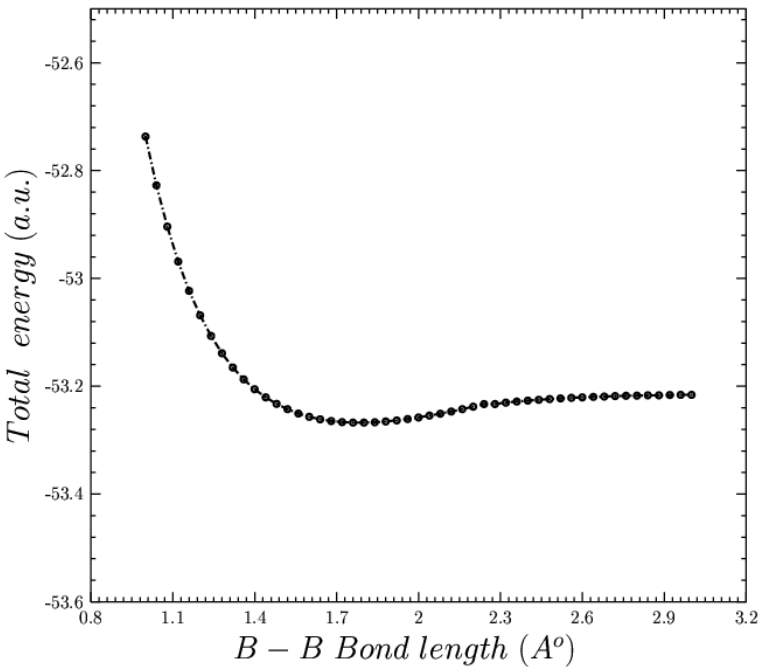

FIG. 5.3. The total energy versus B-B bond length for $M2B_2H_6$ model.

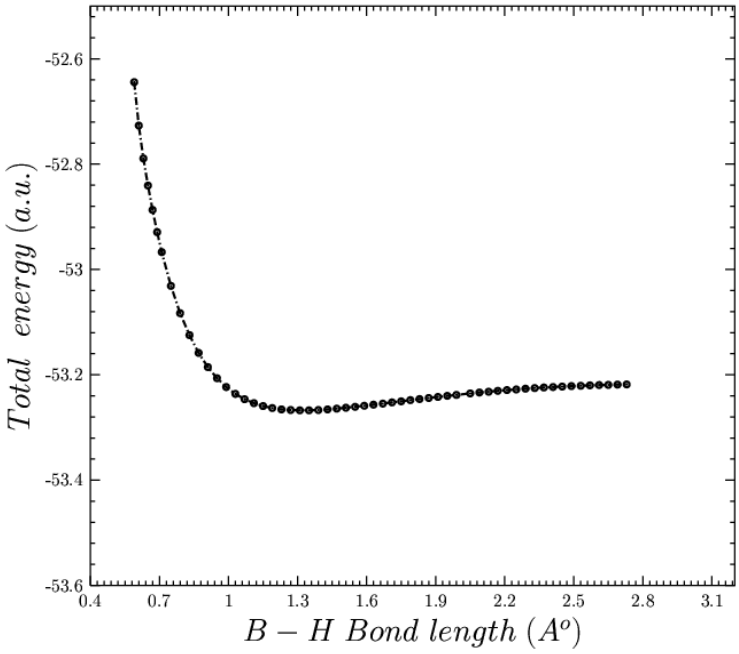

FIG. 5.4. The total energy versus B-H bond length for $M3B_2H_6$ model.

B-B and B-H bond lengths in Figs. 5.2, 5.3, and 5.4, for each optimization step of the models. It is found that, all three models have decomposed to two planar BH_3 molecules by elongating the corresponding bond between BH_3 molecules in B_2H_6 structure. Furthermore the three models of B_2H_6 molecules are found to be passed through the same optimum structure with the same lowest total energy before the dissociation. Therefore the ground state structure of B_2H_6 molecule with minimum total energy of -53.30a.u is obtained during the dissociation process. The total energy of the optimized B_2H_6 structure was reported to be -53.30a.u by Hartree-Fock calculations in Ref. [70]. In the literature, this structure of B_2H_6 was identified with a pair of chemical bridge bond between B-H-B atoms having geometries look like a banana. The optimum structure of B_2H_6 contains two types of H atoms; four H atoms of one type make four normal covalent bonds, but the other two H atoms form bridge bonds (banana bonds) between two B atoms. Figs. 5.5 (a) and (b) show the geometry and the pair of banana bonds for the optimized B_2H_6 structure, respectively. The pair of banana bonds locates in the yz plane perpendicular to the plane of the other four H atoms. Since the banana bonds are formed by the bridge bond involve three atoms (B, H, B) and only two electrons, they are also defined to be three-center-two

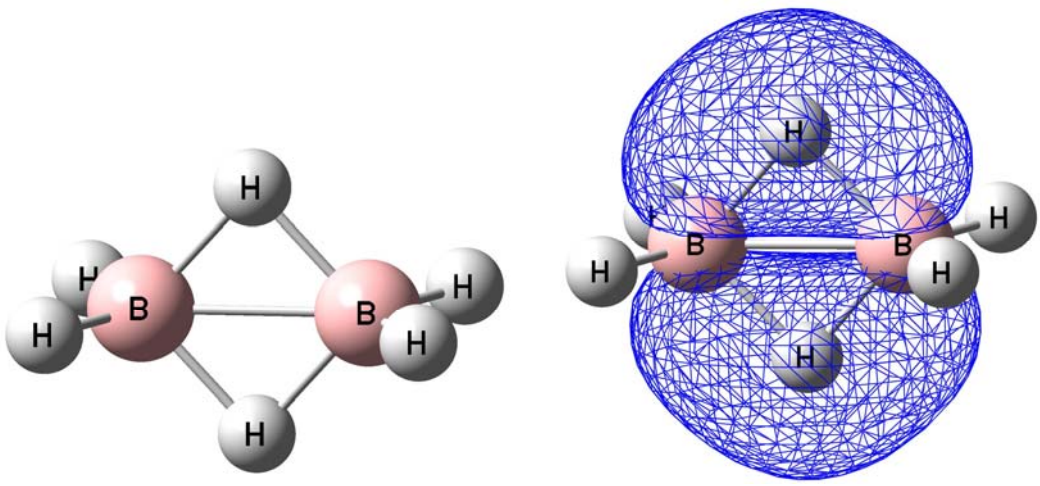

(a) **(b)**

FIG. 5.5. Geometry and the pair of banana bonds for the optimized B_2H_6 structure.

electron-pair bond. The molecular orbital of B_2H_6 due to the pair of banana bonds consists of $2p_y$ atomic orbital of boron and 1s atomic orbital of bridge hydrogen atoms. The length of B-H in the banana and normal covalent bond are found to be 1.315 and 1.185A^o, respectively. These bonds were reported to be 1.316 and 1.187A^o in Ref. [70]. Since the chosen basis vectors are different, the present total energy and bond lengths of the optimized B_2H_6 structure are different a little bit with respect to the ones reported in Ref. [70]. In the present work, the necessary external energy (E_{ext}) to dissociate the optimized structure of B_2H_6 is calculated by

$$E_{ext} = E_{final} - E_{initial} \tag{5.1}$$

Here, E_{final} and $E_{initial}$ represent the total energies of the dissociated and initial optimized structures of B_2H_6, respectively. In the present work, the necessary external energy for the dissociation of B_2H_6 is calculated to be ~1.3eV. The calculated energy to decompose the B_2H_6 molecule is in agreement with the experimental value of 26kcal/mol (~1.13eV) [71]. The activation energy for the dissociation of B_2H_6 was also calculated to be 23-25kcal/mol (1-1.08eV) in Ref. [72] by Hartree-Fock method with modified neglect of diatomic overlap (MNDO). In the same experimental work [71], the boron films were synthesized from B_2H_6 + He gas structure in CVD method by irradiating the surface with UV-laser light (λ = 193.6nm). The present necessary external energy calculated for the dissociation of

B_2H_6 into two BH_3 molecules is also found to be reasonable when it is compared with the UV-laser light energy ~6eV used for the total decomposition of B_2H_6 in Ref. [71]. In the literature, there are certain works in which the external energy to decompose B_2H_6 molecule into two BH_3 molecules was tried to be decreased in the assistance of other media or hydrocarbon solvents [73, 74].

5.3 Adsorption of the fragments of B_2H_6 on Stepped Ge(100) surface

5.3.1 Adsorption of BH_3 on Stepped Ge(100) surface

The adsorption of BH_3 molecule on the stepped Ge(100) surface has been investigated by the same models defined in chapter 4. These models are designed again by considering the single and double open surface bonds on S_A type step-down and step-up terraces. In the first considered adsorption models (MBH_3mod1-MBH_3mod8), BH_3 molecule is adsorbed to the step-down (MBH_3mod1-MBH_3mod4) and step-up (MBH_3mod5-MBH_3mod8) terraces with an open Ge bond taken at the step and close to the step regions. The adsorption of BH_3 on stepped Ge(100) is studied for both buckled-up and buckled-down Ge atoms, separately. The other open bonds of the stepped Ge surface are saturated by H atoms. The adsorption models of BH_3 on stepped Ge surface having single open bond are pictured in Fig. 5.6, by the labels of the surface Ge atoms given in Fig. 3.4. As an example, in MBH_3mod2 structure, BH_3 molecule is adsorbed to buckled-up side of the dimer bond via second Ge atom when the other surface atoms are totally compensated by H atoms. In the present work, the geometries of the adsorption models are optimized by minimizing their total energies. The optimized structures of MBH_3mod1-MBH_3mod8 models are also given in Fig. 5.6. The total energy of each optimized model is listed in Table 5.1. The binding energy of BH_3 in each optimized adsorption model has been also calculated by Eq. (1.1) and tabulated in Table 5.1. The total energy calculations have shown that, the most probable model is MBH_3mod2 in which BH_3 is initially adsorbed to the buckled up Ge atom at the step region of the step-down terrace. Since the total energies of the naked stepped Ge surfaces (having single open bond at

Model	Initial Structure	Optimized Structure
MBH_3mod1	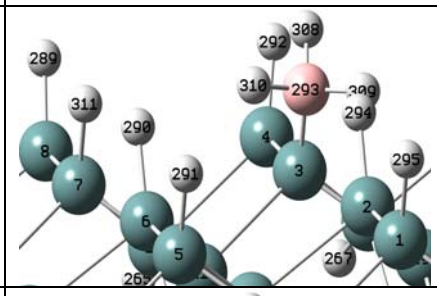	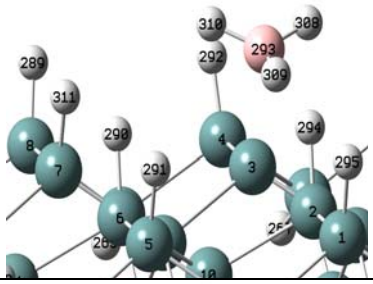
MBH_3mod2	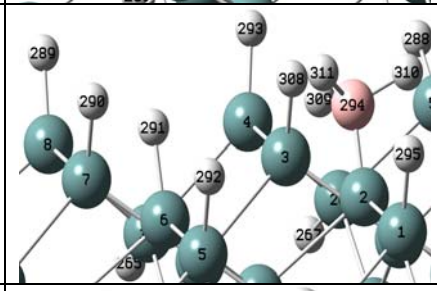	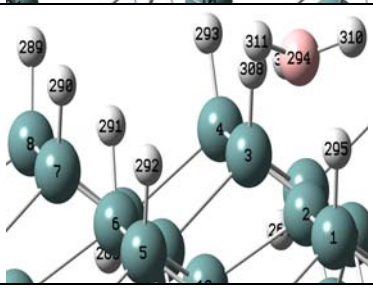
MBH_3mod3	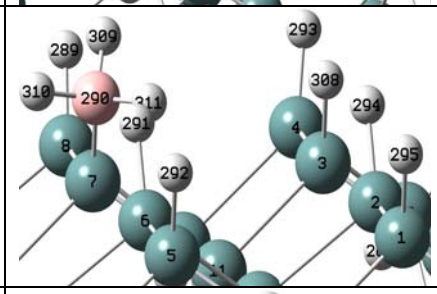	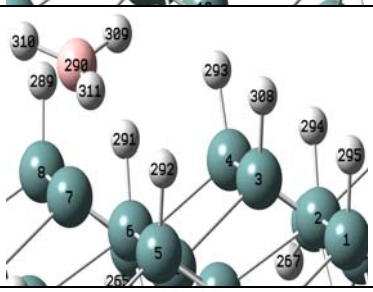
MBH_3mod4	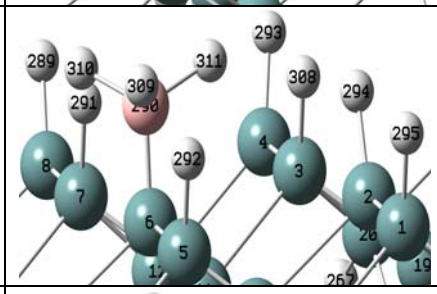	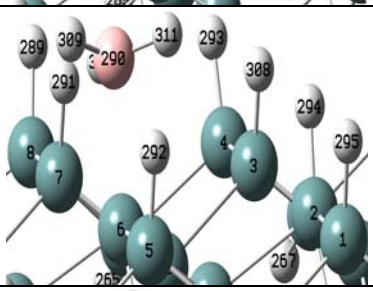
MBH_3mod5	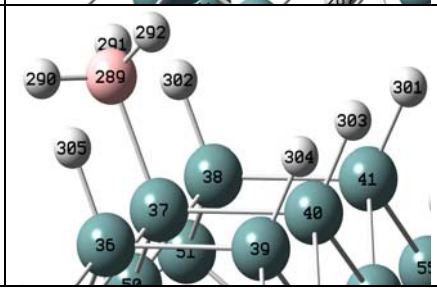	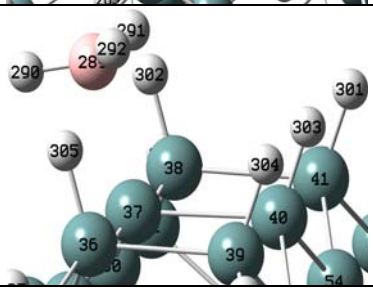

FIG. 5.6. The initial and optimized adsorption models of BH_3 on stepped Ge(100) surface having single open bond.

Model	Initial Structure	Optimized Structure
MBH_3mod6	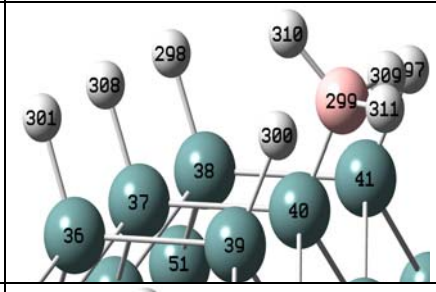	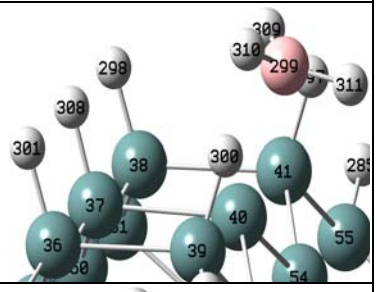
MBH3mod7	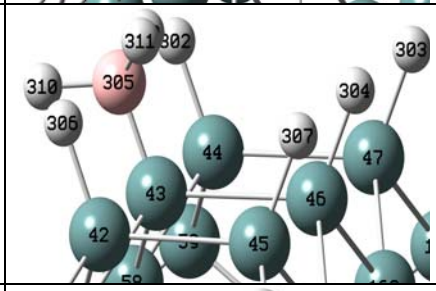	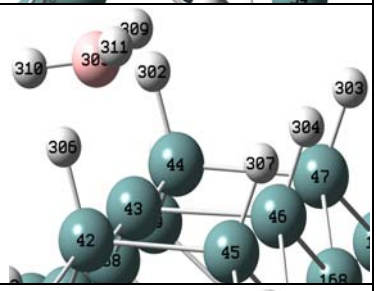
MBH3mod8	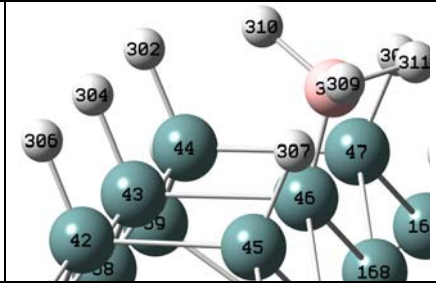	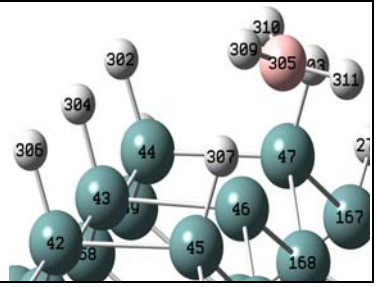

FIG. 5.6. (Cont.)

different sites) have found to be the same approximately (-369402.735a.u – (-369402.736a.u)), the most probable adsorption model (MBH_3mod2) has been also confirmed by the binding energy of BH_3.The minimum binding energy of BH_3 is calculated to be -3.690eV in MBH_3mod2 structure. The total energies of the models (Table 5.1) are found to be very close to each other as it is reported before for the same adsorption models of AsH_3. The maximum energy difference is only ~0.07eV between the step down models (MBH_3mod1-MBH_3mod4) in which BH_3 is initially adsorbed to the step or closed to the step regions. The energy difference is only ~0.02eV for the corresponding models (MBH_3mod5-MBH_3mod8) of the step-up terrace. On the other hand, the maximum total energy difference between the most probable adsorption model (MBH_3mod2) and the step up model with highest total

TABLE 5.1. The structural parameters, the total energy, and the binding energy of BH_3, for the optimized adsorption models of BH_3 on stepped Ge(100) surface having single open bond.

Model	Bond length (A^o)			Tilt angle (degree)	Total Energy (a.u)	Binding Energy (eV)
	Ge-B	B-H	Dimer Ge-Ge			
MBH_3mod1	2.28	1.16	2.46	0.4	-369428.9406	-3.663
MBH_3mod2	2.28	1.16	2.50	3.6	-369428.9416	-3.690
MBH_3mod3	2.29	1.16	2.45	8.8	-369428.9391	-3.631
MBH_3mod4	2.28	1.16	2.50	3.5	-369428.9407	-3.671
MBH_3mod5	2.28	1.16	2.48	3.7	-369428.9413	-3.678
MBH_3mod6	2.28	1.16	2.48	2.6	-369428.9413	-3.675
MBH_3mod7	2.28	1.16	2.49	3.74	-369428.9414	-3.684
MBH_3mod8	2.28	1.16	2.49	2.5	-369428.9407	-3.676

energy is found to be only ~0.02eV. In all adsorption models (MBH_3mod1-MBH_3mod8), BH_3 molecule has been suspended on the open Ge bond after optimization. In most probable adsorption model (MBH_3mod2), BH_3 molecule has suspended on the open bond of the second Ge atom with a Ge-B distance of 2.28A^o. The asymmetric dimer bond structure of the surface is not changed by optimization. The adsorption of BH_3 on stepped Ge(100) surface with two open bonds has been defined by unbridged MBH_3mod9-MBH_3mod14 and bridged BBH_3mod1-BBH_3mod5 models. As it is considered in the previous chapter, the two open bonds are considered at the step region for both terraces, because of the total energies of the adsorption models at the step region are found to be lower than these of the others in the group of MBH_3mod1-MBH_3mod8 models. The two open surface bonds are either

on the same or adjacent dimer bonds. In MBH_3mod9-MBH_3mod14 models, BH_3 molecule is initially adsorbed to one of the open bond when the other bond is open. The two open bonds considered on the step-down and step-up terraces have also allowed the formation of bridged adsorption models (BBH_3mod1-BBH_3mod5). In Fig. 5.7, the initial and optimized models correspond to two open dangling bonds of the surface are pictured by the labels of Ge atoms given in Fig. 3.4. The total energies of the optimized bridged and unbridged adsorption models have been also listed in Table 5.2. The optimized unbridged adsorption models (MBH_3mod9-MBH_3mod14) have expressed only one kind of structure; when the model has two open bonds on the same or adjacent dimer bond, BH_3 remains on the initial adsorption bond leaving the other bond as open (MBH_3mod9-MBH_3mod14). Similarly, in the adsorption model of BBH_3mod3, BH_3 is adsorbed on one of the open bond after optimization by removing the initial bridge between the adjacent dimers. But in the other bridge adsorption models (BBH_3mod1, BBH_3mod2, BBH_3mod4, BBH_3mod5), BH_3 breaks the bridge between the surface Ge atoms on the same (BBH_3mod1, BBH_3mod4) or adjacent (BBH_3mod2, BBH_3mod5) dimers and dissociates into BH_2+H or BH+H_2, after optimization. Therefore when BH_3 is adsorbed on stepped Ge (100) surface in the bridge model it will have high probability to be reduced to BH_2 or BH simultaneously. It is found that BH_3 is dissociated into BH directly in BBH_3mod2 model and two H atoms broken from BH_3 molecule are desorbed from the surface in the form of H_2 molecule. Therefore when the stepped Ge terraces have been exposed to BH_3 gas, BH_3 molecules will be adsorbed to the surface either directly or dissociatively, due to the number and the position of the open bonds. Since the bond structures on the stepped Ge(100) surface are different for each adsorption model considered here, the most probable model is defined by the binding energies (Table 5.2) calculated for the fragments, BH_3, BH_2, and BH. The most probable direct adsorption (non dissociative) model of BH_3 (among MBH_3mod9-MBH_3mod14 and BBH_3mod3 models) is obtained by the optimization of MBH_3mod12 model on the step-down terrace. In optimized MBH_3mod12 model, BH_3 molecule is bound to the surface with a bond length of 2.06A^o and the binding energy of $\sim$ -6eV (Table 5.2). The length and the tilt angle of the dimer bond having BH_3 molecule are found to be 2.52A^o and 4.8^o, respectively.

Model	Initial Structure	Optimized Structure
MBH_3mod9	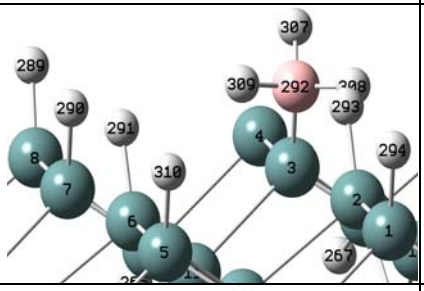	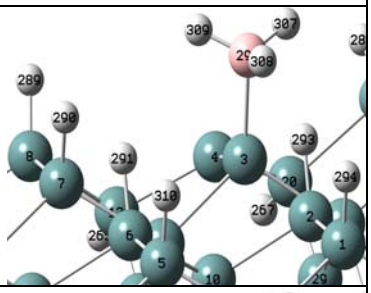
MBH_3mod10	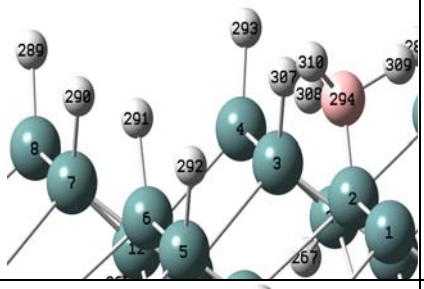	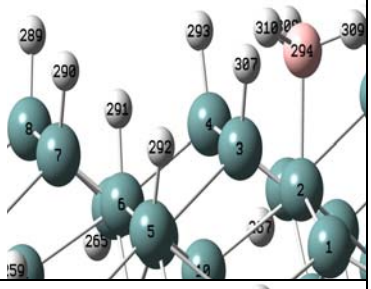
MBH_3mod11	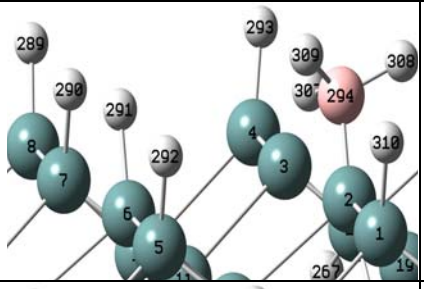	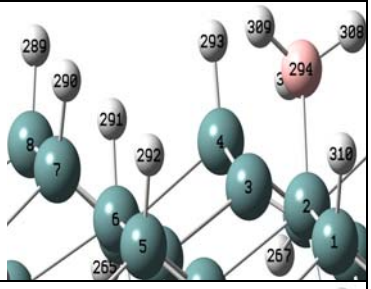
MBH_3mod12	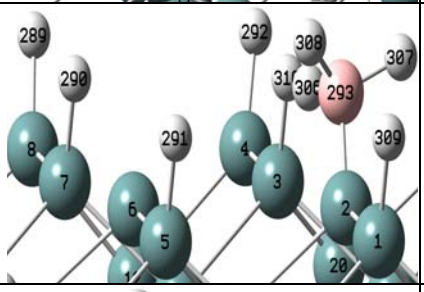	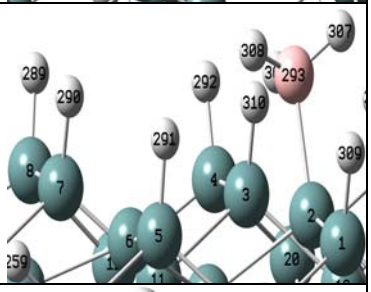
MBH_3mod13	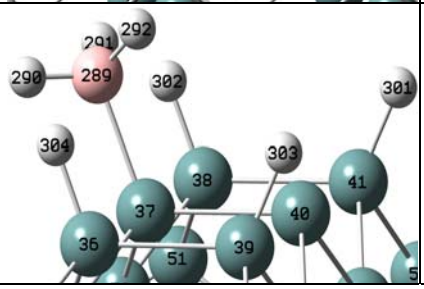	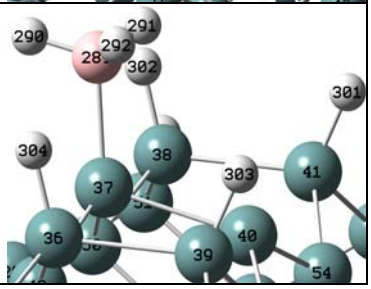

FIG. 5.7. The initial and optimized adsorption models of BH3 on stepped Ge correspond to two dangling bonds of the surface.

Model	Initial Structure	Optimized Structure
MBH3mod14	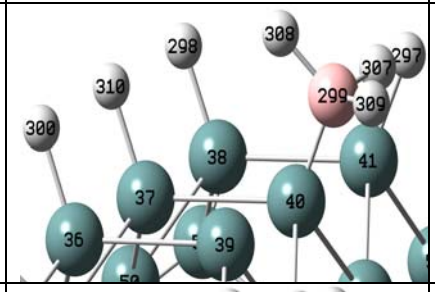	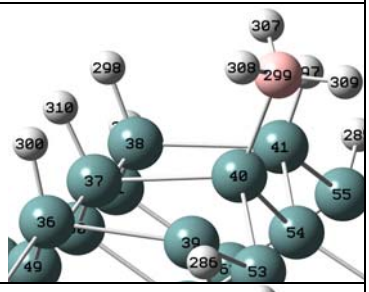
BBH_3mod1	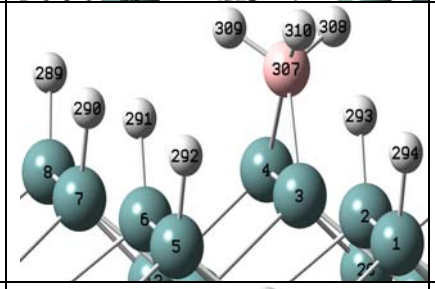	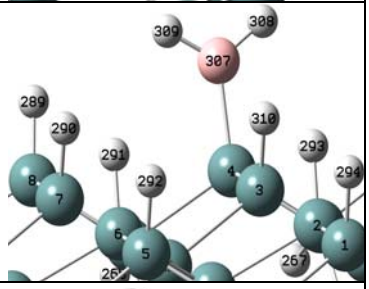
BBH_3mod2	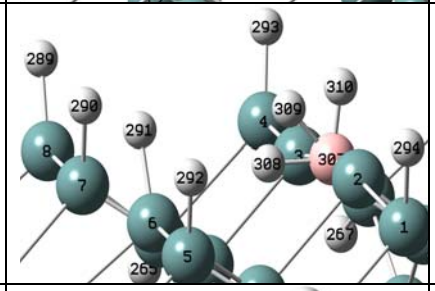	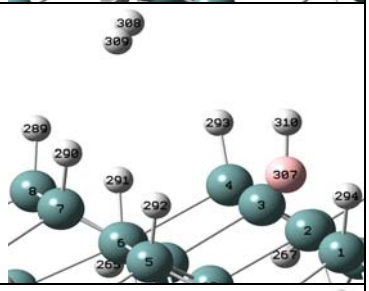
BBH_3mod3	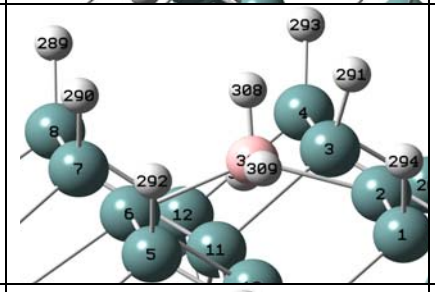	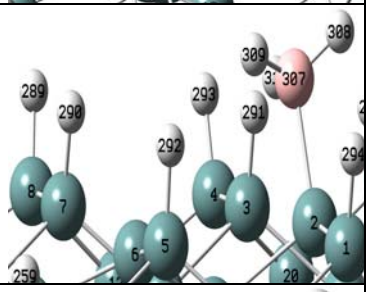
BBH_3mod4	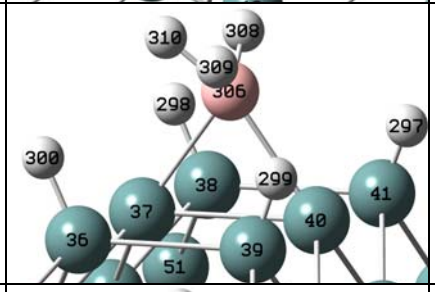	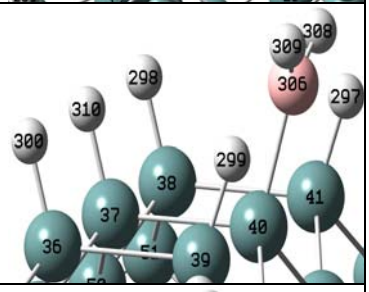
BBH_3mod5	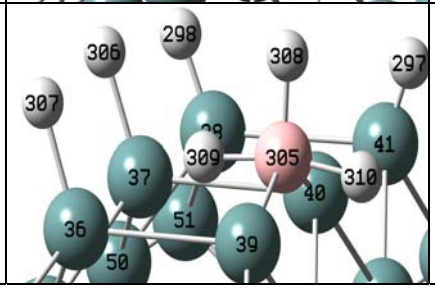	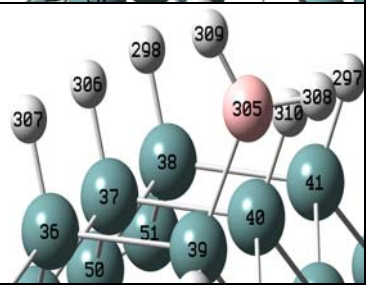

FIG. 5.7. (Cont.)

TABLE 5.2. The structural parameters, the total energy, and the binding energy of BH_3 (or BH_2 or BH), for the optimized adsorption models of BH_3 on stepped Ge(100) correspond to two dangling bonds of the surface.

Model	Bond length (A^o)			Tilt angle (degree)	Total Energy (a.u.)	Binding Energy (eV)
	Ge-B	B-H	Dimer Ge-Ge			
MBH3mod9	2.07	1.16	2.46	25.0	-369428.3148	-5.635
MBH3mod10	2.06	1.16	2.50	18.0	-369428.3222	-5.839
MBH3mod11	2.06	1.16	2.55	6.7	-369428.2825	-5.488
MBH3mod12	2.06	1.16	2.52	4.8	-369428.2990	-5.935
MBH3mod13	2.06	1.16	2.49	17.5	-369428.3187	-5.785
MBH3mod14	2.06	1.16	2.49	18.7	-369428.3005	-5.462
BBH3mod1	1.97	1.16	2.47	3.4	-369428.4090	-7.170 for BH_2
BBH3mod2	2.32	1.17	2.86	20.7	-369428.1551	-7.470 for BH
BBH3mod3	2.06	1.17	2.52	4.7	-369428.3032	-6.046
BBH3mod4	1.97	1.16	2.50	1.5	-369428.4044	-7.039 for BH_2
BBH3mod5	1.97	1.16	2.50	1.9	-369428.4052	-7.060 for BH_2

The total energies of the models in which BH_3 dissociates into BH_2 and H (BBH_3mod1, BBH_3mod4 and BBH_3mod5) are very close to each other (Table 5.2). Since the structures of the substrates of these models are different, the binding energy of BH_2 in these models are calculated to be different. According to the binding energies given in Table 5.2, the optimized BBH_3mod1 on the step down terrace is the most probable geometry explaining the BH_2+H type dissociation. The binding energy of BH_2 in BBH_3mod1 model is calculated to be -7.170eV (Table 5.2).

In optimized BBH_3mod1 model, the length and the tilt angle of the dimer bond with BH_2 molecule are found to be 1.97A^o and 3.42^o, respectively. In another dissociative model (BBH_3mod2), two H atoms are desorbed from the surface and BH is suspended between two Ge atoms on adjacent dimers. In optimized BBH_3mod2 model, the fragment of BH is suspended to Ge atoms with the binding energy of -7.470eV. Hence at this stage of BH_3 gas exposure, BH_3, BH_2, BH, and H will be appeared usually on the stepped Ge surface depending on the positions of the open bonds in front of BH_3 molecules. Besides, if BH_3 molecule decreases to BH directly as in BBH_3mod2 model, the desorption of H atoms from the surface is provided by the formation of H_2 molecules.

5.3.2 Adsorption of BH_2 on Stepped Ge(100) surface

In the next stage, the molecular adsorption of BH_2 on the surface has been confirmed by the optimization of unbridged and bridged adsorption models pictured in Fig 5.8. The total energies of the optimized bridged and unbridged models are tabulated in Table 5.3. It is found that, when BH_2 molecule is adsorbed to one of the two open bonds of Ge(100) surface directly (MBH_2mod1-MBH_2mod5), it remains on the initial adsorption bond leaving the other bond as open, after optimization. Similarly, when BH_2 makes a bridge between the open bonds on the adjacent dimers, it breaks the bridge after optimization and bond to one of the open bond leaving the other bond as open (BBH_2mod2, BBH_2mod3, BBH_2mod5). However in the other optimized bridged models (BBH_2mod1, BBH_2mod4), BH_2 saves its initial position, i.e, makes a bridge between two open Ge bonds on the same dimer. This outcomes of the optimized unbridged and bridged models have excluded the spontaneous dissociative adsorption of BH_2 on stepped Ge(100) surface. Since the molecular adsorption of BH_2 is studied directly, the binding energy of BH_2 (Table 5.3) in MBH_2mod1-MBH_2mod5 models is ~2-2.7eV lower than those (Table 5.2) in the dissociative adsorption models of BH_3. The binding energy of BH_2 in MBH_2mod1-MBH_2mod5 models are also comparable with the ones calculated for the optimized BBH_2mod2, BBH_2mod3, and BBH_2mod5 models. Since the open bond structures of the optimized unbridged (MBH2mod1-MBH2mod5) and bridged (BBH_2mod1-BBH_2mod5) models are completely different, the most probable geometry for the

Model	Initial Structure	Optimized Structure
MBH_2mod1	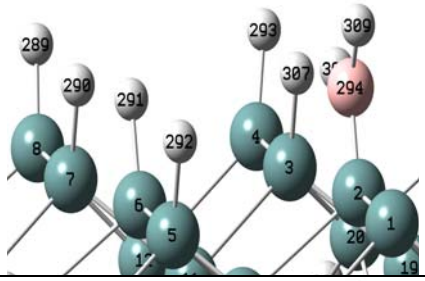	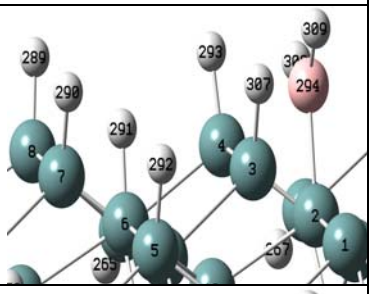
MBH_2mod2	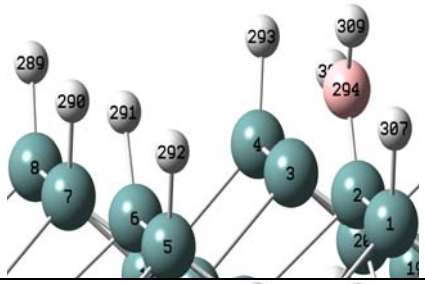	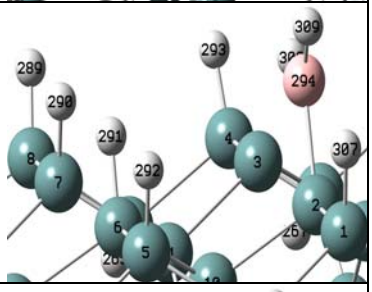
MBH_2mod3	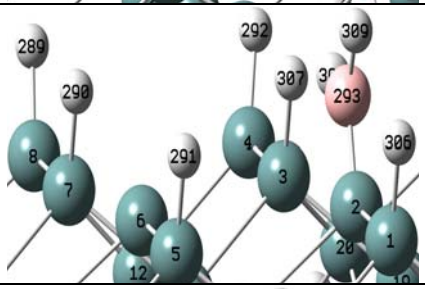	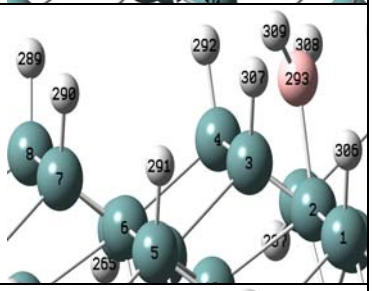
MBH_2mod4	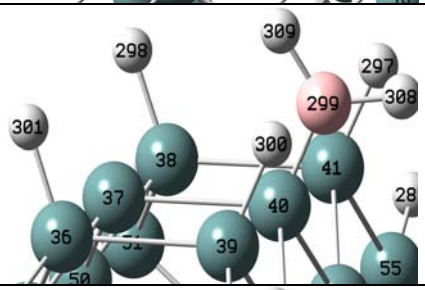	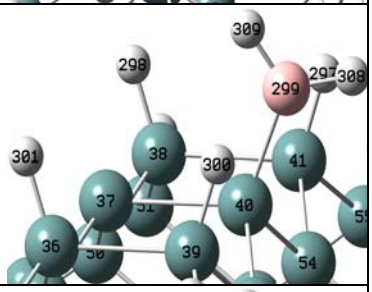
MBH_2mod5	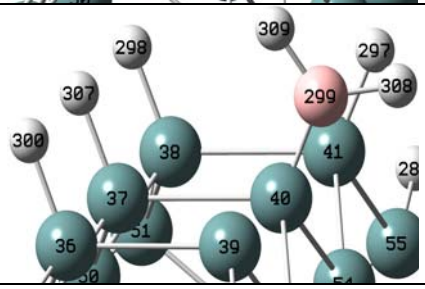	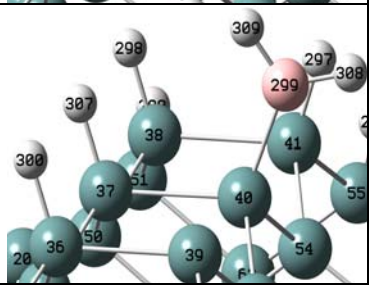

FIG. 5.8. The initial and optimized adsorption models of BH_2 on stepped Ge(100) surface.

Model	Initial Structure	Optimized Structure
BBH_2mod1	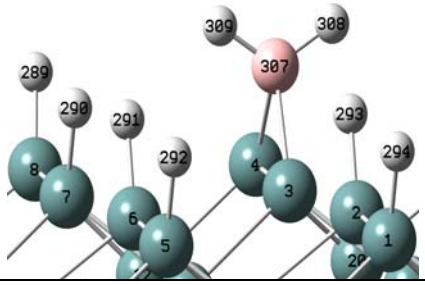	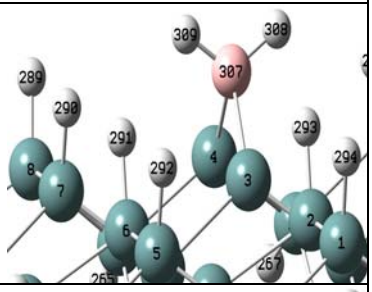
BBH_2mod2	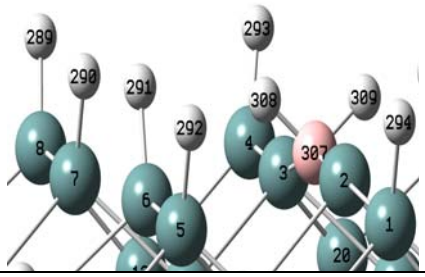	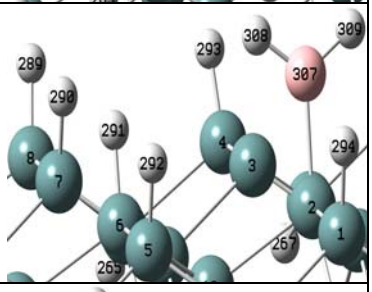
BBH_2mod3	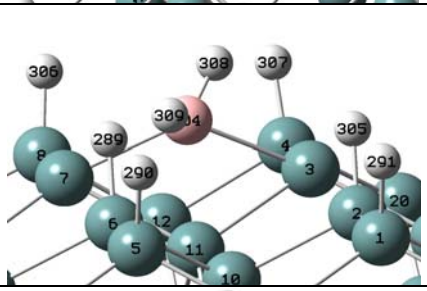	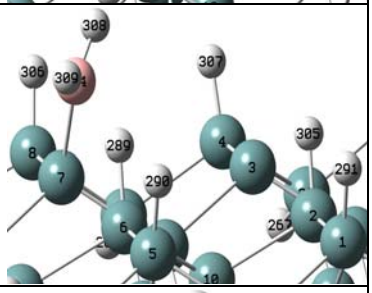
BBH_2mod4	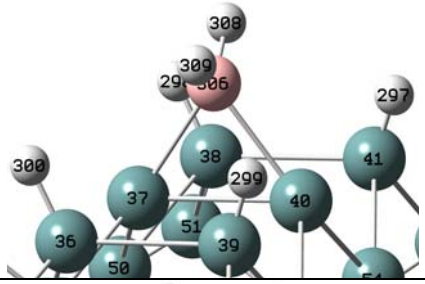	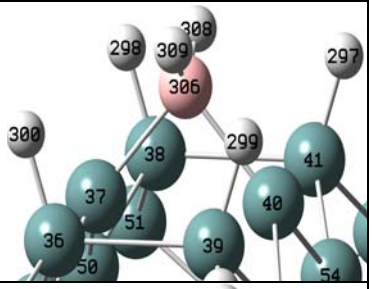
BBH_2mod5	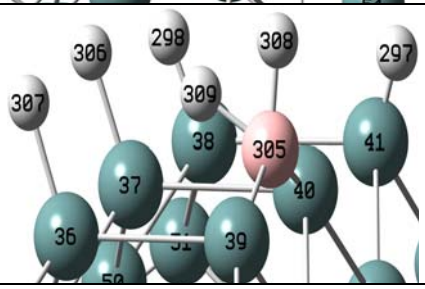	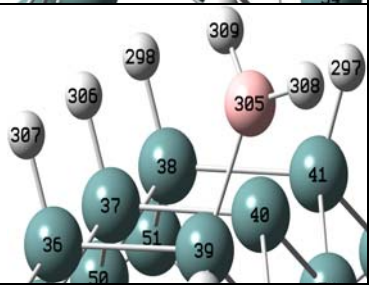

FIG. 5.8. (Cont.)

TABLE 5.3. The structural parameters, the total energy, and the binding energy of BH_2, for the optimized adsorption models of AsH_2 on stepped Ge(100) surface.

Model	Bond length (A^o)			Tilt angle (degree)	Total Energy (a.u.)	Binding Energy (eV)
	Ge-B	B-H	Dimer Ge-Ge			
MBH2mod1	1.97	1.16	2.50	1.1	-369427.7777	-8.990
MBH2mod2	1.97	1.16	2.50	0.6	-369427.7780	-9.731
MBH2mod3	1.97	1.16	2.47	4.7	-369427.7781	-9.731
MBH2mod4	1.97	1.16	2.48	1.9	-369427.7782	-9.045
MBH2mod5	1.97	1.16	2.49	1.4	-369427.7778	-9.212
BBH2mod1	2.0	1.15	2.74	4.6	-369427.7781	-9.007
BBH2mod2	1.97	1.16	2.52	0.7	-369427.7778	-9.728
BBH2mod3	1.97	1.16	2.47	4.7	-369427.7828	-9.859
BBH2mod4	2.0	1.15	2.79	0.7	-369427.7756	-8.977
BBH2mod5	1.97	1.16	2.50	1.5	-369427.7786	-9.231

adsorption of BH_2 on stepped Ge(100) surface is determined by comparing the binding energy values given in Table 5.3. The most probable adsorption model is found to be BBH_2mod3 in which BH_2 is adsorbed to the step down with the binding energy of -9.859eV. In optimized BBH_2mod3 model, BH_2 is bounded to the surface with a bond length of 1.97A^o. The length and tilt angle of the dimer bond having BH_2 molecule is 2.47A^o and 4.7^o, respectively.

5.3.3 Adsorption of BH on Stepped Ge(100) surface

In the laboratory conditions, the adsorption of BH_2 molecule on stepped Ge(100) surface has been expected to be followed by the adsorption of BH molecule when one of the H atoms of BH_2 has formed H_2 molecule with an adjacent H atom and desorbed from the surface. At his stage, the surface H atoms remained by the dissociation of BH_3 (as BH_2+H or BH+H+H) make the built up of H_2 molecules possible.

In the present work, the adsorption of BH on stepped Ge(100) surface has been modeled again by unbridged (MBHmod1-MBHmod5) and bridged (BBHmod1-BBHmod5) models on the step-down and step-up terraces. The initial and optimized adsorption models of BH are totally pictured in Fig. 5.9 by the labels of the surface Ge atoms. In unbridged models, two open bonds are considered either on the same or adjacent dimer bonds. As it is explained for AsH in the previous chapter, BH molecule adsorbed to one of the open bonds when the other bond is open. In bridged models, BH fragment makes a bridge between the surface Ge atoms either on the same or adjacent dimer bonds. It is found that BH in all optimized unbridged (MBHmod1-MBHmod5) and bridged (BBHmod1-BBHmod5) models has a tendency to make a bridge between two surface Ge. The tendency of BH to make a bridge between the surface Ge atoms is also noticed before in the spontaneous dissociation process of BH_3 on the surface of BBH_3mod2 (Fig. 5.7) model. According to the binding energies given in Table 5.4, the most probable adsorption models are obtained when BH makes a bridge between the surface Ge atoms on the same dimer bond of the step-down (BBHmod1) and step-up (BBHmod4) terraces. In optimized structures of these models, BH is bonded to two surface Ge atoms with a bond length of 1.85A^o and the binding enegy of ~ -10 eV. The optimized bridged models, BBHmod2, BBHmod3, and BBHmod5, have also indicated that BH can make a bridge between the adjacent dimers on the same or different dimer rows.

Model	Initial Structure	Optimized Structure
MBHmod1	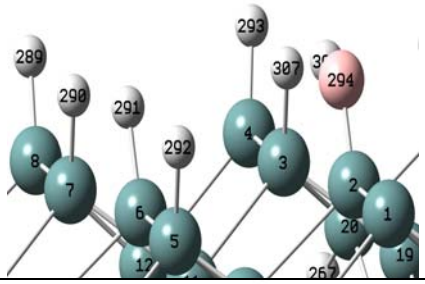	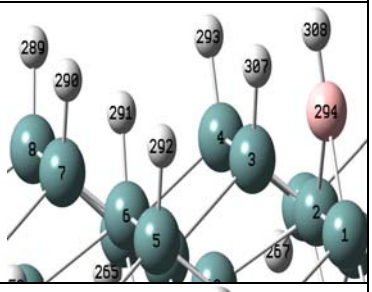
MBHmod2	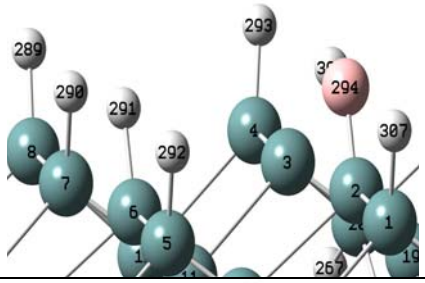	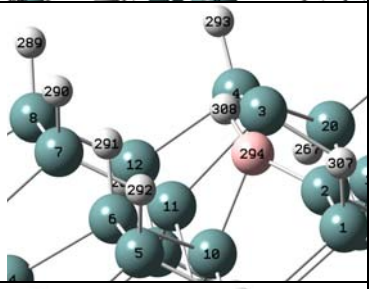
MBHmod3	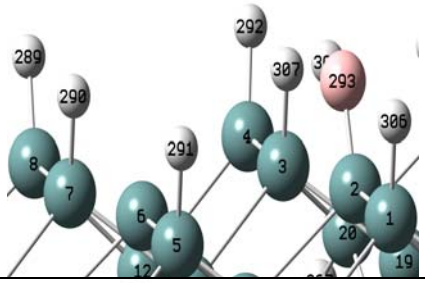	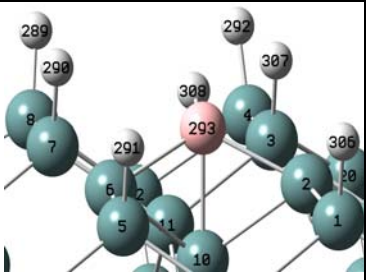
MBHmod4	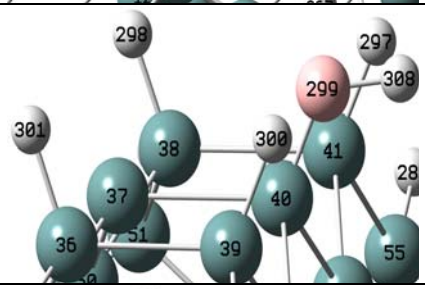	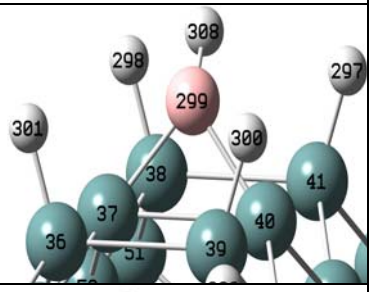
MBHmod5	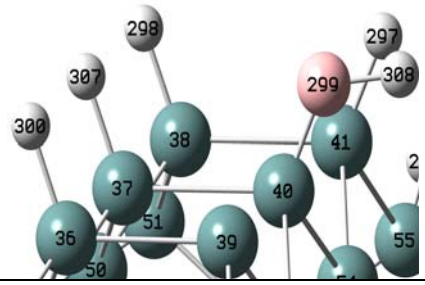	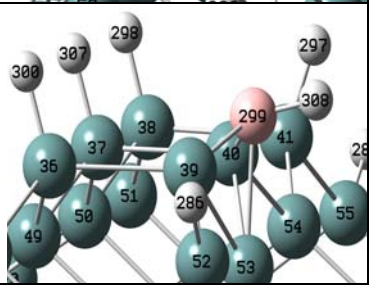

FIG. 5.9. The initial and optimized adsorption models of BH on stepped Ge(100) surface.

Model	Initial Structure	Optimized Structure
BBHmod1	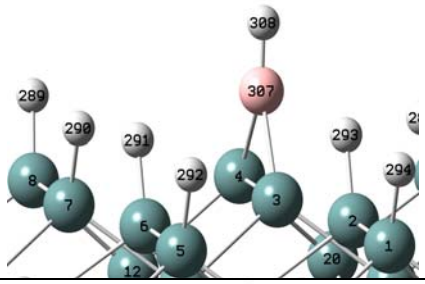	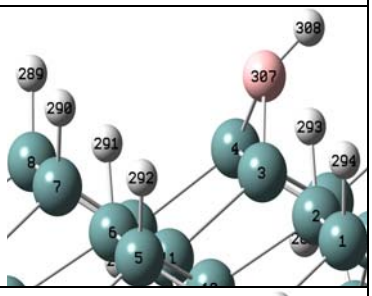
BBHmod2	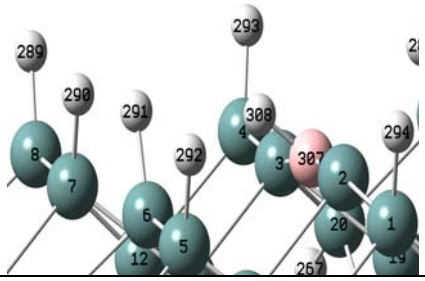	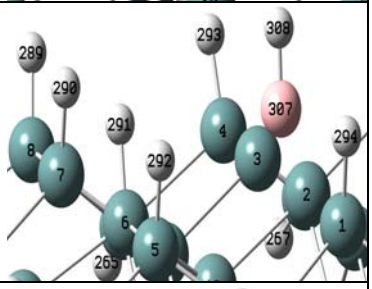
BBHmod3	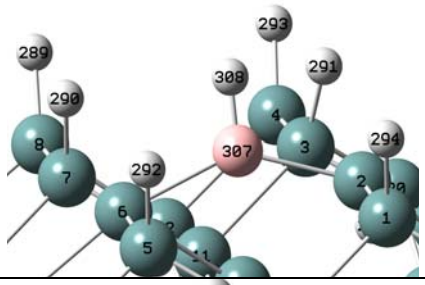	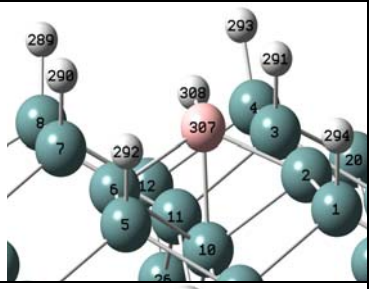
BBHmod4	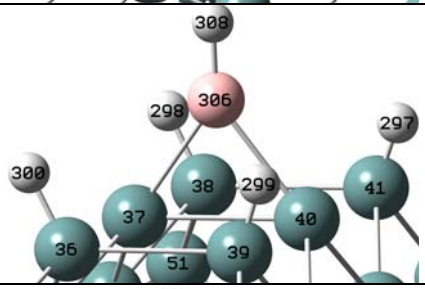	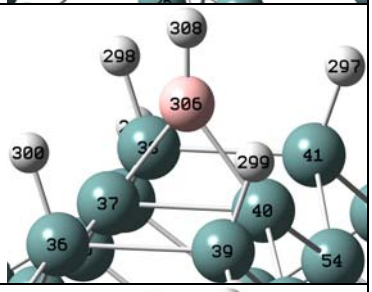
BBHmod5	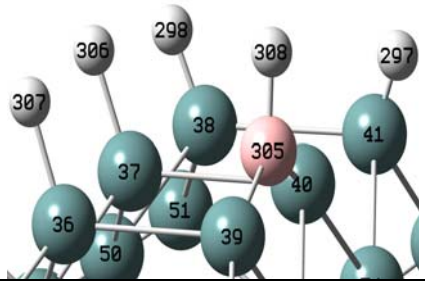	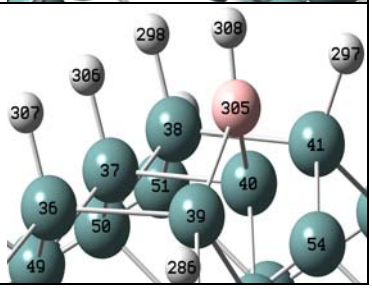

FIG. 5.9. (Cont.)

TABLE 5.4. The structural parameters, the total energy, and the binding energy of BH for the optimized adsorption models of BH on stepped Ge(100) surface.

Model	Bond length (A^o)			Tilt angle (degree)	Total Energy (a.u.)	Binding Energy (eV)
	Ge-B	B-H	Dimer Ge-Ge			
MBHmod1	1.94	1.16	2.36	0.4	-369427.1546	-9.924
MBHmod2	1.88	1.16	2.46	14.3	-369427.0218	-7.042
MBHmod3	2.09	1.16	2.49	9.7	-369427.1150	-9.573
MBHmod4	1.87	1.16	2.46	0.7	-369427.1532	-9.924
MBHmod5	2.08	1.16	2.47	8.7	-369427.1418	-9.790
BBHmod1	1.85	1.16	2.48	4.2	-369427.1610	-10.098
BBHmod2	2.32	1.17	2.86	20.7	-369427.0376	-7.470
BBHmod3	2.08	1.16	2.48	9.48	-369427.1192	-9.684
BBHmod4	1.94	1.1	2.35	0.5	-369427. 1531	-9.924
BBHmod5	2.15	1.17	2.51	10.1	-369427.1031	-8.739

5.3.4 Adsorption of B atom on Stepped Ge(100) surface

In the next stage of the doping process of stepped Ge(100) sample, BH_3 molecule of the Borane gas is expected to be reduced to B atom by

$$BH+H \longrightarrow B+H2$$

reaction. As it is considered in the previous chapter, H_2 molecule built up by H atom of BH fragment and one of the adjacent surface H atom has been desorbed from the surface. The atomic adsorption of B has been examined by again unbridged

(MBmod1-MBmod5) and bridged (BBmod1-BBmod5) models. It is examined whether the bridge model of BH (Fig. 5.9) is broken or not during the desorption of H_2 from the surface. The initial and optimized adsorption models are pictured in Fig. 5.10, and their total energies are given in Table 5.5. It is found that the direct adsorption of B on step-down and step-up terraces is not changed after optimization for unbridged models (MBmod1-MBmod5). In all these models, Boron atom is remained on one of the open bond. It is also found that, the bridge structure in BBmod1-BBmod5 models are not changed after optimization. In optimized bridged models, B atom prefers to make a bridge between two Ge surface atoms either on the same or adjacent dimers. Since the bond structures of the substrates are different, the most probable model for the adsorption of B is determined by taking the binding energy of B in these models into account. It is found that the binding energy of B has the most negative value in BBmod1. In optimized BBmod1 model, Boron atom makes a bridge between two step down Ge atoms on the same dimer bond with the binding energy of -8.977eV. In another similar bridged model of the step up terrace (BBmod4), the binding energy of B is calculated to be -8.631eV. These two bridged models indicate that the bridge structure of BH (in the previous stage) on the same dimer (Fig. 5.9) has been saved on both step-down and step-up terraces during the reduction of BH to B. The bridged structure of B on the same dimer bond of the step-down and step up terraces is characterized with the Ge-B bond length of $\sim 1.76A^o$ and $1.94A^o$, respectively. The length of the dimer bond in the most probable bridged models of B (BBmod1, BBmod4) is found to be 2.62 and $2.40A^o$ for the adsorption on step- down and step- up, respectively. For the same structures, BBmod1 and BBmod4, the tilt angle of the dimer bond having B atom bridge is calculated to be 4.66^o and 0.71^o, respectively.

Model	Initial Structure	Optimized Structure
MBmod1	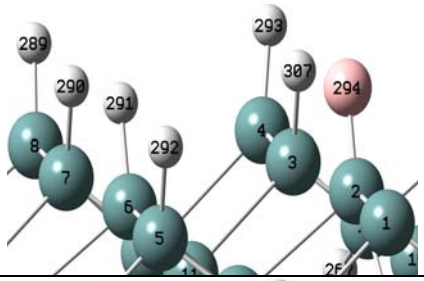	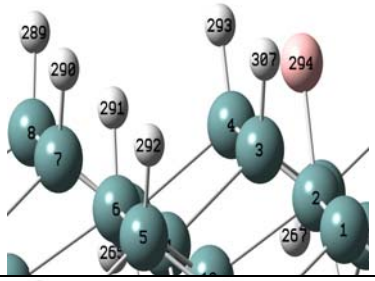
MBmod2	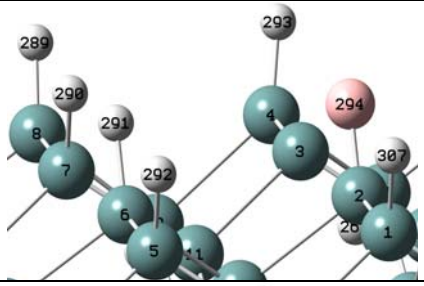	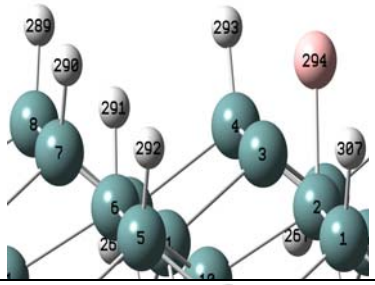
MBmod3	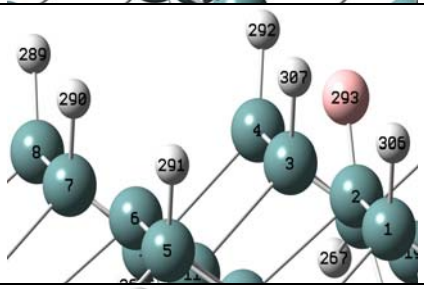	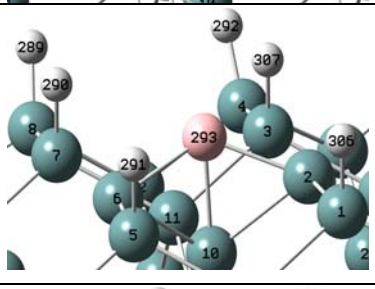
MBmod4	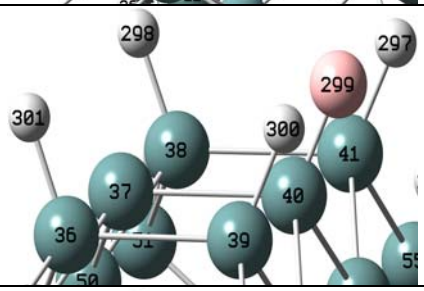	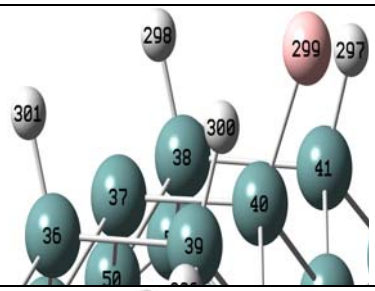
MBmod5	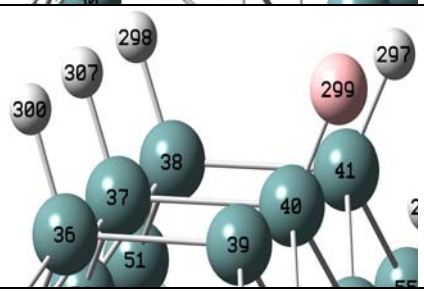	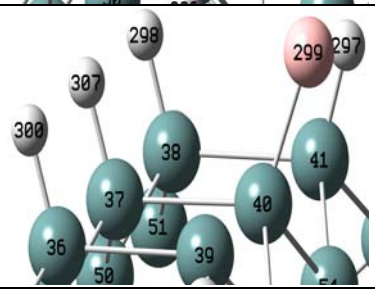

FIG. 5.10. The initial and optimized adsorption models of B atom on stepped Ge(100) surface.

Model	Initial Structure	Optimized Structure
BBmod1	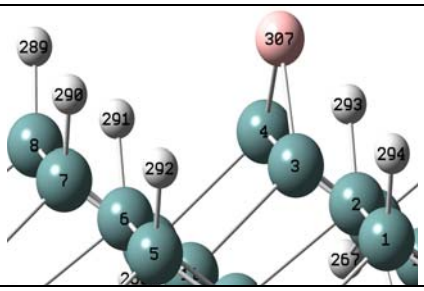	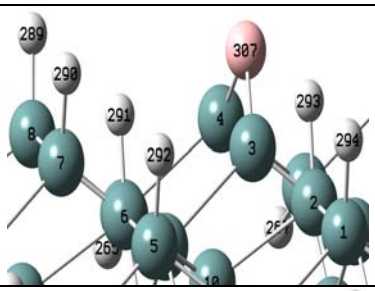
BBmod2	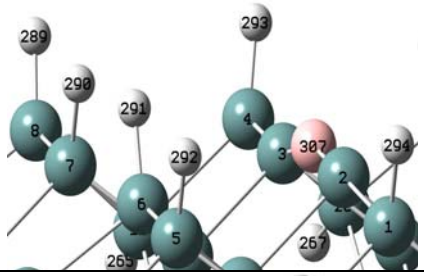	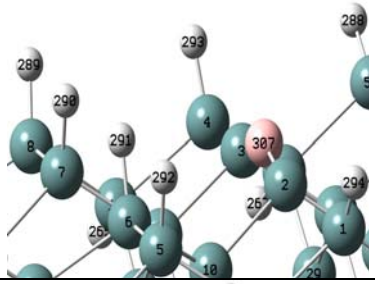
BBmod3	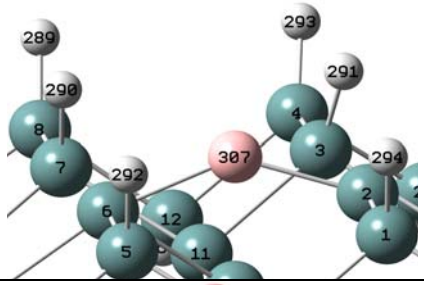	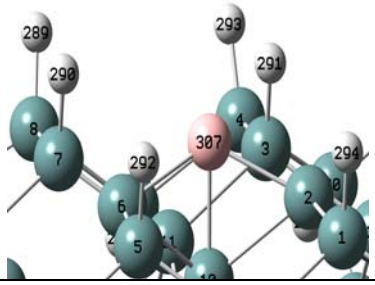
BBmod4	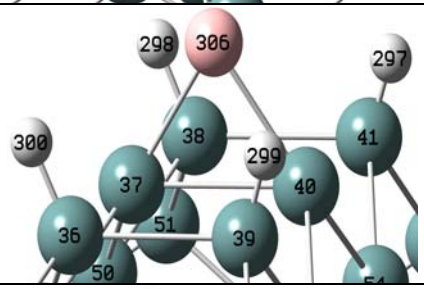	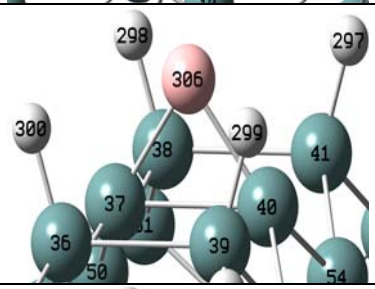
BBmod5	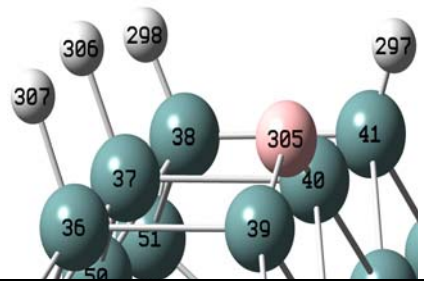	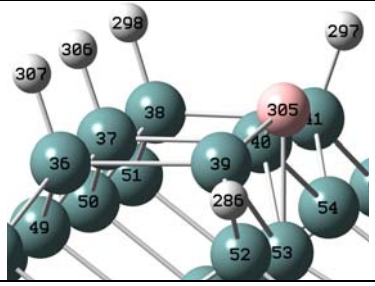

FIG. 5.10. (Cont.)

TABLE 5.5. The structural parameters, the total energy, and the binding energy of B, for the optimized adsorption models of B on stepped Ge(100) surface.

Model	Bond length (A^o)		Tilt angle (degree)	Total Energy (a.u)	Binding Energy (eV)
	Ge-B	Dimer Ge-Ge			
MBmod1	1.93	2.51	1.8	-369426.4733	-7.820
MBmod2	2.09	2.51	0.8	-369426.4588	-8.158
MBmod3	2.06	2.50	9.4	-369426.4683	-8.408
MBmod4	1.92	2.49	2.5	-369426.4736	-7.867
MBmod5	1.92	2.50	2	-369426.4739	-8.053
BBmod1	1.76	2.62	4.7	-369426.5158	-8.977
BBmod2	1.84	3.64	16.6	-369426.4458	-7.801
BBmod3	2.06	2.49	9.2	-369426.4724	-8.522
BBmod4	1.94	2.40	0.7	-369426.5017	-8.631
BBmod5	2.04	2.49	8.2	-369426.4941	-8.602

5.3.5 Diffusion of B atom through the layers of Stepped Ge(100) surface

At this stage of the present work, the p-type stepped Ge(100) is simulated by the diffusion of the B atoms towards the layers of the surface. As it is considered for the diffusion of As atoms in the previous chapter, during the diffusion, B atoms can have a sit between the surface Ge atoms breaking the Ge-Ge bonds or occupy substitutional or interstitial places of the stepped Ge(100) surface. The setting of B atoms between the surface Ge atoms on the step-down and step-up terraces is defined

by BBBmod1 and BBBmod2 structures, respectively. The initial and optimized geometries of these models are pictured in Fig 5.11. The total energies and the binding energies of the fragments for the optimized models obtained at this stage are given in Table 5.6. It is found that, the optimized BBBmod1 and BBBmod2 models show different structures than the optimized structures of BBAsmod1 and BBAsmod2; in BBBmod1 and BBBmod2 models, B atom makes a bridge between the layers of step-down and step-up terraces, respectively, breaking the Ge-Ge bond. The binding energy of B in BBBmod1 and BBBmod2 structures are calculated to be -6.367 and -6.245eV, respectively (Table 5.6). The other models, SBmod1-SBmod3 and IBmod1-IBmod3, given in Fig. 5.11 have defined the substitutional and interstitial occupation sites of B atoms on the stepped Ge(100) surface, respectively. In SBmod1-SBmod3 models, one site of Ge atom in the layers of the stepped Ge(100) surface is initially occupied by B atom. The main structures of these models are not changed after optimization. The binding energy of B is calculated to be -20.155, -23.116 and -13.080eV in optimized SBmod1-SBmod3 structures, respectively (Table 5.6). It is found that the initial structures of IBmod1-IBmod3 models are changed mainly after optimization. The IBmod1 model in which B atom is interstitially in the valley between the step-down and step-up terraces is converted to a bridge model between the layers of the terraces by optimization (Fig. 5.11). Similarly, the IBmod2 model in which B atom interstitially between the 1st and 2nd layers of the step-down terrace is changed to a bridge model between the adjacent Ge atoms on the 1st and 2nd layers of the step-down terrace (Fig. 5.11). It is also found that, the interstitial site of B in IBmod3 has not been saved after optimization. In Optimized IBmod3 structure, B atom has left its interstitial site and gone out from the layers of the surface to make a bridge between the surface Ge atoms on the same dimer. The breakdown of the interstitial models (IBmod1-IBmod3) have indicated that B atoms do not prefer the interstitial sites during the doping process of the stepped Ge(100) surface. The binding energy of B is calculated to be -6.142, -8.552 and -7.031eV (Table 5.6) in optimized IBmod1, IBmod2 and IBmod3 structures, respectively. According to the results given above, the binding energy of B in SBmod1-SBmod3 structures are all more negative with respect to that in all optimized bridged models (BBBmod1-BBBmod2, IBmod1-IBmod3). This outcome

Model	Initial Structure	Optimized Structure
BBBmod1	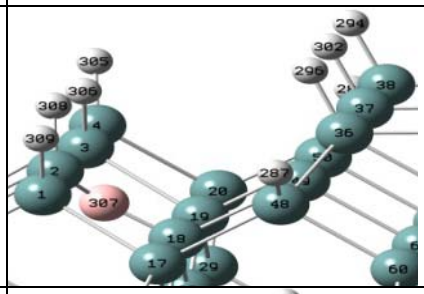	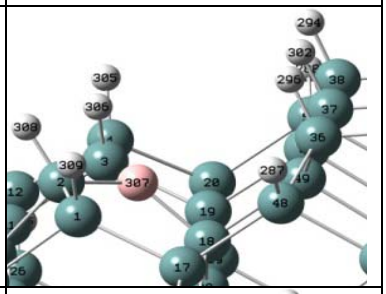
BBBmod2	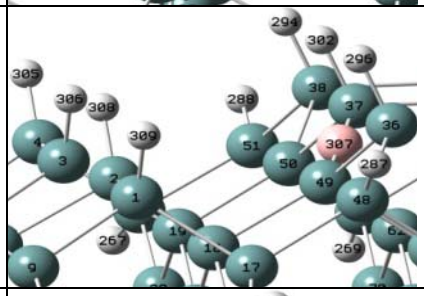	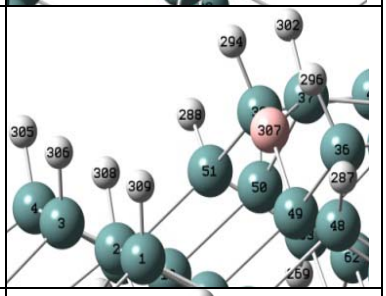
SBmod1	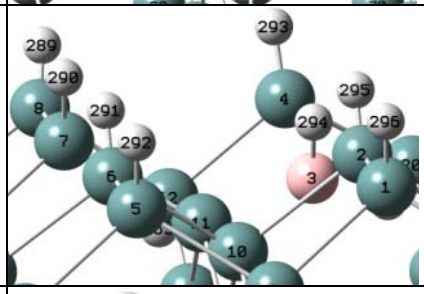	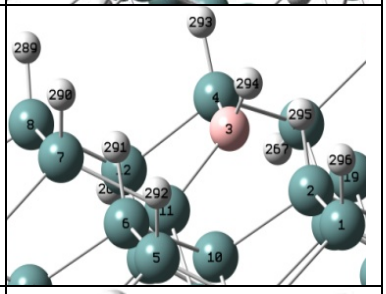
SBmod2	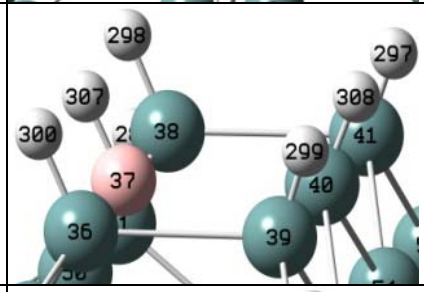	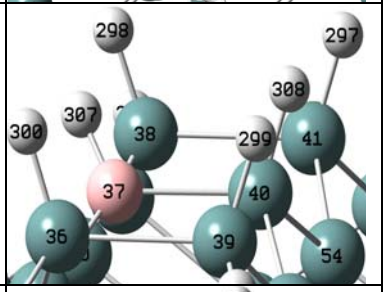
SBmod3	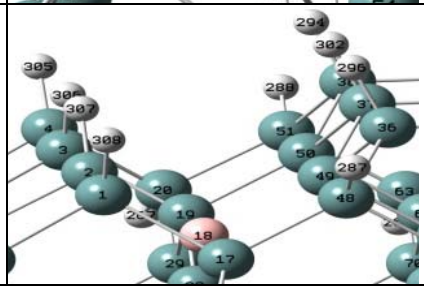	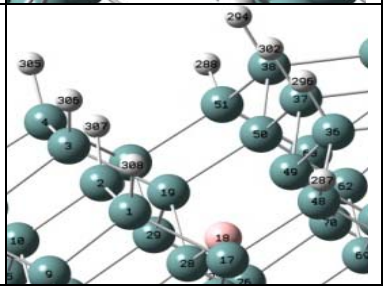

FIG. 5.11. The initial and optimized diffusion models of B atom on stepped Ge(100) surface.

Model	Initial Structure	Optimized Structure
IBmod1	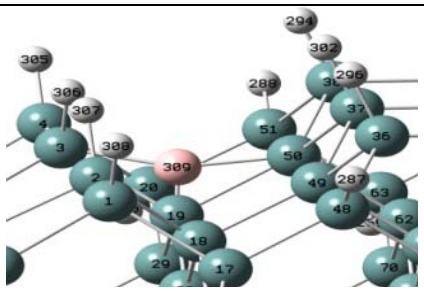	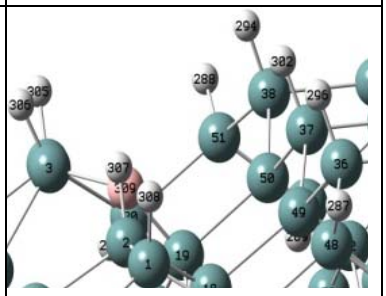
IBmod2	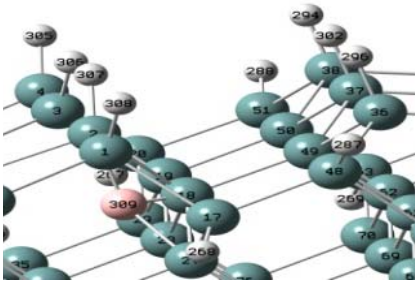	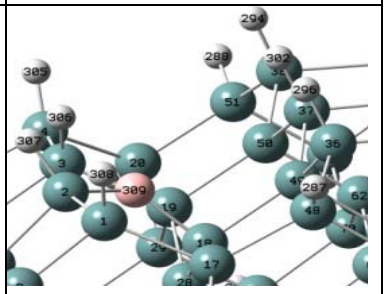
IBmod3	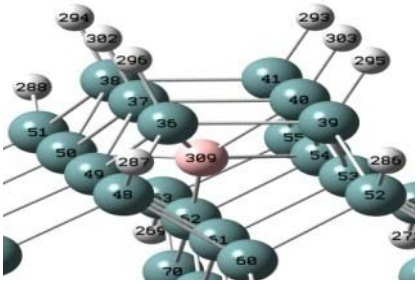	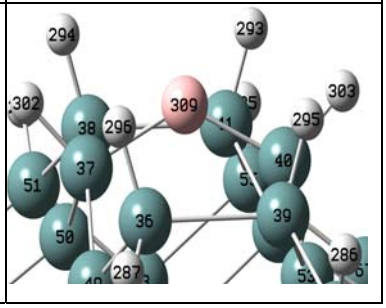

FIG. 5.11. (Cont.)

illustrates that, in the adjusted laboratory conditions, B atoms can temporarily make bridge models between the adjacent Ge atoms on the 1st and 2nd layers of the stepped down terrace, but they permanently prefer the substitutional sites with the most negative binding energies, during the diffusion.

In the present work, the density of states (DOS) of optimized SBmod2 is plotted in Fig. 5.12 for the states around the highest occupied molecular orbitals (HOMO) and lowest unoccupied molecular orbitals (LUMO) of the stepped Ge(100) surface. The DOS of stepped Ge(100) surface based on single point total energy calculations is also included to Fig. 5.12 for comparison. Both profiles seeing in Fig. 5.12 are generated by Gaussian broadening technique with broadening of 0.2eV. This

TABLE 5.6. The structural parameters, the total energy, and the binding energy of B, for the optimized diffusion models of B atom on stepped Ge(100) surface.

Model	Bond length (A^o)		Tilt angle (degree)	Total Energy (a.u)	Binding Energy (eV)
	Ge-B	Dimer Ge-Ge			
BBBmod1	1.91	2.45	11.2	-369427.8506	-6.367
BBBmod2	1.91	2.43	8.8	-369427.8461	-6.245
SBmod1	2.16(dimer) 2.15(back)	---	21.5	-367375.8912	-20.155
SBmod2	2.14(dimer) 2.13(back)	---	18.8	-367375.8970	-23.116
SBmod3	2.22	---	---	-367375.6449	-13.080
IBmod1	1.91	2.44	14.1	-369427.8423	-6.142
IBmod2	1.92	2.40	9.5	-369427.9309	-8.552
IBmod3	1.97	---	---	-369427.8749	-7.031

broadening level is found to be sufficient to observe the features around HOMO and LUMO clearly. As it is mentioned in chapter IV, the passivation of the all dangling bonds of the stepped Ge(100) surface models with and without B atom provide an obvious energy gap between LUMO and HOMO. This energy gap corresponds to the optical gap between the conduction and valance band of bulk Ge. Since the stepped Ge(100) surface is defined by limited number of Ge atoms in the considered cluster models, the energy difference between LUMO and HUMO (~10eV) is much greater than the actual energy gap of bulk Ge (0.67eV) structure.

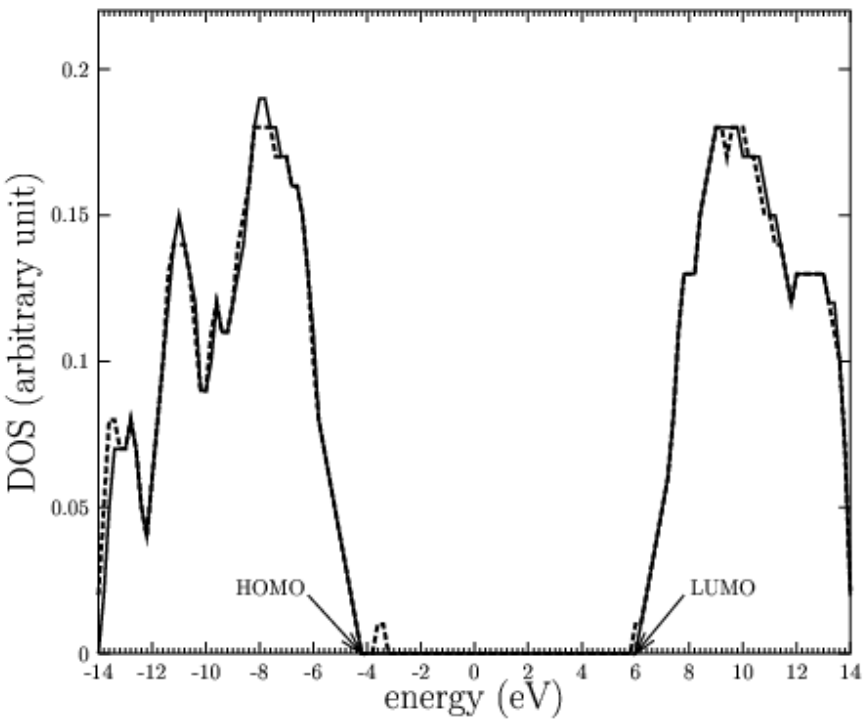

FIG. 5.12. DOS of optimized stepped Ge(100) surface models with (dotted line) and without (solid line) B atom.

Fig. 5.12 is important to see the effect of B atom on DOS of stepped Ge(100) surface; while the energy range between LUMO and HOMO of stepped Ge(100) surface is empty, a feature located at about -3.7eV is obtained by the addition of B atom to the substitutional site of the stepped Ge(100) surface (SBmod2 model). Therefore the substitutional B atom initiates the doping process of stepped Ge(100) surface by giving a feature very close to the HOMO. This feature of B states in Fig. 5.12 defines the acceptor energy level of p- type stepped Ge(100) surface. As it is mentioned in the previous chapter, the small ratio between the number of B atom and Ge atoms in the SBmod2 model (1/180) gives a very small B states height with respect to the height of the Ge states. The B acceptor energy level is presently calculated to be ~0.4eV (referenced to HOMO edge) with respect to the literature value of 10.4meV (referenced to the valance band edge of bulk Ge) [60]. The present total energy calculations with limited number of cluster atoms point out the existence of B acceptor energy level, but it is found to be insufficient for the determination of the exact energy value of the acceptor level.

5.4 Conclusion

In the literature, although a considerable experimental efforts [2, 6, 20-22, 25] have been reported on the growth of p- type flat Ge(100) surface by B_2H_6 gas flow, as far as the author knows, there isn't any theoretical or experimental work examining the doping of the vicinal (stepped) Ge(100) surface. Because of that, the adsorption and decomposition steps of BH_3 (fragment of B_2H_6) obtained in the present work are compared only with the corresponding steps of BH_3 defined experimentally on the growth of p-type flat Ge(100) surface. In these experimental works [2, 6, 20-22, 25], the decomposition steps of B_2H_6 were not analyzed step by step, but especially in Ref. [21], the doping process was controlled by temperature – programmed desorption spectra (TPD) measurements for different B atom concentrations provided by different fluxes of B_2H_6 gas source and substrate temperature. The α peaks (α_1, α_2, α_1^*, α_2^*) observed in TPD spectra of this work [21] in the range of (200-350°C) were associated with the desorption of H atoms from the Ge(100) surface. This outcome strongly indicates the dissociation of BH_3 molecules on Ge(100) surface occur by the heat threatment. Moreover, the H peaks of TPD spectra observed at different substrate temperatures illustrate the step by step dissociation as it is determined in the present work. The high probability obtained presently for the first step dissociation of BH_3 into both BH_2+H and BH+H_2 can be explained by much coordination around the step edge of the stepped Ge(100) to initiate the dissociation. On the other hand, in a very recent work [20], B adsorption on Ge surface was demonstrated to be first increased with increasing B_2H_6 exposure time at 100°C and finally saturated with concentration of $6x10^{14}/cm^2$. Since the concentration of irregular vacancies (empty Ge sites) in Ge sample is limited, the saturation of B atoms concentration on Ge surface was explained as the adsorption of B atoms at Ge surface sites mainly. The saturation of B atoms concentration on Ge surface was also identified in another recent work [6] at 400°C for different flux of B_2H_6 gas flow. These two experimental results [6, 20] have confirmed another result of the present work; B atoms prefer to occupy empty Ge sites instead of interstitial sites of the surface.

CHAPTER 6

CONCLUSION

In this project, a systematic theoretical study has been introduced on the dissociation paths of arsine (AsH_3) and diborane (B_2H_6) gas molecules on stepped Ge (100) surface. The arsine and diborane gas structures are widely used n- and p- type dopant sources for Ge, respectively. The determination of the dissociation paths of the dopant fragments might be an important preliminary step to control the doping processes of the substances. It may facilitate to fix the laboratory conditions, such as the flow rates and the pressures of the dopant sources, the temperature and the pressure of the substances.

The doping processes of the stepped Ge (100) surface by AsH_3 and B_2H_6 gas flow have been modeled by the possible adsorption and dissociation models. These models considered for the dissociation paths of the dopant fragments on stepped Ge (100) surface have been simulated by a substrate Ge cluster having (2x1) and (1x2) asymmetric dimerized domains separated by kink free S_A type step. The most probable adsorption and dissociation models of the AsH_3 and B_2H_6 molecules on stepped Ge (100) surface have been determined by the local minimum energy and /or binding energy calculations based on Hartree-Fock theory.

The total energy calculations have shown that, the step region (both up and down terraces) of the stepped Ge (100) surface has the most attractive sites for the initial stage of the adsorption for AsH_3 molecules. The adsorption of AsH_3 molecule on the sites of the up and down terraces of the step has been provided by the molecular

suspension when there is only one dangling bond on the surface. But, when there are at least two open bonds either on the same or different dimers adjacent to each other, AsH_3 molecule makes an actual bond with the Ge surface; it is adsorbed directly (AsH_3) or dissociatively (AsH_2+H) to the surface having initially two dangling bonds on the same or adjacent dimers, respectively. This is the common result fixed by the binding energies of the considered models for both up an down terraces of the stepped Ge (100) surface. Since the doping processes have been initialized with the cleaved and cleaned substrate surfaces, all the surface bonds should be considered to be available for adsorption. Therefore both molecular and dissociative adsorptions of AsH_3 molecule will be possible and the stepped Ge surface will have H atoms in additions to both AsH_3 and AsH_2 fragments at the initial stage of the doping process. The same result has been also obtained by the other adsorption models in which AsH_3 makes a bridge between the dangling bonds; AsH_3 is adsorbed molecularly and dissociatively on the same and adjacent dimers, respectively breaking the bridge bonds. This outcome has also indicated that AsH_3 and AsH_2 molecules do not prefer the bridge structure at the first stage of the adsorption. The H atoms left by the dissociation of AsH_3 molecules can be either bounded to one of the open surface bonds or desorbed from the surface as H_2 molecules if they are adjacent to other H atoms which are already on the surface by the previous dissociations.

In the next stage, it is found that the fragments of AsH_3 molecules (AsH_2 molecules) make a bridge between the available two dangling bonds on the same dimers by leaving one of the H atoms (AsH). This result has been obtained for all optimized bridged and unbridged models considered on the up and down terraces of the step. The tendency of AsH to the bridged model was also identified for the bridges between the rows of dimers, but, the binding energy of AsH is determined to be less negative in these models. This result has indicated that AsH can prefer the bridged structures on the adjacent dimers if only the other dangling bond of its dimer is not available. Therefore depending on the available open bonds of the Ge surface, AsH_3, AsH_2, and AsH molecules in the unbridged and bridged structures, respectively will be appeared on the surface. As it is considered above, the H atoms left by AsH_3 and AsH_2 molecules can be bonded to the open bonds or desorbed from the surface as H_2.

The present total energy calculations have revealed that the AsH fragment has saved its bridge structure on the dimers of both step-down and step-up terraces when it has lost its H. However, the bridge structures of AsH between the adjacent dimers have been found to be broken during the reduction of AsH to As. Therefore at the end of the dissociation steps As atom in the bridge and unbridged structures will be appeared on the stepped Ge (100) surface. Since AsH_3 molecules have been continuously provided in the doping process by arsine gas flow AsH_3, AsH_2, AsH fragments and H atoms can be totally on the surface in addition to As atoms.

In the last stage of the doping process, As atoms diffuse towards the layers of the stepped Ge (100) surface. According to the optimized models As atoms can make bridges between the Ge atoms on adjacent layers of the substrate when they are diffusing. The total energy calculations have displayed that the As atoms have the most negative binding energy when they occupy the empty sites (irregular vacancies) of the layers of the stepped Ge(100).

The dissociation path of the AsH_3 molecule on stepped Ge(100) surface can be outlined by the following steps:

1- AsH_3---stepped Ge(100) $\longrightarrow$ AsH_3 (unbridged)+stepped Ge(100)

or

AsH_3---stepped Ge(100) $\longrightarrow$ AsH_2 (unbridged)+H+stepped Ge(100)

AsH_2 (unbridged)+H+stepped Ge(100) +H $\longrightarrow$ AsH_2 (unbridged)+H_2+stepped Ge(100)

2- AsH_2 (unbridged)+stepped Ge (100) $\longrightarrow$ AsH (bridged)+H+stepped Ge(100)

AsH (bridged)+H+stepped Ge(100) +H $\longrightarrow$ AsH (bridged)+H_2+stepped Ge(100)

3- AsH (bridged)+stepped Ge (100) $\longrightarrow$ As (bridged)+H+stepped Ge(100)

As (bridged)+H+stepped Ge(100) +H $\longrightarrow$ As (bridged)+H_2+stepped Ge(100)

4- As (bridged)+stepped Ge (100) $\longrightarrow$ As (substitutional)+stepped Ge(100)

The doping process of the stepped Ge(100) surface by p -type dopants have been simulated by the dissociation steps of the B_2H_6 gas molecule. In the present work, first the dissociation of B_2H_6 has been investigated independent of the substrate. It is found that diborane gas molecule dissociates into two BH_3 molecules by external energy of ~1.3eV. In the literature, this first dissociation step was provided by light energy:

B_2H_6+ ~1.3eV (light energy) $\longrightarrow$ BH_3+BH_3

The total energy calculations have shown that, BH_3 fragments departed from B_2H_6 molecule have suspended on the step down terrace of the Ge(100) surface when there is only one dangling bond on the surface. It is found that the actual adsorption of BH_3 on the surface has been provided when at least two surface bonds either on the same or adjacent dimers are open. At the first stage of the adsorption, BH_3 molecules have been adsorbed to the surface either directly or dissociatively, due to the number of initial adsorption bonds. When the adsorption has been satisfied by a single adsorption bond, BH_3 doesn't change its structure (direct adsorption). But, when BH_3 molecule adsorbs to the surface via double bonds (on the same or adjacent dimers) like in the initial bridge models, BH_3 molecule dissociates into BH_2+H or BH+H_2. Therefore at the first step of the adsorption of BH_3, the BH fragment will be appeared on the stepped Ge(100) surface in addition to BH_3, BH_2 molecules and H atoms. This remarkable result has showed that dissociation of BH_3 on Ge(100) surface can be easier than AsH_3's. The fragments, BH_3, BH_2 and BH are found to be bounded to the surface by a single and double adsorption bonds (bridged model), respectively in the optimized models. This outcome has been confirmed with the

optimization of the direct adsorption models of BH_2 and BH. At this step of BH_3 adsorption, desorption of H atoms (in H_2 structure) from the surface has been obviously determined during the reduction of BH_3 to BH.

The most probable adsorption model of BH in bridged structure has been determined to be not changed when H atom is left; the surface B atoms have always preferred to make a bridge between two step down or two step up Ge atoms on the same dimers. The tendency of B atoms to make bridge structures between the Ge atoms of the adjacent layers has been also determined for the diffusion steps. But for the diffusion steps, the most negative binding energy of B atom has been calculated when B atoms have occupied the Ge sites in the layers of the substrate substitutionally.

The dissociation path of the BH_3 molecule on stepped Ge(100) surface can be outlined by the following steps:

1- BH_3---stepped Ge(100) $\longrightarrow$ BH_3 (unbridged)+stepped Ge(100)

or

BH_3---stepped Ge(100) $\longrightarrow$ BH_2 (unbridged)+H+stepped Ge(100)

BH_2 (unbridged)+H+stepped Ge(100) +H $\longrightarrow$ BH_2 (unbridged)+H_2+stepped Ge(100)

or

BH_3---stepped Ge(100) $\longrightarrow$ BH (bridged)+H_2+stepped Ge(100)

2- BH_2 (unbridged)+stepped Ge (100) $\longrightarrow$ BH (bridged)+H+stepped Ge(100)

BH (bridged)+H+stepped Ge(100) +H $\longrightarrow$ BH (bridged)+H_2+stepped Ge(100)

3- BH (bridged)+stepped Ge (100) $\longrightarrow$ B (bridged)+H+stepped Ge(100)

B (bridged)+H+stepped Ge(100) +H $\longrightarrow$ B (bridged)+H_2+stepped Ge(100)

4- B (bridged)+stepped Ge (100) $\longrightarrow$ B (substitutional)+stepped Ge(100)

The total most probable unbridged adsorption models presented in this work are all obtained by the adsorption of AsH_3 and AsH_2 (or BH_3 and BH_2) on buckled down side of the Ge dimer bonds. The small tilt angle initially defined for the asymmetric dimer bonds of the stepped Ge(100) surface is found to be increased in all optimized adsorption models in which one of the dangling bond of the corresponding dimer is open. Besides, the length of the dimer bond directly related to the adsorption is decreased when the adsorption is strong.

In the present work, The DOS have been also calculated for the stepped Ge(100) surface which is substitutionally occupied by As (or B) atom. The feature of As (or B) states obtained very close to the LUMO (or HOMO) in DOS spectrum has showed the beginning of the n – (or p-) type doping of the stepped Ge(100) surface.

In this project, a prototype study has been introduced for the adsorption and dissociation steps of the AsH_3 and B_2H_6 on the stepped Ge(100) surface and the diffusion of As and B atoms in the layers of the stepped Ge(100) surface. Since the periodic boundary conditions are not taken into account the numerical outcomes are not compared directly with the corresponding experimental results. But the adsorption, dissociation and diffusion structures obtained in this work were confirmed either by experimental images or quantities given in the literature. The present work can be evaluated as a preliminary work for the first principles calculations and the experimental works dealing with the kinematics of the AsH_3 and BH_3 dopant molecules on the stepped Ge(100) surface.

REFERENCES

[1] H. Shang, H. Okorn-Schmidt, K. K. Chan, M. Copel, J. A. Ott, P. M. Kozlowski, S. E. Steen, S. A. Cordes, H. S. P. Wong, E. C. Jones, and W. E. Haensch, Tech. Dig. Int. Electron Devices Meet. 441 (2002).

[2] A. B. Greytak, L. J. Lauhon, M. S. Gudiksen, and C. M. Lieber, Appl. Phys. Lett. 84, 4176 (2004).

[3] C.O. Chui, and K. C. Saraswat,"Germanium Nanodevices and Technology" in Advanced Gate Stacks for high mobility semiconductors, vol. 27, chp. 13, p 293, edited by A. Dimoulas, E. Gusev, P. C. Mc Intyre, and M. Heyns, Springer deries in advanced microelectronics, Springer Berlin Heidelberg, (2007).

[4] R. E. Jones, S. G. Thomas, S. Bharatan, R. Thoma, C. Jasper, T. Zirkle, N. V. Edwards, R. Liu, X. D. Wang, Q. Xie, C. Rosenblad, J. Ramm, G. Isella, H. von Känel, J. Oh, and J. C. Campbell, Tech. Dig. Int. Electron Devices Meet. 793 (2002).

[5] P. R. Bandaru, S. Sahni, E. Yablonovitch, J. Liu, H. Jun Kim, and Y. H. Xie, Mater Sci Eng. B 113, 79 (2004).

[6] J. M. Hartmann, J. F. Damlencourt, Y. Bogumilowicz, P. Holliger, G. Rolland, and T. Billon, J. Cryst. Growth 274, 90 (2005).

[7] W. C. Dunlap Jr., Phys. Rev. 94, 1531 (1954).

[8] J. S. Saby, and W. C. Dunlap Jr., Phys. Rev. 90, 630 (1953).

[9] F. A. Trumbore, Bell Syst. Tech. J. 39, 169 (1960).

[10] P. V. Pavlow, and V. A.Uskov, Soviet Phys. Solid State 8, 2377 (1967).

[11] T. Canneaux, D. Mathiot, J. P. Ponpon, S. Roques, S. Schmitta, and C. Dubois, Mater Sci Eng. B 154–155, 68 (2008).

[12] A. Satta, E. Simoen, T. Clarysse, T. Janssens, A. Benedetti, B. De Jaeger, M. Meuris, and W. Vandervorst, Appl Phys Lett. 87, 172109 (2005).
[13] S. K. Mandal, S. Das, and C. K. Maiti, Mat Sci Semicon Proc. 8, 353 (2005).
[14] R. J. Zambrano, F. A. Rubinelli, W. M. Arnoldbik, J. K. Rath, and R. E. I. Schropp, Sol. Energ Mat. C 81, 73 (2004).
[15] L. Radic, A. F. Saavedra, K. S. Jones, and M. E. Law, J. Vac. Sci. Technol. B 24, 478 (2006).
[16] M.S. Carroll, and R. Koudelka , Semicond Sci Tech. 22, S164 (2007).

[17] S. Brotzmann, and H. Bracht, J Appl Phys. 103, 033508 (2008).

[18] P. Tsouroutas, D. Tsoukalas, I. Zergioti, N. Cherkashin, and A. Claverie, Diffusion and activation of phosphorus in germanium. Mat Sci Semicond Proc., (2008). doi:10.1016/j.mssp.2008.09.005.

[19] Y. Kawamura, Y. Shimizu, H. Oshikawa, M. Uematsu, E. E.Haller, and K. M. Itoh, Physica B 404, 4546 (2009).

[20] Y. Yamamoto, K. Köpke, R. Kurps, J. Murota, and B. Tillack, Thin Solid Films, 518, S44 (2010) .
[21] H. Kim and J. E. Greene, J. Vac. Sci. Tech. A 17, 354 (1999).
[22] Q. Lu, T. R. Bramblett, M. A. Hasan, N.-E. Lee, and J. E. Greene, J. Appl. Phys. 78, 6027 (1995).
[23] F. Gao, D. D. Huang, J. P. Li, M.Y. Kong, D. Z. Sun, J. M. Li, Y. P. Zeng, and L.Y. Lin, J. Crys. Growth 223, 489 (2001).
[24] S. Kamatsu, M. Kasamatsu, K. Yamada, and Y. Moriyoshi, J. App. Phys. 71, 5654 (1992).

[25] E. Tutuc, S. Guha, and J. O. Chu, Appl. Phys. Lett. 88, 043113 (2006).

[26] M. Takenaka, K. Morii, M. Sugiyama, Y. Nakano, and S. Takagi, Jpn J. of Appl. Phys. 50, 010105 (2011).
[27] W.E. McMahon and J.M. Olson, J. Crystal Growth 225, 410 (2001) .
[28] S. Gan, L. Li, M. J. Begarney, D. Law, B.-K. Han, and R. F. Hicks, J. Appl. Phys. 85, 2004 (1999).
[29] E. Suvar, J. Christensen, A. Kuznetsov, and H.H. Radamson, Mat. Sci.

and Eng. B 102, 53 (2003).
[30] Chi On Chui, K. Gopalakrishnan, P. B. Griffin, J. D. Plummer, and Krishna C. Saraswat, Appl. Phys. Lett. 83, 3275 (2003).
[31] B. A. G. Kersten, H. J. W. Zandvliet, D. H. A. Blank, and A.van Silfhout, Surf. Sci. 322, 1 (1995).

[32] T. Sato, T. Sueyoshi, T. Amakusa, M. Iwatsuki, and H. Tochihara, Surf. Sci. 340, 328 (1995).

[33] H. Shigekawa, K. Hata, K. Miyake, M. Ishida, and S. Ozawa, Phys. Rev. B 55, 15448 (1997).
[34] T. Sato, T. Iwatsuki, and H. Tachihara, J. Electron Microsc. 48, 1 (1999).
[35] C. Tegenkamp, J. Wollschla ger, H. Pfnür, F. J. Meyer zu Heringdorf, and M. Horn-von Hoegen, Phys Rev. B 65, 235316 (2002).

[36] H. J. W. Zandvliet, Phys. Rep. 388, 1 (2003).

[37] C. Tegenkamp, and H. Pfnür, Surf. Sci. 574, 205 (2005).

[38] J. Wollschläger, and C. Tegenkamp, Phys. Rev. B 75, 245439 (2007).

[39] R. M. Tromp, R.J. Hamers, and J.E. Demuth, Phys. Rev. Lett. 55, 1303 (1985).
[40] R. J. Hamers, R.M. Tromp, and J.E. Demuth, Phys. Rev. B 34, 5343 (1986).

[41] S. D. Kevan, Phys. Rev. B 32, 2344 (1985).

[42] C. Collazo-Davila, D. Grozea, E. Landree, and L.D. Marks, Surf. Sci. 375, 293 (1997).
[43] X. R. Qin, and M. G. Lagally, Phys. Rev. B 59, 7293 (1999).

[44] K. Hata, S. Yasusda, and H. Shigekawa, Phys. Rev. B 60, 8164 (1999).

[45] T. Shirasawa, and S. Mizumo, and H. Tochihara, Surf. Sci. 600, 815 (2006).

[46] B. Stankiewicz, L. Jurczyszyn, Surf. Sci. 601, 1981 (2007).
[47] R. E. Schlier, and H. E. Farnsworth, J. Chem. Phys. 30, 917 (1959).

[48] D. J. Chadi, Phys. Rev. Lett. 43, 43 (1979).

[49] P. E. Wierenga, J. A. Kubby, and J. E. Griffith, Phys. Rev. Lett. 59 2169 (1987).

[50] N. C. Bartelt, T. L. Einstein, and C. Rottman, Phys. Rev. Lett. 66, 961 (1991).

[51] D. J. Chadi, Phys. Rev. Lett. 59, 1691 (1987).

[52] H. J. W. Zandvliet, Phys. Rev. B 61, 9972 (2000).

[53] J. B. Foresman and AEleen Frisch, "Exploring Chemistry with Electronic Structure Methods", Gaussian, Inc. Pittsburgh, 1995.

[54] Chemistry 6440/7440, http://www.slideworld.com/slideshows.aspx/Chemistry-6440--7440-ppt-519616, last visited date 26.07.2011.

[55] Hartree- Fock Method, http://en.wikipedia.org/wiki/Hartre-Fock_method, , last visited date 26.07.2011.

[56] A. Szabo and N. S. Oslund, " Modern Quantum Chemistry: Introduction to Advanced Electronic Structure Theory", New York, McGraw-Hill 1989.

[57] M. J. Frisch, G. W. Trucks, H. B. Schlegel, G. E. Scuseria, M. A. Robb, J. R. Cheeseman, V. G. Zakrzewski, J. A. Montgomery, R. E. Stratmann, J. C. Burant, S. Dapprich, J. M. Millam, A. D. Daniels, K. N. Kudin, M. C. Strain, O. Farkas, J. Tomasi, V. Barone, M. Cossi, R. Cammi, B. Mennucci, C. Pomelli, C. Adamo, S. Clifford, J. Ochterski, G. A. Petersson, P. Y. Ayala, Q. Cui, K. Morokuma, D. K. Malick, A. D. Rabuck, K. Raghavachari, J. B. Foresman, J. Cioslowski, J. V. Ortiz, B. B. Stefanov, G.Liu, A.Liashenko, P. Piskorz, I. Komaromi, R. Gomperts, R. L. Martin, D. J. Fox, T. Keith, M. A. Al- Laham,C.Y.Peng, A. Nanayakkara, C. Gonzalez, M. Challacombe, P. M. W. Gill, B. G. Johnson, W. Chen, M. W. Wong, J. L. Andres, M. Head-Gordon, E. S. Replogle and J. A. Pople, Gaussian2003 Rev. D.01(Gaussian, Inc. Wallingford CT, 2004).

[58] C. C. J. Roothaan, Rev. Mod. Phys. 23, 69 (1951).

[59] G. G. Hall, "The Molecular Orbital Theory of Chemical Valency. VIII. A Method of Calculating Ionization Potentials". Proceedings of the Royal Society London A 205, 541 (1951).

[60] C. Kittel, “Introduction to Solid State Phys.”, 8th Ed., USA, 2005.

[61] Y. Yoshimoto, Y. Nakamura, H. Kawai, M. Tsukado, and M. Nakayama, Phys. Rev. B 61, 1965 (2000).

[62] M. Needels, M.C. Payne, and J.D. Joannopoulos, Phys. Rev. B 38, 5543 (1988).

[63] T. Shirasawa, S. Mizuno, and H. Tochihara, Surf. Sci. 600, 815 (2006).

[64] Y. Takagi, Y. Yoshimoto, K. Nakatsuji, and F. Komori, J. Phys. Soc. Jpn. 72, 2425 (2003).

[65] H. Ueba, Surf. Sci. 603, 831 (2009).

[66] Y. Negishi, H. Kawamata, F. Hayakawa, A. Nakajima, and K. Kaya, Chem. Phys. Lett. 294, 370 (1998).

[67] J. Wang, M. Yang, G. Wang, and J. Zhao, Chem. Phys. Lett. 367, 448 (2003).

[68] Ş. Katırcıoğlu, Surf. Rev. Lett. 14, 507 (2007) .

[69] A. Chroneos, R. W. Grimes and C. Tsamis, J. Mater. Sci:Mater Electron 18, 763 (2007).

[70] F. Wang, W. Pang, and M. Huang, J.Electron Spectrosc. 151, 215 (2006).

[71] T. P. Fehlner and S.A. Fridmann, Inorg. Chem. 9, 2288 (1970).

[72] S. Komatsu, M. Kasamatsu, K. Yamada, and Y. Mariyoshi, J. Appl. Phys. 71, 5654 (1992).

[73] B. M. Mikhailov, and Y. N. Bubnov, Organaboron Compounds in Organic Synthesis, Harwood Academic Publishers, Amsterdam, 1984.

[74] Yu-Bo Fan, Zong-Biao Ding, Quan-Rui Wang, and Feng-Gang Tao, Chem. Phys. Let. 328, 39 (2000).